The Stickiness Curves of Dairy Powder

A thesis presented in partial fulfillment of the requirements for the degree of Master of Technology in Bioprocess Engineering at Massey University

Jenny Y. Zuo

B. Tech (Hons)

2004

ABSTRACT

Powder stickiness problems encountered during spray drying are important to the dairy industry. Instantaneous stickiness is a surface phenomena that is caused by exceeding the glass transition temperature of the amorphous sugar in the powder, usually lactose in dairy powders. Instantaneous stickiness occurs at a certain temperature above the T_g of amorphous lactose and has been denoted as the critical "X" value. Whether powder particles are sticky or not depends on whether there is enough liquid flow on the surface between the particles. Two particles stick to each other when there is enough liquid flow to form a bridge between them after the contact. This project aimed to measure the instantaneous sticky point conditions for various dairy powders and to relate these to the operating conditions to give a commerical outcome for the dairy industry.

The particle-gun rig was developed to simulate the conditions in the spray drier and the ducting pipe and cyclone. The stickiness of powder particles occurs after a short resident time in the particle-gun. Thus, stickiness is a surface phenomenon and the point of adhesion is the instantaneous sticky point. The amount of deposit on the plate was measured at a temperature, with increasing relative humidity. At a particular temperature and relative humidity, the powder stuck to the stainless steel plate instantaneously. This was observed by a sudden change in % deposition on a % deposition verse RH plot. The $T-T_g$ plot and stickiness curve profile were developed to determine the critical "X" value for the dairy powders.

The critical 'X' value is the temperature which exceeds the T_g of amorphous lactose when instantaneous stickiness occurs. The critical "X" values for various dairy powders including WMP, SMP, MPC, whey protein, buttermilk, white cheese powder and GUMP powder were found to be 33-49°C, 37-42°C, 42-51°C, 50°C, 37-39°C, 28.5°C, and 40,7°C respectively. In addition, the slope of the trend line in the $T-T_g$ plot, indicates how quickly the particular powder becomes sticky once the instantaneous sticky point has been exceeded. The particle-gun rig demonstrated that powders with greater than 30% amorphous lactose are more likely to cause blockage than powders with less than 30%.

Both the critical 'X' value and the slope are unique to the powder. The stickiness curve was used to relate the powder surface stickiness condition with the drier outlet temperature and relative humidity. It was recommended to operate at conditions below the stickiness curve for a powder to avoid any chamber or cyclone blockages caused by stickiness. The slope enables a decision to be made about how close to the critical point a plant should be run for a particular powder. The inlet air temperature or concentrate feeding rate can be used to move the operating conditions towards or away from the stickiness curve, according to the operating situations.

ACKNOWLEDGMENTS

The completing of my masterate thesis is a learning experience of skills gained from both research work and life experience as regards the good nature of many human beings.

My gratitude goes to my primary supervisor, Tony Paterson, thank you for your consistant support, guidance, patience and help towards gaining confidence (especially in presentations). I am very grateful to have had the opportunity to do a Masterate under your supervision. My secondary supervisor, John Bronlund: thank you for your help and guidance (especially at the beginning and end of my project). Thank you to Mary Paterson for proof reading my thesis.

Thanks to Technology New Zealand for their sponsorship of this project and Fonterra Research Centre for their assistance with this project. In particular, thanks to Tuan Troung, David Pearce, Shabeshe Paramalingam, Kenneth Bidlake, and the Longburn site drier supervisors and operators.

I would like to express my thanks to Gary Radford and Steve Glasgow of the Institute of Food, Nutrition and Human Health, for the use of various pieces of equipment.

Many thanks to my friends and colleagues; they are acknowledged for creating an enjoyable and stimulating atmosphere that has made the time spent at Massey very pleasant. In particular, I would like to thank Rachel, Anna, Kellie, Stephen, Craig, Adi, Heath, Jeremy and John. A special thanks to Roland for your helpful discussion on my project, and getting me involved in the activities that helped me to learn more about New Zealand culture and how to be a real kiwi (BBQs; watching a Super 12 rugby game in the Wellington Westpac stadium). Thanks to the Hodgkinson family who have provided me love and support through the years that I spent in Palmerston North. Also, thank you to Sarah for her understanding and support, especially during my final stages of writing up.

And last but not least, I would like to thank my grandmother, mum and dad, JieJie and aunt Lili for both giving and encouraging me to seek for myself a demanding and meaningful education. This study could not have taken place without that precious gift. I love and appreciate you all.

TABLE OF CONTENTS

LIST OF FIGURES

LIST OF TABLES

CHAPTER 1

PROJECT OVERVIEW

1.1 BACKGROUND

The stickiness of dairy powder particles and adhesion of the particulate mass to chamber walls and ducting surfaces are common severe problems in drying operations. Such problems include chamber, cyclone blockages and frequent downtime for cleaning; hence it has a significant economic impact in the dairy industry. It is estimated that the overall product loss due to the stickiness problem would be $4 million per year over all Fonterra operations. Coping with stickiness in spray driers has been a matter of trial-and-error experimentation to find conditions which avoid or control the sticky characteristic of a given composition. Therefore, it is desirable to be able to predict the stickiness conditions and then control the problem during processing.

1.2 PROPOSED SOLUTION

The two main stickiness mechanisms identified by Foster (2002) are (1) Powders that contain more than 42% total fat (greater than 1.95g/m^2 surface fat content), when exposed to a temperature above 40°C where the fat becomes completely molten and form liquid bridges between the adjacent powder particles, and (2) The glass transition temperature of the amorphous sugar present in the powder is exceeded sufficiently to make the amorphous sugar behave as a viscous liquid and form liquid bridges when particles come into contact. Hence, it is important to be able to identify this critical temperature condition which exceeds the T_g of amorphous sugar to an amount, that allows the viscous liquid to be sufficiently liquid to enable liquid bridges to form when two particles come together or a particle impacts on the wall of a duct.

Preliminary work carried out by Chatterjee (2003) shows promising results in using a particle-gun rig to mimic the air conditions in ducting and constructing the 'stickiness curve' to relate the measurements to the industry process conditions. This work used the same rig with some modification to generate stickiness curves in the industry process

temperature range. Some preliminary work was done in order to implement the stickiness curve in the plant more constructively.

1.3 PROJECT OBJECTIVES

The specific objectives of this research were:

1) To identify conditions under which dairy powders become instantaneously sticky using a particle-gun rig. The knowledge gained from the understanding of the stickiness mechanism helps to appreciate the causes of adherence in powder particles.

2) To relate these sticky conditions to plant operating conditions, to give a commercial outcome for the dairy industry.

3) To recommend the best way to control powder stickiness during the drying process in terms of its composition. To recommend changes in the operating conditions for the spray drier.

1.4 THESIS STRUCTURE

A literature review helped this research work stay in focus and it only included the topics that relate to this project such as the stickiness mechanisms and glass transition temperature of amorphous materials. Understanding these fundamental facts provides a good grounding for the following chapters. Chapter three discusses the materials and methods used and explains the dairy powder samples selected and experimental work carried out using the particle-gun rig. Instantaneous stickiness occurs at a certain temperature above the T_g of amorphous lactose and has been denoted as the critical "X" value. Chapters four and five concentrate on the identification of the critical "X" value for powder instantaneous stickiness and use this information to construct a stickiness curve for various powders selected. A preliminary work with the aim to implement the stickiness curve in a plant environment is discussed in chapter six, with a case study on skim milk powder (SMP). Chapter seven summarises the project in a nut shell and provides the recommendations for this research.

CHAPTER 2

LITERATURE REVIEW

2.1 INTRODUCTION

Powder stickiness between particle-particle (cohesion) and particle-wall (adhesion) is a major problem in the dairy industry, especially in spray driers. It can cause cyclone blockage, long downtimes for cleaning, and lowered process capacity, thereby reducing process efficiency and yield. In order to carry out the objectives of this work, it was essential to understand the related areas. These areas include the dairy powder related stickiness mechanisms, the theory on glass transition and its relation to the critical sticky point, and the tests and measurements used to investigate stickiness behaviour.

2.2 STICKINESS MECHANISMS

Stickiness and caking are closely related phenomena and are commonly encountered problems during the spray drying process and storage of dairy powders. Stickiness is a time, temperature and humidity dependent phenomena [Roos *et al.* (1996)]. With time, stickiness can lead to crystallisation and caking which is due to the formation of solid bridges between the particles.

Stickiness due to electrostatic or molecular attraction forces is insignificant compared to liquid bridging because of its unpredictable and irregular pattern [Peleg (1993)]. In addition, Chen (1994) found no effect of charge on the particles as related to the deposition rate in the spray driers. Therefore, the initial stage of stickiness is almost always due to sufficient flow that forms a liquid bridge between two particles' surface at their contact point. The driving force for the flow is surface tension [Downton *et al.* (1982), Wallack and King (1988)].

Product temperature and moisture content are two of the important factors that influence the stickiness of dairy powder and other sugar-containing foods [Downton *et al.* (1982)]. Above a particular relative humidity and temperature condition when undergoing spray drying, particles like fructose from fruit juice and lactose from milk behave in an adhesive or cohesive fashion. Such a change from non-sticky behaviour to

sticky behaviour happens with only a small change in the temperature and moisture content [Bhandari *et al.* (1997), Chuy and Labuza (1994), Hennigs *et al.* (2001)]. It is the state of the powder particle's surface (sticky or not) that determines whether the particles bounce off the walls, adhere to the wall or cohere to other particles that are already adhering to the walls. The temperature and water content are related to the particle conditions.

It has been well established that stickiness is a property of surface phenomena. It is governed by its composition, powder exposure conditions, surface properties, viscosity, and physical properties [Chatterjee (2003), Foster (2002)].

The onset of powder stickiness is the focus of this project, particularly where powder becomes instantaneously sticky. The following liquid bridging mechanisms for sticking have been identified and are the main focus of this project.

2.2.1 Viscosity

The surface properties of the drying particles are related to the surface viscosity. The viscosity, as a result of water removal, increases rapidly as the glass transition is approached. A typical viscosity of an amorphous material in the glass state is equal to or above the order of 10^{12} Pa. s. The viscosity decreases as the material changes from glass to a rubbery state due to conditions that are above the glass transition temperature (T_g) and are reported to have a viscosity ranging from 10^6-10^8 Pa.s. The viscosity of food systems is a function of temperature, once it transforms in the rubbery state associated with stickiness and caking [Roos (1995a)]. Downton *et al.* (1982) reported the critical viscosity of stickiness of amorphous sugars at $T\text{-}T_g$ values in a range from 10-20°C which means that the sticky point temperature is 10-20°C higher than the glass transition temperature. The magnitude of the $T\text{-}T_g$ parameter is the fundamental indicator of amorphous material related to stickiness and adhesion.

Downton *et al.* (1982) proposed a model for estimating the critical viscosity (μ_c) for dry particle stickiness to occur. The equation 2.1 shows that the viscosity is influenced by the surface tension (γ), contact time (τ) and the distance (KD) over which

flow must occur. The critical viscosity is a constant value of viscosity for the stickiness to occur at short-time contacts (e.g. 1-10s) and is predicted from equation 2.1 to be in a range of 10^6 to 10^8 Pa.s. The sticky-point temperature measurement test of Lazar *et al.* (1956) was used to measure the sticky-point temperature over a range of moisture contents for a sucrose/fructose mixture. It was found that all measured viscosity data lie well within the predicted critical viscosity range and fall within the range of 0.32×10^7 to 4.0×10^7 Pa.s. It was concluded that the proposed model provides a good understanding of the stickiness phenomenon with a more quantitative and mechanistic approach.

$$\mu_c = \frac{\kappa\gamma\tau}{KD} \tag{2.1}$$

Where "κ" is a dimensionless proportionality constant (κ=1 assumed), "D" is actual particle sizes (1-10μm),"K" is the fraction of the particle diameter required as the bridge width (0.01-0.001 for a sufficiently strong bridge).

Wallack and King (1988) used a similar model, the Frenkel model (equation 2.2), to predict the critical viscosity range of maltodextrin/sucrose/fructose and coffee extract in a short contact time. It was found that the measured viscosity lay within the predicted critical viscosity range of 10^6-10^8 Pa.s. for maltodextrin/sucrose/fructose and $10^5 - 10^7$ Pa.s. for coffee extract. "a" is the particle radius, "x" is the interparticle bridge size formed by viscous flow and is estimated from scanning electron micrographs of particles which have undergone sticking and are then freeze dried. "a/x" is approximately equal to 0.1. It shows that stickiness of particles occurs by viscous flow driven by surface energy. The Frenkel model demonstrates the relationship between the viscosity of material with the particle radius and powder surface energy. In order to prevent the stickiness, the viscosity should be raised by either increasing the particle radius of the powder, and/or decreasing the powder surface energy.

$$\mu = \frac{3}{2}\frac{\gamma\pi a}{x^2} \tag{2.2}$$

Both researchers Downton *et al.* (1982) and Wallack and King (1988) use surface tension (γ) of 70 mN/m for interstitial concentrate and "τ" is the particle contact time 1-10s for the method used by Lazar *et al.* (1956) for determining stickiness. The standard falling ball method was also used for measurement of viscosity. The results confirmed that the sticky mechanism of viscous flow is driven by surface energy. The models show that increasing the surface-tension driving force or longer contact times would increase the tendency toward sticking, while greater viscosity or larger particle size decreases the sticking tendency. The viscosity relates to conditions of temperature and moisture content under which stickiness occurs [Le Meste *et al.* (2002)].

The viscosity of material can be considered constant in the glassy state ($\geq 10^{12}$), but the viscosity changes dramatically above glass transition temperature (T_g). Therefore, it can be said that viscosity is dependent on the temperature above glass transition temperature ($T>T_g$, e.g. T_g+100K) [Bhandari and Howes (1999)]. Williams *et al.* (1955) proposed the Williams-Landel-Ferry (WLF) equation (equation 2.3) to relate relaxation time of mechanical properties to temperature above its glass transition temperature. The measured sucrose/fructose viscosity data of Downton *et al.* (1982) was found to fall within the predictions range of the WLF equation.

$$\ln \frac{\mu}{\mu_g} = \frac{-C_1 (T - T_g)}{C_2 + (T - T_g)} \tag{2.3}$$

Where μ is the viscosity and μ_g the viscosity at glass transition temperature, T_g is the reference temperature, T is the temperature, and C_1 and C_2 are 'universal' constants, (17.44 and 51.6 respectively for many materials). Aguilera *et al.* (1995) used the WLF-type relationship with adjustable C1 (-11.16) and C2 (10.7) coefficients to investigate caking of the amorphous fish hydrolysate powder. It is now widely understood that the universal constants given by Williams *et al.* (1955) are not universal and should be allowed to vary for different materials.

Roos and Karel (1991b) and Roos (2002) have applied the WLF equation to predict the viscosity of the glass as a function of temperature for the crystallisation rate of various amorphous sugars (lactose, sucrose, sucrose/fructose).

2.2.2 Liquid Bridging

As introduced earlier, almost all cases of sticking and caking are caused by liquid bridging rather than electrostatic or molecular attraction forces. It is important to prevent the formation of liquid bridges; and therefore, the caking and sticking of powders can be avoided. In real situations, liquid bridging can only occur when at least some of the particle surface is viscous (or if there is a presence of an external moisture or a second liquid phase) [Adhikari *et al.* (2001)].

For the sticking process to occur, the particle surface has to become fluid at the particular contact point or points. Peleg (1993) gave the mechanisms by which this may be caused by:

- Direct wetting or moisture condensation on the surface forms a film of saturated solution around the particle.
- Re-crystallised amorphous material causes adsorbed water to be liberated onto the particle surface.
- The glass/rubber transformation of amorphous material on the surface is caused by temperature exceeding glass transition temperature. The surface becomes a very viscous "rubbery" state and therefore flows.
- Melting on the surface (e.g. fat-containing particles).

It is assumed that stickiness due to insufficient drying before particles collide with one another or with the walls of the drying apparatus is not the case here. The powder particle state is dried powder, under normal operation conditions.

The first case is not appropriate for amorphous material, because it is very hygroscopic and any surface moisture would be absorbed into the particle rather than remaining on the surface. However, the condition of the amorphous material does depend on the temperature and moisture in the surrounding air. This could depress T_g, giving the third case above. Re-crystallisation of amorphous material happens during storage, because of its long relaxation time. Therefore, stickiness due to insufficient

drying (≥ 50% RH) and crystallisation are not applicable here. All spray-dried powder is assumed to be dried and contain amorphous carbohydrate present in the powder.

For this work on the sticking of dairy based powder, it would appear that the two mechanisms of liquid bridging involve either amorphous carbohydrate glass/rubbery transformation and/or fat-melting on the surface, particularly in powders which have a high fat content.

2.2.2.1 Amorphous Carbohydrate Sticking Mechanism

Amorphous lactose is formed when water is removed so quickly that there is no time for the lactose to crystallize, or by freeze-drying. Molecules either do not have time to arrange themselves or they are held in the frozen water matrix and hence cannot crystallize. This results in the random arrangement of α- and β- lactose molecules in the solid powder matrix. Amorphous lactose has a number of important properties, such as being hygroscopic; it absorbs moisture very readily from its surroundings, and it is subject to a phenomenon known as glass transition [Roos (1995b) ,Bhandari and Howes (1999), Roos *et al.* (1996)]. Lactose in amorphous rubber form is responsible for powder stickiness in the dairy industry, while crystalline lactose powders can be sticky only under extremely high temperature and humidity conditions [Bronlund (1997)]. Amorphous lactose crystallisation occurs at a water content of about 6.8 g (g x 100)$^{-1}$ of lactose corresponding to an equilibrium relative humidity of 37% at room temperature [Roos (2002)]. Aguilera *et al.* (1995) reported that amorphous lactose crystallizes at 42-52% RH. Such change can lead to release of water and/or encapsulated milk fat in the case of dairy powders.

Amorphous lactose becomes sticky when its glass transition temperature is exceeded sufficiently that the decrease in viscosity causes flow at the surface and liquid bridges can form between particles which causes particles to adhere together [Brooks (2000), Foster (2002)]. The glass transition temperature can be exceeded by either an increase in temperature to above T_g and/or an increase in moisture content and water activity to suppress the T_g.

It is very common for speciality powders to have another carbohydrate added in solution or dry form. If these carbohydrates are added in solute form (i.e. prior to spray drying) then the carbohydrate will be in the amorphous form in the final product. However, the mechanism of liquid bridging is applicable to all amorphous carbohydrates present in dairy products. Foster (2002) investigated properties of amorphous carbohydrates such as sucrose, maltose, glucose, galactose, fructose and sugar mixtures in relation to stickiness.

2.2.2.2 Fat-melting Sticking Mechanism

Milk fat contributes to sticking of dairy powders during processing and storage, especially for high fat powders such as cream powders and cheese powders. In processing, high fat powders cause smearing, in which the powder builds up on the inside of the chamber, cyclones and fluidised beds [Burr (1999), Crofskey (2000)]. Free fat content varies with different process conditions. For example, more free fat is observed in roller drying than spray drying [King (1965)].

Milk fat contains a mixture of lipids, and 98.5% of its constituents are triglycerides. Different triglycerides (differing in types of fatty acid, the length of chain and the degree of saturation) have different melting points, thus milk fat has a large melting range. Norris *et al.* (1973) using a Diferential Scanning Calorimeter (DSC) showed that the triglycerides in milk fat have a melting range approximately -40°C to +40°C. A typical DSC thermogram for milk fat shows three melting ranges: -40°C-0°C, 0°C - 20°C, and the highest melting region 20-37°C which is the main melting peak. Although the resolution of the peaks in the DSC thermogram differ due to different heating rates, the temperatures at which the peaks occur remains constant.

Fat complexes with protein in a finely emulsified state and is said to be encapsulated fat [Buma (1971a), King (1965)]. Buma (1971a) stated that fat which is not encapsulated is known as extractable fat or "free" fat. A detailed study of free fat content in relation to the powder properties defines that free fat originates from four different sources. These are:

Surface fat, which is present as pools or patches of fat on the outer most particle surface;

Outer layer fat, consists of fat globules in the surface layer of the powder particle and it can be directly reached by fat solvent;

Capillary fat, consists of fat globules inside the particle, which can be reached by fat solvents via capillary pores or cracks;

Dissolution fat, consists of fat globules, which can be reached by the solvent through holes left by already extracted globules.

It is the free fat on the surface and some on the outer layer that contributes mostly to the sticking mechanism. This is mainly because they have the ability to pool the fat together and form liquid bridging when the fat is in its molten state. Some high fat content powder, the capillary fat near the surface also pooled by molten fat on the surfaces. In most cases the capillary fat and dissolution fat do not contribute to sticking or caking. Foster (2002) used confocal laser scanning microscopy (CLSM) to observe the pooling effect of fat in low fat cream powder. The observations were carried out at 20°C before and after being heated to 55°C. The result supported the fat-melting mechanism for sticking and caking, as the surface fat pooled at the particle contact point/s and formed agglomerated particles.

The mechanism for sticking and caking due to milk fat is described by Foster (2002) shown in Figure 2.1. Liquid bridging in high fat dairy powders occurs when there is enough molten fat on the surface when they are exposed to a process temperature above 40°C.

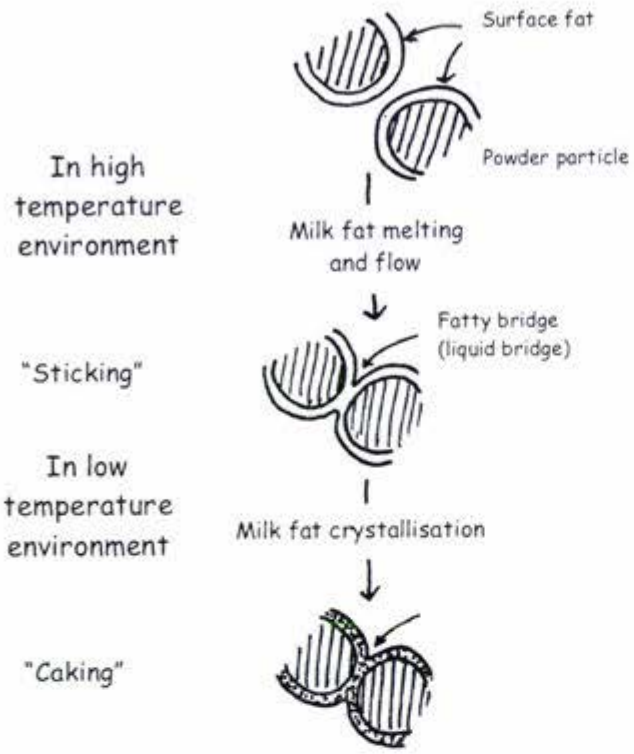

Figure 2.1 Milk fat-melting mechanism (taken from Foster (2002)).

Free fat was extracted by washing the powder with an organic solvent-petroleum ether (boiling point 40 to 60°C) for the desired time. Then the solution was filtered through filter paper to separate the powder and the solvent. The powder residue was washed with the solvent and dried. The solvent residue containing the extracted fat was allowed to evaporate until the extracted fat residue reached a constant weight. The free fat content is calculated as a percentage of the total mass of the powder sample. It was observed that as extraction time increases, the amount of free fat extracted increases. Kim *et al.* (2002) extracted free fat from commercial SMP (0.01fat g/g powder) and WMP (0.266 fat g/g powder) at an extraction time of 10 mins, 24 hrs and 48 hrs. The amount of extracted free fat in WMP increased from 0.019 g/g powder to 0.028 g/g powder. However, the surface fat of free fat is of interest for the liquid bridge mechanism. Foster (2002) estimated an extraction time of 10s for the surface fat of a low fat cream powder (55% total fat) because a constant free fat content measured with extraction time less than 20s was observed using the standard free fat extraction

procedure. Buma (1971a) also suggested that an extraction time as short as 10 s or at least 1 min would be needed to measure the surface fat.

The differences in spray drying process parameters from manufacturer to manufacturer have minor importance to the composition of the powder surface [Foster (2002), Fäldt and SjÖholm (1996)]. However, difference in particle size has an effect on the amount of free fat that can be extracted, the reason being that small powder particles have much more surface exposed to the solvent than larger particles during extraction [Buma (1971b), Fäldt and SjÖholm (1996)].

Surface fat content can be estimated from the total fat content and specific surface area. Foster (2002) looked at the relationship between the surface fat content and total fat content for different powders with varied levels of fat. The data was expressed in terms of the specific surface area in order to consider the particle size effects in the free fat extraction.

Total fat content measurement used the Majonnier fat extraction procedure. Figure 2.2 taken from Foster (2002) shows a fairly linear relationship between surface fat content and total fat content when the total fat content is above 30%.

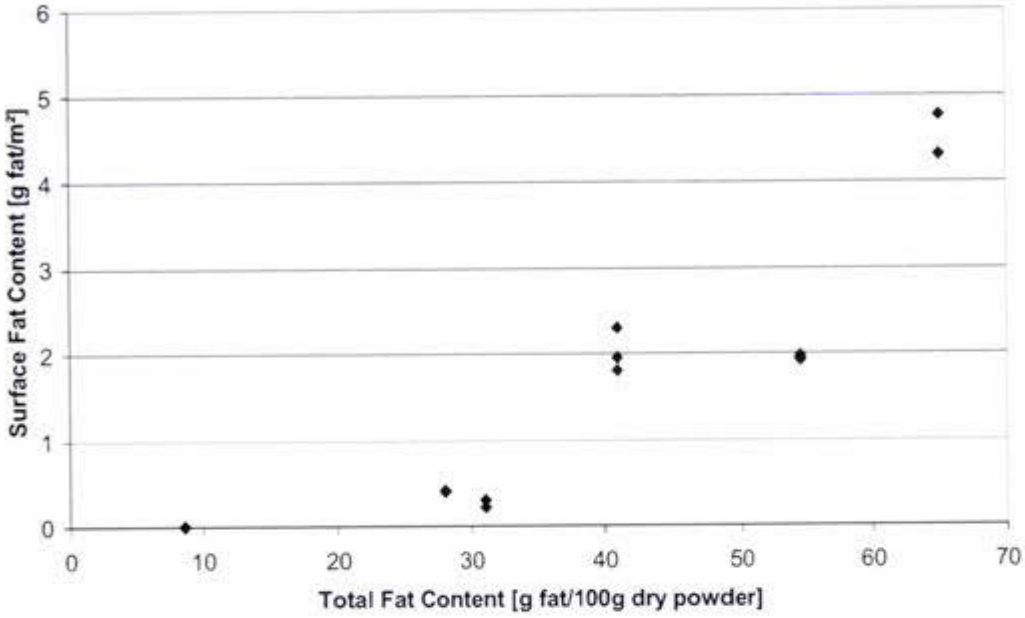

Figure 2.2 The relationship between total fat content and surface fat content expressed in terms of the specific surface area (Foster (2002)).

Crofskey (2000) examined the effect of the fat-melting mechanism in low and high fat cream powders, using an air gun to fire powder particles at a plate and measure the percentage of powder stuck to the plate. The RH was kept relatively low to avoid the lactose changing its state while increasing temperature. Surface tension of the fat decreases as the temperature increases. The fat is able to flow over the particle surface when its surface tension becomes equal to or less than the surface tension material of its contact. The critical surface tension point for low fat cream powder was found to be around 40°C. Furthermore, as temperature increases to a point of flow, fat viscosity is decreasing and this pulls more fat from the capillary fat near the surface to the surface and increasing the total area of fat coverage. However, for high fat cream powder, at a temperature above 40°C, there was no increase in powder stickiness as the particles are covered with a layer of fat. No further fat can be drawn from inert fat.

Although, surface fat-melting to form liquid bridges is one of the attributes to sticking and caking in dairy powder, it is agreed by Fäldt and Bergenståhl (1995) and King (1965), that lactose crystallisation is the other attribute for gaining surface fat from encapsulated fat. This can happen during storage; if amorphous lactose crystallises, as a

result of an increase in temperature or moisture stresses, disrupting the encapsulated fat, forcing fat to spread to the powder particle surface [Fäldt and Bergenståhl (1995), King (1965)]. In the case of milk powder, King (1965) noted that when it absorbs moisture and develops into a dry, hard and powdery texture, this coincides with the release of fat. At the critical moisture content of 8.9%-9.2%, fat was released for a powder with a fat content of 27-28%. Lactose crystallisation was observed during this time with a polarizing microscope. The crystallisation ruptured the continuous matrix of the SNF (solid not fat) and made the fat accessible to the solvent.

Researchers have used the Electron Spectroscopy for Chemical Analysis (ESCA) to estimate the amount of surface fat on the powder in conjunction with free fat extraction method. The ESCA analysis provides direct information about the powder surface independent of particle size and melting point of oil phase. In addition, the powder surface coverage of other components such as protein and carbohydrate is also detectable. The result is the two approaches have a good correlation. For powder with a higher fat content, the surface fat coverage is high, so is the free fat [Fäldt *et al.* (1993), Fäldt and SjÖholm (1996), Kim *et al.* (2002)].

2.3 GLASS TRANSITION

In a 'glass' state, the material is solid and brittle and has an amorphous, liquid-like structure with an extremely high viscosity, $\eta \geq$ of the order of 10^{12} Pa.s [Noel *et al.* (1990), Bhandari *et al.* (1997), Downton *et al.* (1982)]. The glass state can transform into a less viscous, liquid rubbery state by escalating the temperature and/or water plasticization. Such phase transformation is referred to as glass transition and the temperature at which this happens is known as glass transition temperature (T_g) [Roos (1995b)]. Glass transition temperature profiles are often reported as a function of water activity, relative humidity or concentration (%solid). Glass transition is a second order transition and is characterized by a change in specific heat capacity.

Materials transforming from 'glass' to a 'rubbery' state as a function of temperature is well established and this transition temperature is dependent on moisture content [Lillford and Fryer (1998)]. The glass transition temperature (T_g) is being recognized as

a fundamental parameter to explain and control phenomenon such as stickiness, caking and unwanted agglomeration for amorphous and semicrystalline foods, particularly in the case of low molecular weight carbohydrates [Bronlund (1997), Foster (2002), Brooks (2000), Adhikari *et al.* (2001), Bhandari and Howes (1999), Downton *et al.* (1982), Bhandari *et al.* (1997), Roos and Karel (1991b), Chuy and Labuza (1994)] .

In dairy foods, the main amorphous components are carbohydrates and proteins. However, often the amorphous carbohydrates govern the transition temperatures corresponding to changes of physical properties. Glass transition occurs due to a water content dependent temperature range decreasing with increasing water content [Roos (2002)]. Milk fat does not affect the glass transition temperature of milk powders and it is immiscible with lactose and other water-soluble substances [Jouppila and Roos (1994a), Jouppila and Roos (1994b)].

In general, the glass transition temperature of carbohydrates decreases as molecular weight decreases [Noel *et al.* (1990), Roos Y. (1993)]. Jouppila and Roos (1994a) found skim milk powder with enzymatically hydrolysed lactose (T_g=49°C) had substantially lower T_g than the regular milk powder (T_g =92°C). Lactose (MW 342) in milk hydrolyzes to glucose (MW 180), and galactose (MW 180) and this decreases the T_g in skim milk powder and critical water content and water activity. The T_g for anhydrous galactose and glucose are 30 and 31°C, respectively, but the T_g for lactose is 101°C [Roos Y. (1993), Bhandari and Howes (2000)]. The low T_g of the galactose and glucose mixture causes more severe glass transition characterized problems than does anhydrous lactose during processing and storage.

The glass transition temperature is important to this work as it is widely recognized that it characterizes amorphous materials for phenomena such as stickiness, caking and crystallisation when an amorphous materials' glass transition temperature is exceeded [Chuy and Labuza (1994), Downton *et al.* (1982), Jouppila. K. *et al.* (1997), Jouppila and Roos (1994a), Jouppila and Roos (1994b), Lloyd *et al.* (1996), Roos and Karel (1991a), Roos and Karel (1991b)]. Bhandari *et al.* (1997) found a correlation

between T_g and the spray drying behaviour of sugars and fruit juices with a maltodextrin additive.

Lloyd *et al.* (1996) showed that the caking of spray dried lactose is related to the onset temperature of T_g. They confirmed the viscous flow of the product above T_g by compressing an amorphous lactose powder at various temperatures in a compacted product increasing above the onset temperature of $T\text{-}T_g$. The temperature change ($T\text{-}T_g$ factor) is the difference between the actual temperature of the powder (T) and its glass transition temperature (T_g); in turn this $T\text{-}T_g$ factor determines the rate of various changes [Brooks (2000), Foster (2002), Roos (1995b), Roos *et al.* (1996), Chatterjee (2003)]. It is therefore desirable to know what T_g is at a particular moisture condition, and how the $T\text{-}T_g$ factor relates to stickiness in dairy powders. The glass transition temperature can be determined either by measuring it directly or predicting it from the moisture content or water activity.

2.3.1 Determination of Glass Transition Temperature

There are several methods by which the glass transition temperature can be directly measured. These analytical methods detect the sudden change in physical properties of the material at T_g. These change of physical properties include heat capacity, free molecular volume, thermal expansion coefficient, dielectric coefficient and viscoelastic properties.

Differential thermal scanning calorimetry (DSC) is one of the most common techniques found in the literature for determining T_g of amorphous material such as spray-dried skim milk and freeze-dried skim milk powder [Ozmen and Langrish (2002), Jouppila and Roos (1994a)]. DSC measures the temperature and heat flows associated with transitions in materials as a function of time and temperature.

Foster (2002) reviewed the literature for the possible causes for different glass transition temperature measurements. The reasons for variation measured by DSC are outlined as follows:

- Scanning rate used (higher rate results in higher T_g value from true value). Chuy and Labuza (1994) measured the glass transition temperature of carbohydrate material and found that the glass transition temperature was lower at slower scanning rates and higher at higher scanning rates. They explained that the lower observed temperature values at the slowest heating rate may be due to the longer residence time of the sample at any temperature during heating, which increases the probability for viscous flow, crystallisation of the amorphous carbohydrate, and collapse. The rate of 5°C/min is used by Roos and Karel (1991a, 1991b, 1991c).

- Location of the T_g on the DSC curve. Due to different interpretations of T_g values from the DSC curve, for example of amorphous lactose, some researchers use onset, mid-point or endset for T_g data [Ozmen and Langrish (2002)]. Up to 10°C differential is expected when comparing the T_g value for amorphous lactose found in the literature by different researchers.

- Enthalpy relaxation peaks.

- Preparation of DSC pan. It has the potential for uptake of moisture by the powder, because amorphous carbohydrates have a hygroscopic nature, which means they absorb moisture very quickly if the DSC pan is not fully filled under dry conditions. This would raise the moisture content of the powder and result in a lower T_g value. In addition, Brooks (2000) noted that freeze-dried sugars still hold some moisture, which can acts as a plasticiser, even after dehydration over a strong desiccant. It is therefore the residual moisture that has an effect on the glass transition temperature and has to be accounted for in the T_g data.

In food systems such as milk powder, the main components are carbohydrate, protein and fat. Jouppila and Roos (1994a) used DSC to determine the glass transition temperature of freeze-dried milk powder products (such as 0%fat skim milk powder, 10.7% fat milk powder, 18.6% fat milk powder, whole milk powder, and hydrolysed lactose skim milk powder) at different water content levels. It was found that the T_g values of those milk powders (except the hydrolysed lactose skim milk powder)

containing lactose were almost equal to those of pure lactose. This indicates that proteins do not interact with lactose in terms of glass transition temperature, and the physical state of SNF in milk powders is governed mostly by lactose. Protein does, however, have some affect on the crystallisation of amorphous lactose [Jouppila and Roos (1994b), Foster (2002)]. It is also likely to affect the rate of change of stickiness with time for a given powder. Other observations show that milk fat did not affect the T_g of milk powders due to their immiscible properties with SNF or moisture. However, T_g could not be determined from the DSC curves for powders containing fat at the RH range of 23.9 to 44.4% because of the dominant fat-melting endotherm in the same temperature range [Jouppila and Roos (1994a)].

Other useful techniques and sometimes more sensitive methods include dynamic mechanical thermal analysis (DMA/DMTA) and mechanical spectroscopy. These techniques measure the effect of a sinusoidally varying stress on dynamic moduli or viscosity. Nuclear magnetic resonance (NMR) spectroscopic technique and electron spin resonance spectroscopy (ESR) are useful techniques when studying the molecular mobility and diffusion of the glass transition temperature of particles [Bhandari and Howes (2000)]. Peleg (1993) extensively listed the references of studies where methods other than DSC or DMA were used to determine the glass transition temperature.

2.3.2 Prediction of Glass Transition Temperature

The Gordon-Taylor equation (eq. 2.4) is the empirical formula that is used to predict the influence of moisture content on the T_g (e.g. anhydrous solute and water component [Jouppila and Roos (1994a)]) or to estimate the glass transition temperature of a mixture of sugars [Hennigs *et al.* (2001) ,Roos and Karel (1991a)].

$$T_{gm} = \frac{(w_1 T_{g1} + k w_2 T_{g2})}{(w_1 + k w_2)} \tag{2.4}$$

Where T_{gm} is the glass transition temperature of the mixture. Examples of mixture components that have been studied are α-lactose-water or maltodextrin-sucrose. w_1, w_2, T_{g1} and T_{g2} are the mass fraction and glass transition temperatures of component 1

(lactose) and component 2 (water), respectively. k is a constant for the solid component and it was derived experimentally.

$$T_{gm} = \frac{w_1 T_{g_1} + (\Delta C_{p2} / \Delta C_{p1}) w_2 T_{g_2}}{w_1 + (\Delta C_{p2} / \Delta C_{p1}) w_2} \tag{2.5}$$

The Couchmann-Karasz equation (eq. 2.5) is another mathematical formula for determining T_g of a polymer mixture. The ratio of change in heat capacity is similar in form to the constant k in the Gordon-Taylor equation. The Couchmann-Karasz equation can expand further and be applied for multi-component mixture systems such as water, glucose and sucrose [Roos (1995a)]. For an *'n'* component system, the extended Couchmann-Karasz equation is shown in equation 2.6.

$$T_{gm} = \frac{\sum_{i=1}^{n} w_i \Delta C_{pi} T_{gi}}{\sum_{i=1}^{n} w_i \Delta C_{pi}} \tag{2.6}$$

For dairy powders, the glass transition temperature is more readily predicted from the water activity rather than the moisture content of the powder. In a practical sense, moisture content of the powder includes not only the moisture associated with sugars but also moisture associated with other components (such as protein) which have no effect on the T_g of the powder. However, water activity of dairy powders is fairly constant with varied levels of its components (i.e. sugars, protein and milk fat). So, the T_g is constant with constant water activity. In addition, water activity can also be easily measured with a calibrated RH probe.

Brooks (2000) fitted a non-mechanistic equation to the literature data; a third order model developed (eq. 2.7) to predict the T_g of amorphous lactose from the water activity of the powder. In the same line of thought, Foster (2002) summarized the T_g/moisture content and T_g/water activity profile for amorphous glucose, galactose, fructose, sucrose, maltose and maltodextrin powders from data available in literature, and

fitted equations to the data, so that the prediction of T_g was made from individual sugars present in the powder.

$$T_g = -530.66(a_w)^3 + 652.06(a_w)^2 - 366.33a_w + 99.458 \qquad (0<a_w<0.575) \tag{2.7}$$

Foster (2002) also proposed a mathematical equation (eq. 2.8) for predicting the T_g of a multi-component powder. The prediction is based on the weighted addition of the individual T_g values for the amorphous sugars present, at given water activity of the powder. This method was found to have an overall better fit than the Couchmann-Karasz equation, especially for the prediction of the T_g of amorphous lactose in dairy powders.

$$T_g = \sum_{i=1}^{n} x_i T_{gi(a_w)} \tag{2.8}$$

2.3.3 The 'T-Tg' Factor

Amorphous carbohydrate associated with the stickiness phenomena is a viscosity related mechanism. When the temperature exceeds its glass transition temperature, the viscosity decreases, allowing flow between the particles. The rate of sticking for amorphous material is governed by how much the T_g, is exceeded ($T-T_g$). The individual parameters of temperature and relative humidity might not directing result in structural changes, but the resulting $T-T_g$ can cause dramatic structural change leading to sticking, caking, collapse and crystallisation. It is therefore, only $T-T_g$ that is important, not the actual temperature and moisture conditions required to achieve it (Brooks 2000). Bhandari *et al.* (1997) and Roos and Karel (1991b) have used the concept of $T-T_g$ to describe the sticking behavior of amorphous powder. Bhandari and Howes (1999) and Bhandari (2001) suggest the critical viscosity of sticky powder in sugar-rich food is reached at a temperature 10-20°C above T_g, and assumed that the temperature of surface of particles during spray drying should not reach 10-20°C above the T_g.

The semilogarithmic plots of the sticky point temperature measurement and the glass transition temperature versus moisture content for sucrose : fructose (7:1) mixture

show them parallel with each other [Adhikari *et al.* (2001)]. The sticky point temperature is almost 4-11°C higher than the glass transition temperature ($T_{g\,end}$).

Brooks (2000) demonstrated that the 'T-T_g' factor of amorphous lactose is a combination of different temperature and relative humidity changes giving this constant value of temperature difference, resulting in the same caking strength with time. The T-T_g of amorphous lactose for onset instantaneous stickiness is 25°C (Table 2.1). However, in order to avoid sticky powder, storage below glass transition or continuation of processing below T-T_g of 10°C were recommended. Foster (2002) found the T-T_g values of amorphous sugars where instantaneous sticking occurred (Table 2.1). The crical T-T_g value for instantaneous stickiness would probably be less than the values given in Table 2.1. Burr (1999) found the specific T-T_g of cheese powder caused mainly by amorphous lactose is 10°C.

Keir (2001) found the stickiness behavior of milk powders did differ from that of pure amorphous lactose. With regard to Brooks (2000)'s recommendation, the T-T_g of 10°C for safe processing is too conservative, and Keir (2001) further stated that the T-T_g required for stickiness to occur may be 30°C or higher, especially considering the short time in the driers. The stickiness changes in dairy powders are obviously affected by the composition of the powder.

Table 2.1 The specific 'T-T_g' factor for instantaneous sticking.

Amorphous Carbohydrate	'T-T_g' factor (°C)
Lactose	25.0*
Sucrose	20.3
Maltose	19.0, 25.3, 29.0
Glucose/Lactose	35.0, 37.4
Galactose/ Lactose	30.8
Fructose/ Lactose	41.3

*Brooks (2000) critical instantaneous stickiness;
Foster (2002) instantaneous stickiness occurred.

2.4 DEVICES TO MEASURE POWDER STICKINESS PHENOMENA

Researchers have developed and reported various techniques to measure powder cohesion and adhesion phenomena over the last 50 years but most of these measure the stickiness of the powder when the particles are stationary or moving in slow motion. A review focused on the most relevant methods follows.

2.4.1 Shear Cell Method

The powder is placed in a box and it is split in half horizontally or vertically. It is equipped with a means of applying various normal stresses and shear stress to the top half of the cell and while the lower half held stationary (Jenike, 1964). It was found that for each normal stress there is a particular shear stress which causes failure. This tensile strength analysis provides a direct indication of the interparticle forces that support before it yields. It was used to correlate the flowabiltiy of a powder especially through chutes and hoppers.

2.4.2 Blow Test

The blow test was developed by Paterson *et al.* (2001) to measure the caking strength of milk powder. In this test, air was passed through a small diameter tube held at a fixed height and angle above a powder bed. The powder bed is pre-conditioned at different water activities. The velocity of air was increased until a channel was formed in the bed and this flowrate recorded as a measure of the caking strength or stickiness of the powder. The blow test was also used to distinguish between fat caking and amorphous lactose caking in dairy powders Foster (2002). Burr (1999) also used the test for the investigation of caking strength of cheese powder in different storage conditions.

Brooks (2000) modified the blow test by including a segmented distributor and a glass enclosure. The segmented distributor enables more samples and multiple readings to be taken over a period of time. The glass enclosure enables the control of powder conditions in the bed, air at desired temperature and relative humidity ready for the blow test. Brooks (2000) found the same caking strength (a particular value of $T-T_g$) with time resulted with different combinations of temperature and water activity. Amorphous

lactose becomes instantaneously sticky at a $T-T_g$ above 25°C. Foster (2002) used the same test to observe this particular value of $T-T_g$ for other amorphous carbohydrates that may be present in dairy powders and the caking mechanism under different storage conditions.

This test allows a continuous reading to be taken over time and the ability to observe the time-dependent side of sticking and caking problems under constant $T-T_g$. Thus, it is possible to quantify the development with time of inter-particle forces caused by the viscous flow of an amorphous material. This is useful in the study of powder conditions for storage where the residence time is long enough for stickiness to develop over time. While it can be shown that stickiness can develop very fast under certain temperature and relative humidity conditions (Paterson *et al.* 2004) it is not generally a suitable device for measuring the instantaneous stickiness needed by a particle impacting the walls of a spray drier or the ducting after the drier.

2.4.3 Sticky-point Temperature Test

The so-called "sticky-point temperature" test was originally developed by Lazar *et al.* (1956). The principle of the tester has been applied and modified by several researchers to determine the sticky point of the amorphous sugar powders for different temperature and moisture contents of the material (Hennigs *et al.* (2001), Downton *et al.* (1982), Chuy and Labuza (1994) and Wallack and King (1988)). The principle of the test involves placing a powder sample with a known moisture content in a test tube, which is immersed in a controlled temperature bath. The tube is closed to the atmosphere with a rotating mercury seal, and a small propeller embedded in the sample. The bath temperature is raised slowly while the propeller is stirred periodically (i.e. quarter turn per second) either by hand or through mechanical means. The sticky-point temperature is referred to as the temperature at which the force experienced to drive the propeller increases sharply. The sticky point temperature is a function of moisture content. Thus the sticky point decreased with increasing moisture content. The test is repeated with other moisture contents, and the sticky point temperatures are plotted against moisture content. The combination of temperature and moisture point lying above the curve causes the onset of product stickiness and is to be avoided, while the region below the

curve is the non-sticky safe regime. Downton *et al.* (1982) reported that sticky-point measurements are repeatable within ±1 K. The bath heating rate was 1°C/3 min then 1°C/5 min as the sticky point was approached [Downton *et al.* (1982), Wallack and King (1988)]. Chuy and Labuza (1994) examined the effect of different heating rates on the sticky point (1°C/3 min, 5°C/min and 10°C/min). In general, a lower temperature was observed at the slowest heating rates compared to faster heating rates for any given powder from the same storage conditions. A slow heating rate would provide a longer residence time, therefore increasing the probability for viscous flow and stickiness.

Downton *et al.* (1982) and Wallack and King (1988) have related the sticky-point temperature to viscosity/temperature data. The sticky point of sucrose/fructose powder is superimposed upon the curves representing the viscosity data. The experimental viscosity value of 0.32×10^7 to 4.0×10^7 mPa.s. lies within the predicted critical viscosity range of 10^6-10^8 [Downton *et al.* (1982)]. The results of Wallack and King (1988) gave similar agreement with the predicted viscosity data range on maltodextrin/fructose powder.

Overall, the sticky-point temperature test is a measure of powder stickiness behaviour in a mildly agitated situation and the results vary with heating rate, particle sizes, stirrer rotational speed and techniques.

2.4.4 Fluidised-bed Rig

The 'bench-top-scale fluidised-bed' rig was developed by Toy (2000) and was based on a study (fluidisation test) carried out by Dixon (1999). This rig was used to measure powders' cohesive stickiness property in a fluidised bed situation, with changing temperature and humidity conditions. This setup involves supply of humid air at different temperatures to a small-scale fluidised-bed. The powder particles surface properties changed as the conditions of the air were changed until the bed lost fluidisation. This was achieved by a controlled wet-bulb temperature via a water bath (range 0-80°C) to give the desired saturation humidity; this saturated air was then heated and immersed into another hot water bath for a desired dry bulb temperature (experimental range 40-80°C) before delivering it into the fluid bed. The water baths' temperatures were controlled,

monitored and recorded by setting conditions at a desired temperature and humidity. The air velocity varied between 0.22 ms^{-1}–0.42 ms^{-1} and showed no effect on the stickiness end point.

The measurement in the 'bench-top-scale fluid bed' rig was done by visual observation of the stickiness end point or total seizure of the bed in a particular temperature/humidity environment. Chatterjee (2003) stated that the observed end points occurred when complete seizure of the particle bed occurred, and this was categorised by an adhered particle mass which would be revitalised temporarily for a short period with rigorous shaking or vibration, but would collapse very soon after. Chatterjee (2003) found lactose in an amorphous form is the stickiest powder, and in a crystalline form is the least stickist powder. The degree of stickiness is due to the amount of amorphous lactose present and the different particle sizes.

This technique can be used to determine the stickiness curve on a temperature versus water activity or relative humidity profile, but cannot be used on cohesive dairy powders which will not fluidise such as high fat powders.

2.4.5 Cyclone Stickiness Testing Device

The stickiness cyclone testing device was developed by Boonyai *et al.* (2002) and it was designed to measure particle-particle and particle-wall stickiness during spray drying. The set-up consists of a system that provides humidified and dry air mixture at a specified RH, adjusted by the their flow rates and a cyclone test chamber. When the desired level of RH was researched, approximately 1 g of powder sample was introduced into the cyclone chamber from the top opening. The powder particles travel in a rotary fashion at the bottom of the cyclone chamber. A travelling time of 1-2 min was sufficient for the powder stickiness to occur under appropriate temperature and humidity conditions Boonyai *et al.* (2004). A stickiness curve is determined in a similar way to the fluidised-bed rig.

This test has the advantage over previous methods in that the particles will be travelling at similar velocity to those encountered in the transport system for the powder after a spray drier, but the conditions actually used are at temperatures below and relative

humidity conditions above those actually experienced by the particles leaving a spray drier. There is also a question as to whether the history or RH ramping rate affects the measurement of the stickiness curve by this technique.

2.4.6 Particle-gun Rig

The shear cell method, blow test and sticky-point temperature tests measure the development of stickiness/ caking between stationary or almost stationary particles. They are not directly applicable to measuring the instantaneous stickiness of high velocity moving particle; the situation found in spray driers and the ducts after the driers. Research conducted by Moreya & Peleg (1981) has shown that physical properties such as 'stickiness', are mainly characteristic properties of the particle surface and can occur at much shorter times than those necessary to reach equilibrium with the interior of the particle. The occurrence of 'instantaneous' agglomerate formation of incipient stickiness in food powders has also been examined by Wallack & King (1988). A new technique, the particle-gun rig has been developed to measure the onset of instantaneous stickiness with particles travelling and hitting walls at velocities, temperatures and relative humidity similar to those encountered industrially.

O'Donnell *et al.* (2002) originally developed an apparatus to supply air with both a controlled temperature and relative humidity, at a variety of flow rates up to 114 l/min. Crofskey (2000) invented the rig to achieve an optimal powder delivery system where the equilibrated particles went through the gun and were fired at a stainless steel plate. The percentage of powder deposit on the plate is measured and calculated for a constant temperature with varied humidity. The initial sticky point at a particular temperature and humidity was identified from the %deposition versus relative humidity plot. Those conditions were then used to generate the 'stickiness curve' of that powder.

The particle-gun rig is very useful in terms of controlling air velocity, temperature and relative humidity to mimic the actual spray drier operating condition in the plant. Chatterjee (2003) used the rig to observe the stickiness properties of a wide range of dairy powders including cream powder, cheese powder, skim and whole milk powders. It

was confirmed that the stickiness is indeed a surface phenomenon and is affected by the surface composition of a particle.

2.5 STICKY POINT CURVE

Chatterjee (2003) used both "bench-top-scale fluid bed" and "particle-gun" rigs to generate a 'stickiness curve' for various dairy-based powders. A typical stickiness curve is temperature versus relative humidity or water activity plotted that so it can directly relate to spray drying outlet conditions. During drying, the product temperature is generally approaching the outlet air temperature [Masters (1991)].

The measured sticky-point data from a stirrer-type sticky-point device Hennigs *et al.* (2001), a fluidised-bed device Chatterjee (2003), Bloore (2000), Boonyai *et al.* (2004) from the cyclone tester and the particle-gun rig Chatterjee (2003) of skim milk powder are shown in Figure 2.3. There are differences in sticky-point obtained from the different techniques. The stirrer-type test shows powder becomes sticky at lower temperatures at the same RH and at lower RH's at the same temperature, than the fluidised-bed and particle-gun methods. This could be because the sample was measured in an almost static bed giving more contact points and less distance between particles. Although, the fluidised-bed device and the particle-gun rig make measurements while the particles are moving there are different sticky-points obtained under similar RH and temperature air conditions.

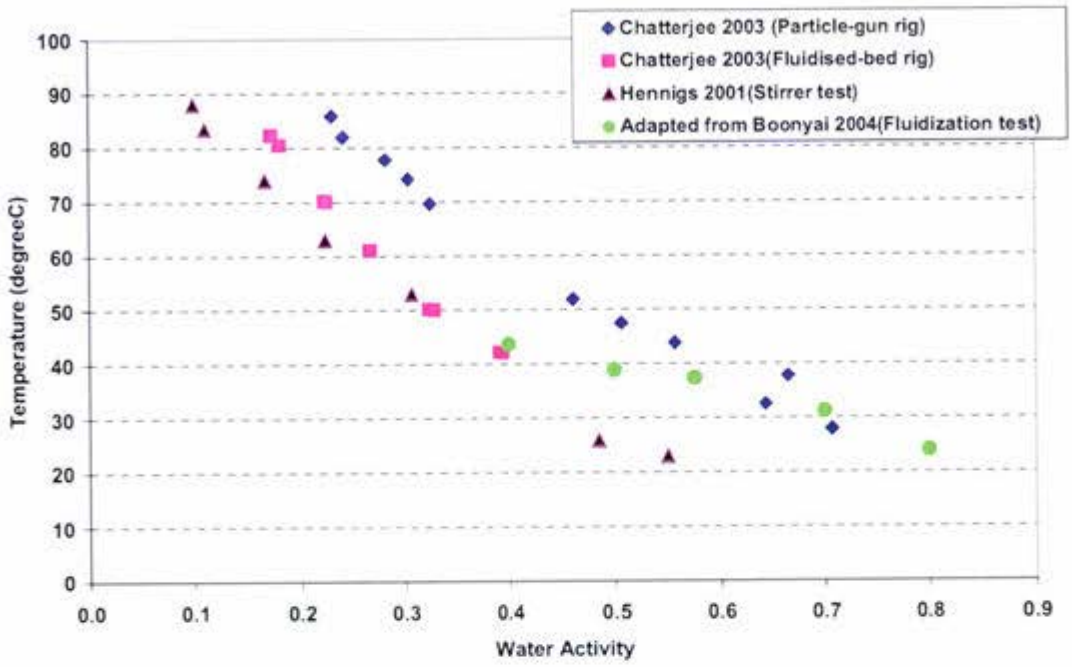

Figure 2.3 Comparison of sticky-point for skim milk powder measured by different techniques.

The sticky-point temperature difference between the different techniques varied from powder to powder, and depends on the individual powder properties. For example, the stickiness-point of amorphous lactose (Figure 2.4) has the largest difference between the two techniques and whole milk powder (Figure 2.5) has the least difference.

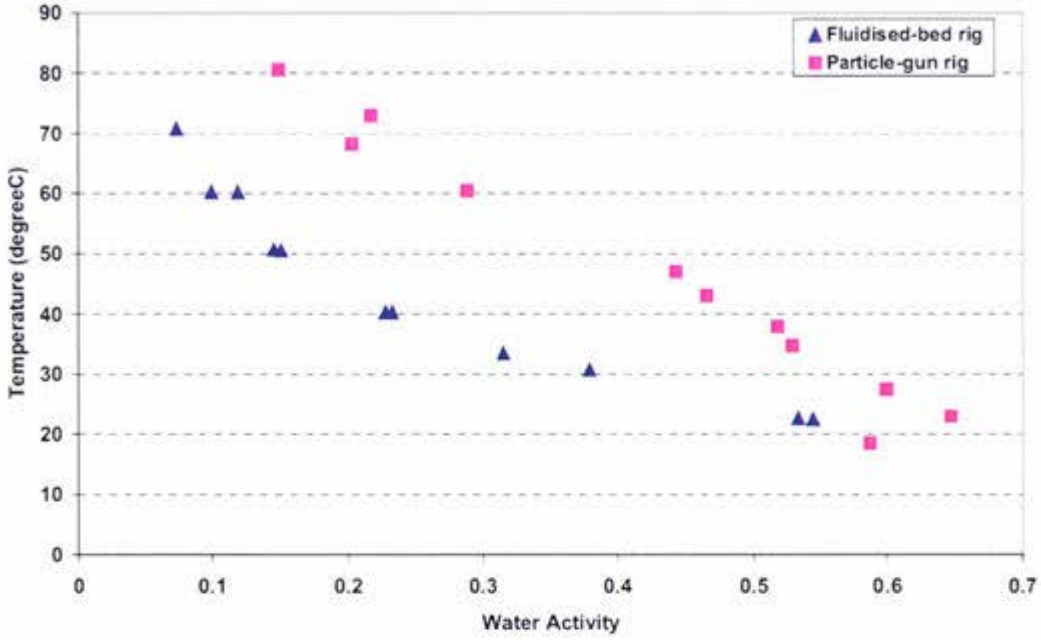

Figure 2.4 Comparison of sticky-point obtained by fluidised-bed rig and particle-gun rig for amorphous lactose (adapted from Chatterjee (2003)).

The differences in sticky-point temperature determined from the two techniques are probably due to the velocity the particles were travelling at. In the fluidised-bed rig, the air velocity was in a range between 0.22-0.42 $m.s^{-1}$, compared to the particle-gun rig of 20 $m.s^{-1}$. Particles travelling at lower speeds will have lower kinetic energy and will require less force to hold them together on impact. Particles travelling at higher speeds might knock off the particles that are loosely adhering to each other. It can be concluded that the particle stickiness is affected by the kinetic energy of the particles. Powders travel at high speed in the ducting pipeline and in the chamber during spray drying and hence the particle-gun rig is probably more applicable as a measure of the stickiness of powders during processing in the dairy industry. Data from all measuring techniques needs to be compared to industrial experience to confirm which are the most applicable.

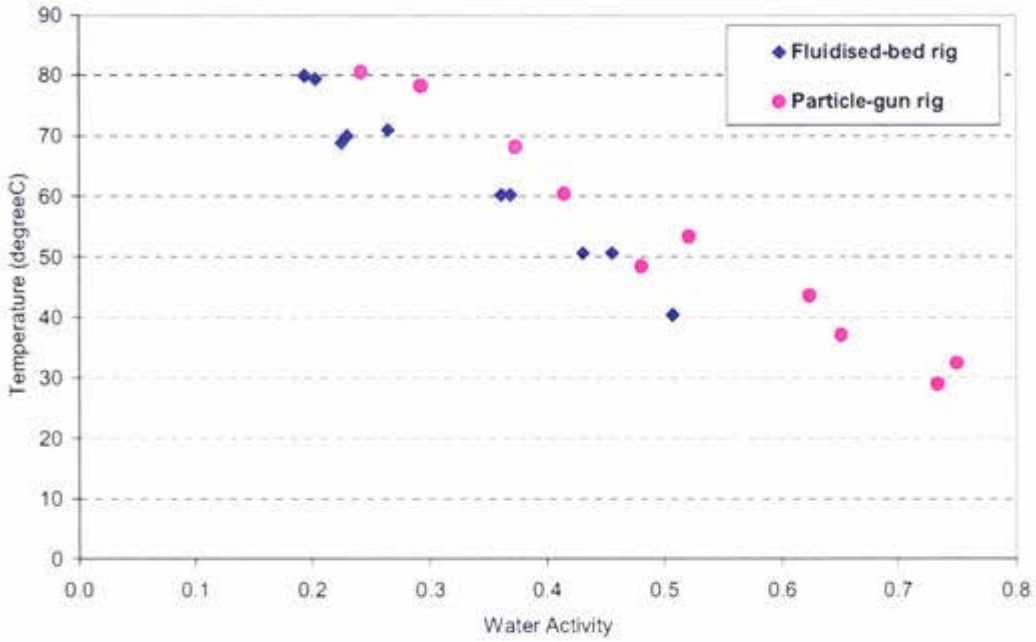

Figure 2.5 Comparison of sticky-point obtained by fluidised-bed rig (adapted from Chatterjee (2003) and particle-gun rig for whole milk powder.

Another factor that might have an influence on the stickiness data gathered by other researchers is the pre-conditioning of the powder. Once the powder has been pre-conditioned to a desired temperature and relative humidity over a period of time, the internal structure of the powder might have changed and this might enhance the likeliness of stickiness to occur at a given set of conditions. This effect will be looked at on the particle-gun in future work.

The stickiness curves of whey powder obtained from the cyclone stickiness test Boonyai *et al.* (2004), amorphous lactose measured by the particle-gun rig are shown in Figure 2.6. (The composition of the whey powder has not been given in the reference so it has been compared to the pure lactose data of Chatterjee 2003.) There is a general trend of constant temperature difference between the two stickiness curves. Amorphous lactose would be expected to become sticky earlier than the whey powder because it has a higher amorphous lactose content. However, this is not the case shown in Figure 2.6. Furthermore, from Figure 2.6 it could predicted that if the same whey powder was tested, the curve generated from the cyclone stickiness test would become sticky earlier than the

curve generated from the particle-gun rig. The difference could be due to the fact that powder particle travelling time for the cyclone stickiness test was about 1-2 min and it was less than 0.05 second for particle-gun rig. As well as this, the cyclone tester ramped the RH values up over time. This will have given some level of conditioning to the powder during the tests and probably explains the difference between the tests, considering the margin of error ± 5°C. Comparisons with data obtained industrially about where plants actually become sticky will be needed to determine which of the two tests is more appropriate.

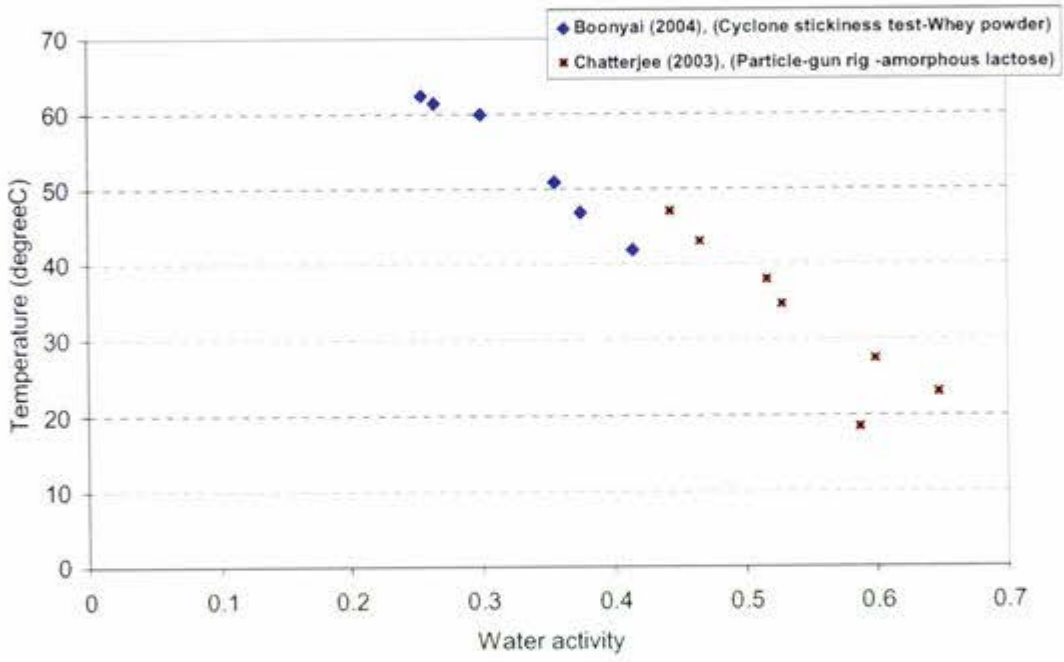

Figure 2.6 Stickiness curve for whey powder measured by the cyclone stickiness test (adapted from Boonyai (2004)) and Amorphous lactose powder measured by particle-gun rig (adapted from Chatterjee (2003)).

The stickiness curve is important in terms of demonstrating the instantaneous stickiness on particle surfaces which occur at a particular value above T_g lactose of dairy-based powder. It can therefore be related to the actual spray drying process parameter and be possible to predict and monitor the process in the sense of stickiness control.

2.6 PROJECT PLAN

Dairy powder sticking to the wall of chambers and to each other during spray drying is a prevalent problem in the industry. The formation of liquid bridging caused by decreased viscosity at the surface was explained for how particles stick. The amorphous sugar and fat-melting mechanisms were responsible for sticking in dairy powders. The degree of each mechanism attributed to the stickiness problem is dependent on the composition of the powder. The introduction of the glass transition temperature theory has helped researchers to investigate the conditions at which the powder becomes sticky enough to cause the problem.

Since there is a short residence time during spray drying, the conditions which are of interest for instantaneous stickiness are those of short contact times. The particle-gun rig is to be used in this work as it can provide information about powder sticky responses to change in temperature and water activity conditions. The stickiness curve is useful to display a critical value when the T_g is exceeded causing instantaneous stickiness of a powder due to the amorphous sugar present. Chatterjee (2003) used the rig for different dairy powders at low temperature (28°C-52°C).

This work is to be focused on developing stickiness curves for various dairy powders at higher temperature ranges (i.e. 60-80°C around the processing temperature) in order to observe if there is a trend between powder stickiness and its composition. From the stickiness curve, the conditions for instantaneous powder stickiness can be identified and related to plant operating conditions. The recommendation for an optimization of process can then be made.

CHAPTER 3

MATERALS AND METHODS

3.1 INTRODUCTION

The variety of compositions in dairy powders is thought to be an important factor in relation to particular powder stickiness curves. The materials used here are commercial products of Fonterra. There are hundreds of product specifications that the company produces; the process of selecting the samples used in this work is explained in the material section.

O'Donnell *et al.* (2002) initially developed an apparatus that can constantly supply air with controlled temperature and humidity conditions. The bubble column was suggested as the simplest way to saturate the air supply under pressure. Crofskey (2000) worked on the invention of the particle-gun and used it for investigating caking problems in cream powders. Further fine-tuning and development on the particle-gun test rig was carried out by the Fonterra Research Centre (FRC) in conjunction with Massey University. Chatterjee (2003) used the rig to generate the "stickiness curves" for different dairy based powders and high fat powders such as cream powder, that are difficult to handle by the bench-top-scale fluidised-bed rig at low temperatures (<50°C) and high (72.5%) relative humidity.

The particle-gun rig was used because it gave control over the air velocity, temperature and moisture that mimics the conditions in spray drier ducting. It is assumed that the surfaces of the particles leaving the drier are in equilibrium with the drier outlet air temperature and relative humidity. It is the critical temperature and humidity conditions at which the powder becomes sticky in a matter of seconds (instantaneous stickiness) that is of interest, as powder stickiness is a surface phenomenon. The measurement of % deposition at a particular temperature and relative humidity provides information on the instantaneous sticky point of powder. The experimental set-up and protocol are explained in the methods section.

3.2 MATERIALS

Lactose, fat and protein are the prime components in dairy based powders. Lactose and fat are responsible for the stickiness phenomena. The composition of lactose and fat were the basis for selecting samples because they are the main components causing powder stickiness. Fonterra Co-operative limited supplied the powders and their bulk composition data (Appendix A1). A 2-D lactose-fat composition plot is shown here to cover the desired range and also the samples that were available (Figure 3.1).

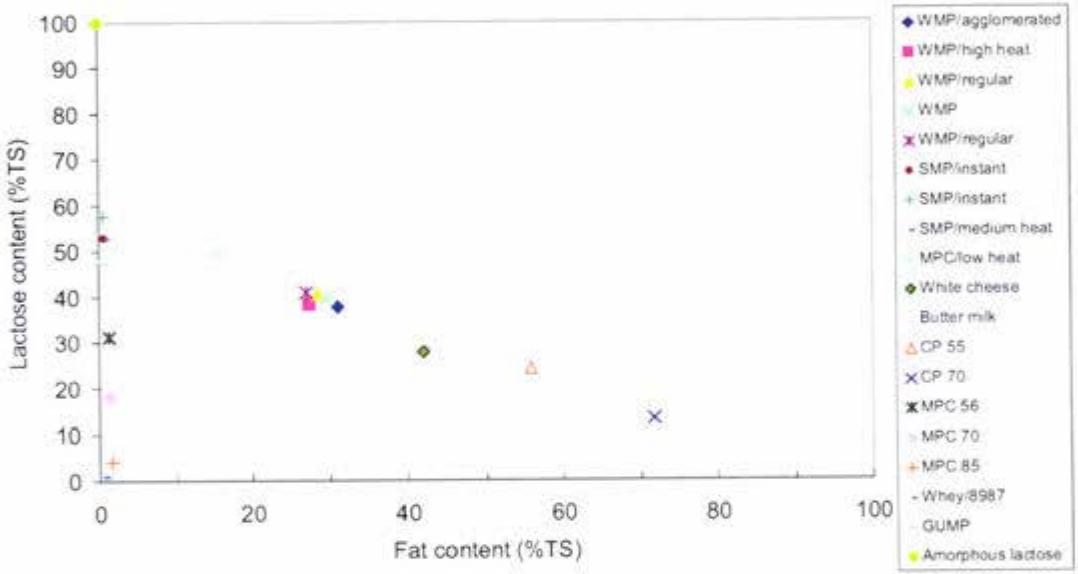

Figure 3.1 Selected dairy powder compositions (2-D Matrix) for experimental work.

The powders were selected to cover a wide range of lactose and fat composition. Cream powder, cheese powder and buttermilk powder are relatively high in fat and low in lactose content. Skim milk powders (SMP) are high in lactose and low in fat. Whole milk powders (WMP) have lactose and fat content in the middle range. Whey protein powder is high in protein and low in lactose, and milk protein concentrate (MPC) was low in both lactose and fat.

Amorphous lactose was made in the pilot plant spray drier at Massey University. The details for preparing amorphous lactose can be found in Brooks (2000) page 3.4.

3.3 METHODS

3.3.1 The Particle-Gun Rig

The particle-gun rig was used to simulate the drier conditions and to measure the point at which a powder becomes instantaneously sticky. The rig is constructed in two parts: a constant humidity air supply system and the particle feeding system that enables the particle to "fire" on the plate at the desired velocity (Figure 3.2). A constant air temperature was used to fire dairy powder particles at a collection plate. The relative humidity of the air was increased and the % deposition recorded. Four different temperatures between 60-80°C were used as they correspond to the spary drier outlet air temperature tange. The 'gun' fittings mean that the exposure time of powder particle is less than 0.05 seconds, which is a sufficient penetration time for the surface stickiness to manifest.

Figure 3.2 The particle-gun rig.

O'Donnell *et al.* (2002) built an apparatus that produces air with both controlled temperature and relative humidity, at a desired throughput by saturating the air at one pressure and then lowering the pressure through a pressure regulator. This principle was

used by Fonterra to develop an equivalent apparatus. The schematic diagram of the particle-gun rig is given in Figure 3.3.

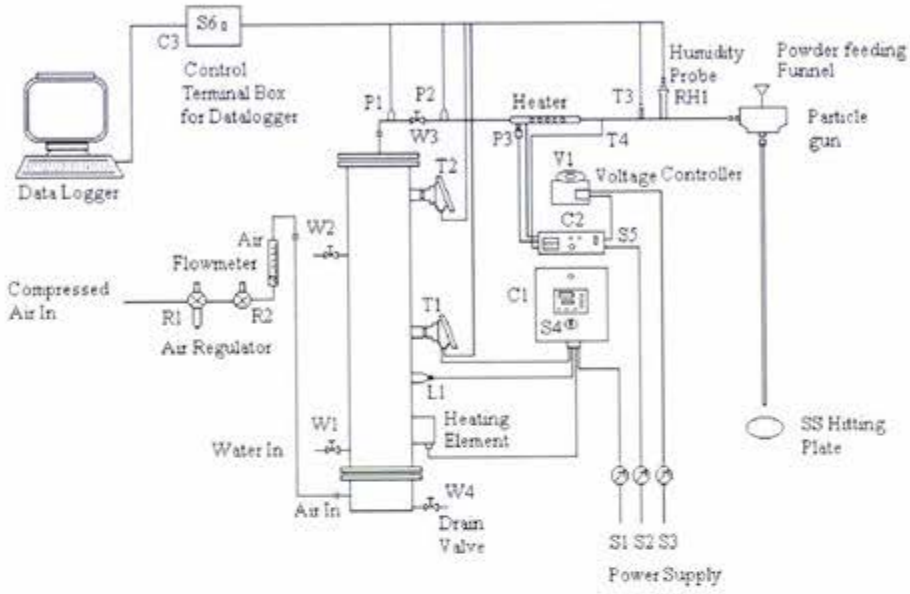

Figure 3.3 A schematic diagram of the particle-gun rig.

A constant air supply was ensured by passing compressed air through two pressure regulators. R1 eliminates any pressure fluctuation from the compressor. R2 controls the pressure for the bubble column. The air passes through an air-flow meter before entering in the column. A steel bubble column was used to saturate the air under higher pressure. The column was filled up with water and the temperature kept constant through a heating element. The air stream was bubbled through the column of water at a pressure of up to 8 bar and then passed through an expansion valve (W3) to release the pressure to a lower pressure. The relative humidity of the low pressure air stream is set by the ratio of high (P1) and low (P2) pressures. The air stream is then passed through an in-line air heater which enables a desired air outlet temperature to be achieved. This temperature change can have an effect on the relative humidity of air, hence control of the outlet condition. The relative humidity of air can also be adjusted by increasing the water temperature in the column, allowing more water vapor in the air to be carried

through the column. The reading of water temperature in the column, the pressures and humidity of air readings for the system were recorded and displayed on the computer.

Figure 3.4 This part of the particle-gun shows where powder feed from the glass funnel and firing on the stainless steel plate occur.

The velocity of the air was kept constant at 20 ms^{-1} at the particle-gun tip. Typical velocities in industrial cyclones are in the region of 20-45 ms^{-1} Masters (1991), and it was the velocity recommended by Crofskey (2000). Figure 3.4 shows the particle feed system. The constant temperature and humidity air stream entered into a vortex chamber. A venturi effect was used to create a suction through the glass funnel which fitted in a hole on the centre of the vortex chamber. The degree of suction created was dependant on the position of the glass funnel into the firing tube.

The temperature and humidity differences between the air leaving the air-heater and the air at the tip of the gun were found to be significant Chatterjee (2003). The heat loss was due to the lines and fitting for carrying the air and the mixing of the ambient air through the suction of the glass funnel. Modifications were made to the particle-gun for

this experimental work in order to minimize the heat losses. In addition, the air temperature and relative humidity were measured at the tip of the gun to define the final conditions.

3.3.1.1 Experimental Set-up

The operation procedure of the particle-gun rig was taken mainly from Chatterjee (2003) as the same procedure was used there. A detailed step-by-step description of the particle-gun start-up has been given by Chatterjee (2003).

A control terminal box recorded all the measuring devices of the process variables installed on the rig. All the data was then transmitted to the computer for display. Those variables that correspond to the display on the computer that were included are:

P_Humid: Pressure of air (P1)

P_outlet: Pressure of air after being stepped-down (P2)

T_Outlet: Temperature of air measured after being heated by air-heater (T3)

RH_Oultet: Relative humidity of the air before travel through to the vortex chamber (RH1)

RH_Calc: Calculated relative humidity value. The differential pressure between P1 and P2 is inversely proportional to the relative humidity of the outlet air.

T_Humid: Temperature of saturated air in the top of the water column (T2)

Y_Calc: Calculated amount of moisture in the air at P2

T_Water: Temperature of the water in the column (T1)

The final temperature (°C) and relative humidity (%RH) of the air was measured at the tip of the gun by a rotronic HYGRO PALM; a portable humidity and temperature measuring instrument The probe's- +/- 1 digit of the display was calibrated before use against saturated salt solutions. The system was adjusted to ensure the desired condition

was met. The temperatures and relative humidity of the air displayed on the screen was recorded at each run for reference purposes.

The temperature and humidity profile during processing was displayed on the computer screen. This enabled better control of the system, monitoring the changes in the system quickly in terms of temperature and humidity. When the system had reached a constant state, the experimental work was started.

The relative humidity of the outlet air can be increased by either increasing the water temperature (wet-bulb temperature) in the column or reducing the differential pressure between P1 and P2, (lower pressure at pressure regulator (R2)). The air-heater can also be used in the control of the relative humidity; heating-up the air would result in a decrease in relative humidity.

For these experiments the water temperature was set at 68°C, and the temperature of the air was first set by the air-heater, then the relative humidity was adjusted to carry out the experiment. It took a long time (approx. 1 hour) for the system to reach a static condition, especially for higher temperature experiments. This experiment was carried out by first fixing the temperature of the air and then increasing the relative humidity of the air for the runs. Four different temperatures between 60-80°C were used as they correspond to the process outlet air temperature range. It worked out that the experimental work achieved different RH's at one temperature per day and approximately one powder with 4 temperatures per week. It varied from powder to powder. At times there was a maximum of three powders done within a week when there was a sample available for experiments. At extreme air conditions, either high temperature and/or high relative humidity, the powder became less free-flowing through the funnel as the particles tended to stick to the funnel walls, thereby taking longer to feed the same amount of sample through. Reducing the amount of sample helped in this regard, since the deposition was calculated as a percentage.

The velocity of the air was kept constant at 20ms^{-1} at the particle-gun tip. High velocities in the particle-gun rig were used (20 ms^{-1}); this is because typical velocities in industrial cyclones are in the region of 20-45 ms^{-1} Masters (1991), and it was the velocity

recommended by Crofskey (2000). The discharge valve and pressure regulator (R2) were used to control the air velocity at $20ms^{-1}$, while adjusting the relative humidity to a desired condition. In order to have a better control over the fluctuation which may save waiting time between each run, further work could change the discharge valve to a pressure regulator.

3.3.1.2 Experimental Protocol

Once the constant air velocity, temperature and RH for a test run were reached, the conditions were recorded in a data log sheet. The protocol for carrying out the experiment is described here:

A rounded stainless steel plate of 75 mm in diameter was weighed by Sartorius BP 210S, a 5 significant figure weighing scale. This was placed directly under the particle-gun (distance below 15cm) shown in Figure 3.4. Chatterjee (2003) recommended that a net of 25 grams of powders be used for all test runs. The weight of the powder used depended on the maximum deposition that could be handled on the plate, (in some situations the powder over deposited on the plate, thus causing errors in the experiment), and the types of powders used (some powders are more inherently sticky than others, so less powder was used for stickier powders). Hence, the amount of the powder used varied from 25 grams to 5 grams and the percentage of deposition was calculated as the measure of stickiness.

%deposition (dry weight) = (Weight deposit on the plate / Total weight of feed) *100

The plate was weighed before and after the experiment, so the difference is the weight of the deposit. The beaker for containing the powder was measured before and after each experiment, so the exact total weight of the feed powder was measured. In order to limit the time the powder sample was exposed to the ambient air where it could pick-up the moisture from the air, the sample was weighed just before the feeding started. The ambient condition might have effected the powder condition at feeding; however, it was assumed that the powder particle surface gained equilibrium with the air condition supply once it was fed into the gun. The effect of ambient conditions will be investigated in future work.

The rig was set up to supply air at 20 $m.s^{-1}$ at a predetermined temperature and relative humidity. A sample of powder was fired through the gun and the % deposition recorded. The relative humidity of the air was then adjusted to a new higher value while maintaining the same dry bulb temperature at the tip and a new sample of powder was fired through the gun. This was repeated for increasing RH values.

The particle-gun rig data of % deposition versus RH as a function of temperature shows that the further the critical RH is exceeded the more sticky the powders become. Thus, the particle-gun can identify not only the critical stickiness point of a powder at a temperature, but also enables one to get a feel for how quickly the powder will become a problem when it enters the stickiness regime. This feature is unique to this technique. Further analysis on the data can be found in chapter 4 and 5.

CHAPTER 4

MEASUREMENT AND PREDICTION OF THE CRITICAL "X": STICKINESS TEMPERATURE FOR DAIRY POWDERS

4.1 INTRODUCTION

The liquid-bridging mechanism that occurs when dairy powders become sticky and stick to one another is also the reason that the powder particles become sticky in the duct lines in processing, and is caused by the glass transition temperature of amorphous lactose being exceeded and transforming the amorphous lactose into a rubbery state (Figure 4.1). The glass/rubber state change occurs at the glass transition temperature (T_g) of amorphous lactose; however, liquid-bridging forms at some point above the T_g line due to decreased viscosity of the amorphous lactose which therefore flows. The sticking of amorphous sugars was found to be a viscosity related mechanism and the rate of sticking dependent on the extent to which the T_g of powder is exceeded. Therefore, the viscosity is a function of temperature difference ($T-T_g$). "X" is denoted as the critical temperature difference above T_g of amorphous lactose, where the amorphous lactose is sufficiently liquid for the powder particles to become instantaneously sticky. T_g and consequently "X", is a function of water activity or water content of the amorphous lactose. The higher the value of "X", the more tolerant the powder is to higher RH and/or temperature condition with regard to stickiness. For example, it is expected that the "X" of WMP will be larger than the "X" of SMP, since there is less amorphous lactose present in the powder.

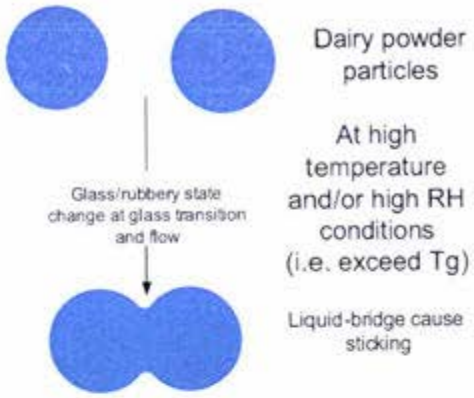

Figure 4.1 The liquid-bridging mechanism caused by T_g amorphous lactose being exceeded.

Brooks (2000), Foster (2002) and Keir (2001) have demonstrated that the rate of sticking is related to the T-T_g of the powder and it is not important what RH and temperature conditions are used to obtain that T-T_g value. They also concluded that the higher the T-T_g value, the higher the rate of stickiness. The rate of sticking has been graphed on a log scale due to the large difference in rates for low and high T-T_g values. Using the log scale, a fairly linear relationship can be seen between the log of the rate of sticking and the T-T_g of the powder. Under certain RH and temperature combinations the rate of stickiness development was so quick, that it could be regarded as instantaneous. The value of T-T_g at which this occurred is an indication of where the powder would be expected to caused problems in transport lines.

The value of T-T_g enables us to correlate the rate and degree of stickiness, as it is dependent on temperature and RH. The prediction of T_g of amorphous lactose was based on the third-order empirical equation and was calculated from the water activity or moisture content of dairy powders [Brooks (2000)].

In this chapter, lactose was the only sugar in SMP, WMP and MPC solutions; therefore, the T_g of amorphous lactose was used as the reference line, and the "X" value above the T_g of lactose was observed. If there are two or more amorphous sugars present, the T_g of multi-components can be predicted from equation 2.8 [Foster (2002)]. The measurement and prediction of "X", the minimum T-T_g value that causes instantaneous stickiness of the other specialty powders, including buttermilk, low fat/high lactose WMP and vitamin fortified milk powder (GUMP) were also observed.

The value for "X" has been shown to have a practical significance in determining the onset of stickiness in dairy powders rather than the glass transition temperature. Expressing the effects of temperature and RH as a single parameter of $T-T_g$ is the most appropriate method to represent the stickiness of dairy powders. The particle-gun rig was developed to simulate the conditions in the spray drier and the ducting pipe and cyclone. The stickiness of powder particles occurs after a relatively short residence time in spray driers. Thus, stickiness is a surface phenomenon and the point of adhesion is the instantaneous sticky point 'X'.

Instant skim milk powder was first used to demonstrate and explain the typical results obtained from the particle-gun experiment in section 4.2. All the sample powder tested followed the same analysis to obtain the critical "X" value through the $T-T_g$ plot and the stickiness curve. The samples are grouped into SMP, WMP, MPC, and specialty powders and their critical "X" values are represented in table forms (section 4.3). The critical "X" value for amorphous lactose in this work were compared with Chatterjee (2003) in section 4.4. Lastly, an equation was generated from multi-regression analysis based on the samples tested. This equation predicts the critical "X' value for total fat content less than 42% and only amorphous lactose present in dairy powders.

4.2 AN INSTANT SKIM MILK POWDER

The raw data collected from the particle-gun rig was % deposition at a particular temperature and relative humidity condition for the air at the tip of the gun. Figure 4.2 shows a typical set of results for skim milk powder when the air temperature was kept constant and the relative humidity of the air was gradually increased. The data typically show very little deposition as the RH was increased at a particular temperature, until a critical relative humidity value was reached. At this point, namely the instantaneous sticky point, the deposition starts and increases with increased values of relative humidity. This information was then used to plot the stickiness points for the powder on a temperature versus RH graph, namely the stickiness curve (Figure 4.3).

Any condition below the T_g+X line was identified to be a non-sticky safe process region and any condition above the T_g+X line was identified to be a sticky region. This

can be used as the chart in the plant and the operators can use it to adjust process parameters in order to control the stickiness level. The stickiness in dairy powders is due to the amorphous sugars present, with the composition being used to predict the T_g curve based on the water activity and the temperature of the powder surface. The temperature difference above T_g is important for controlling stickiness behavior of a particular powder.

As mentioned earlier, the raw data was first collected as % deposition of powder on the plate at a constant temperature and increasing relative humidity. For a particular temperature, zero % deposition occurs up to a certain critical relative humidity. At this instantaneous sticky point, a sudden increase in % deposition occurs which increases as RH is increased further. These deposition data points are plotted and fitted with a straight line and the intercept is identified to be the critical relative humidity or water activity for the instantaneous stickiness point. The % deposition vs RH (%) plot (Figure 4.2) shows that a powders' instantaneous stickiness condition occurs at reduced RH% for increasing temperatures. Therefore, the powder adhesion phenomenon is a function of temperature and humidity.

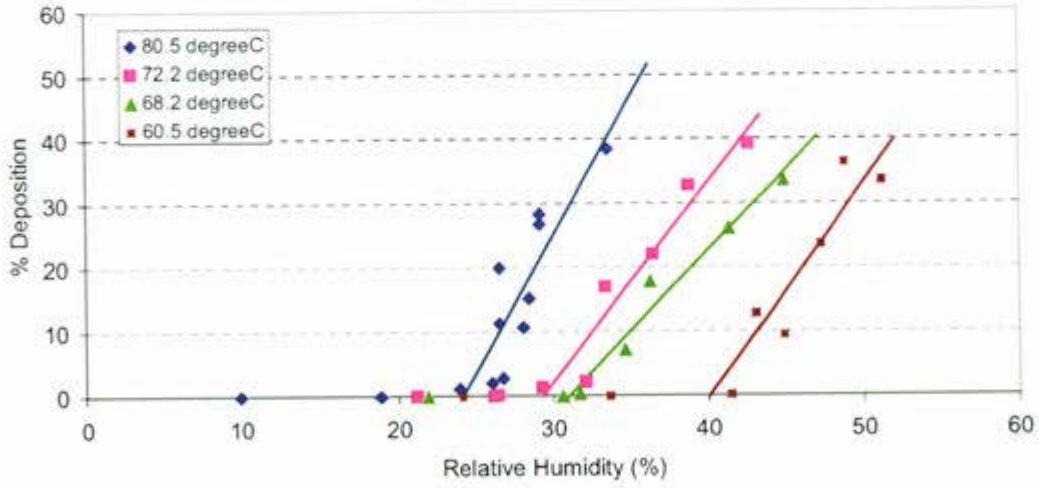

Figure 4.2 The % deposition of dry instant skim milk powder plotted against relative humidity at constant temperatures.

The stickiness curve (Figure 4.3) shows that the T_g+X approach works. In this plot, the intercept RH value from raw data (Figure 4.2) at various temperatures is used to plot the instantaneous stickiness point for the SMP. A T_g+X line was fitted to the data using a least square of errors technique. The resulting critical 'X' value was 37.3°C. The critical values of 'X' obtained from Figure 4.3 and Figure 4.4 are virtually the same, considering the experimental error.

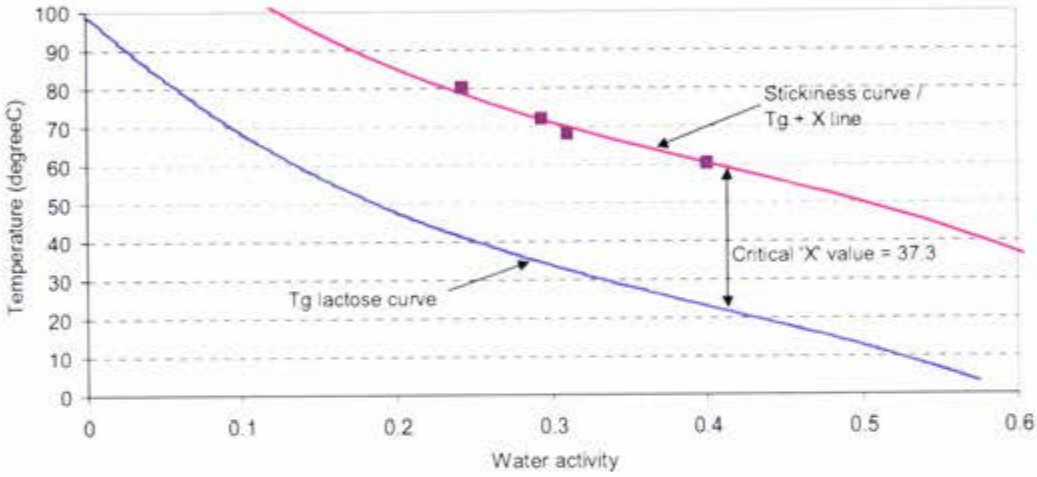

Figure 4.3 The stickiness curve of the instant SMP from four experimental points fitted the curve above T_g of amorphous lactose.

The T_g of amorphous lactose was predicted from water activity or relative humidity based on the fitted empirical cubic equation [Brooks (2000)]. Figure 4.4 plots % deposition against (T-T_g) and this has collapsed the data from different temperatures onto one line showing that there is one common T_g+X value at which instantaneous stickiness for the powder occurs. The data were fitted by a regression line and the intercept found and this was taken as the critical temperature "X" above T_g of amorphous lactose.

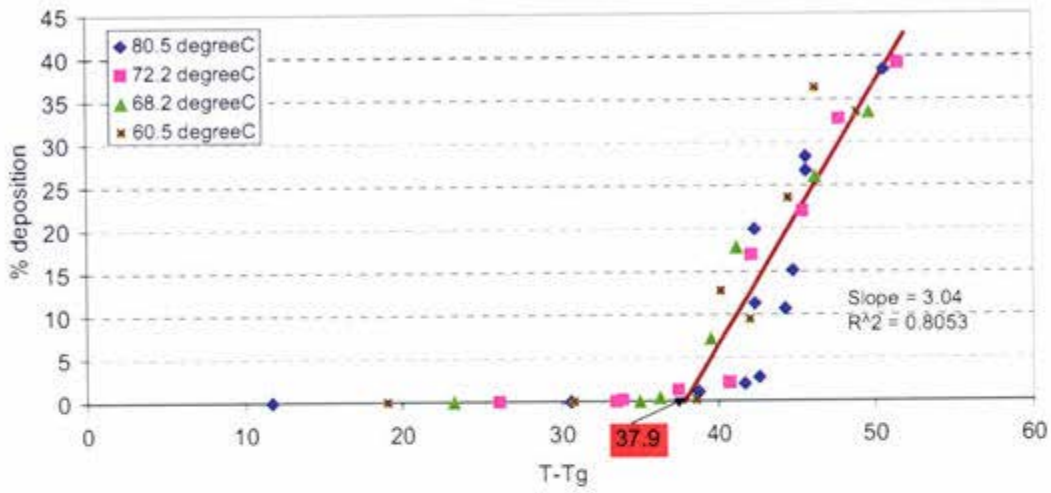

Figure 4.4 % deposition plotted against T-T_g for four different temperature data sets.

T-T_g is the temperature change of the powder above its T_g. At a certain T-T_g, the powder deposit on the plate dramatically shoots up. This critical point of change in % deposition indicates the instantaneous sticky point, and was found by extending the trend line to zero % deposition. The critical T-T_g value, also known as the critical 'X' value for the SMP, was found to be 37.9°C and slope 3.04 by this method.

The % deposition is a function of T-T_g, where all the data collapsed into a common intercept which is defined as the critical point "X". One of the advantages of using T-T_g plot is the distinctive stickiness point effect of amorphous lactose is highlighted, and slope of the trend line indicates how fast the powder became sticky. The "X" value can be used to construct the stickiness curve parallel to the T_g amorphous sugar curve.

Figure 4.4 can also be used to identify the temperature above T_g where a given %deposition occurs, based on the slope of the trend line. The slope of the trend line is a measure of powder sensitivity with respect to temperature and RH changes above the critical sticking curve. The larger the slope, the more sensitive the powder is, meaning a small change in temperature and/or RH above the Tg+X line results in large impacts on

the stickiness of powder deposition on the plate. This is demonstrated in Figure 4.5. Different powders will have different critical 'X' values and slopes.

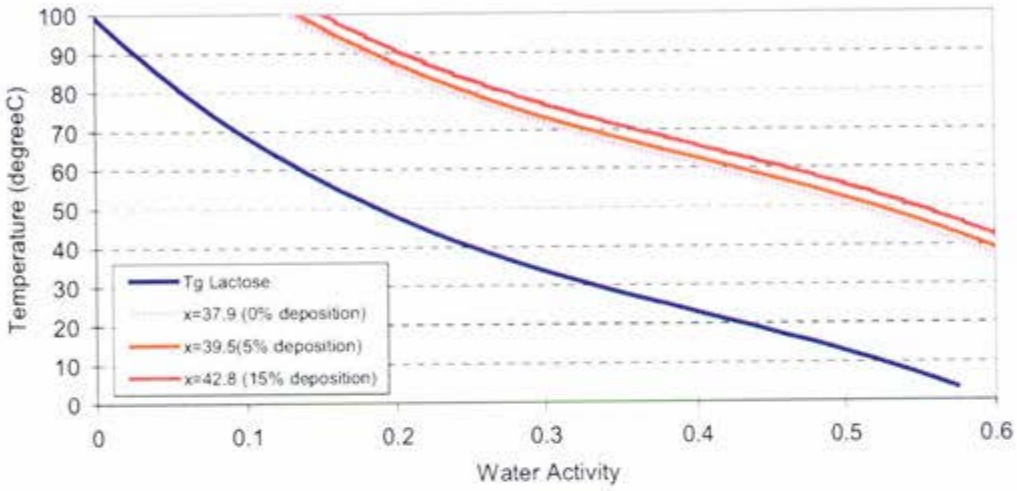

Figure 4.5 The slope of the trend line ($T-T_g$ plot) show how fast is the powder response to temperature and relative humidity change exceed the stickiness curve line.

Due to the time constraints (it took about a week to generate a stickiness curve for four temperatures) doing replicates for every powder was unrealistic. However, a replicate of the same batch of instant SMP sample was done on a different date. The purpose of this exercise was to test the repeatability of the experiment.

The $T-T_g$ and stickiness curves of the two sets of experimental data are shown in Figure 4.6 and 4.7.

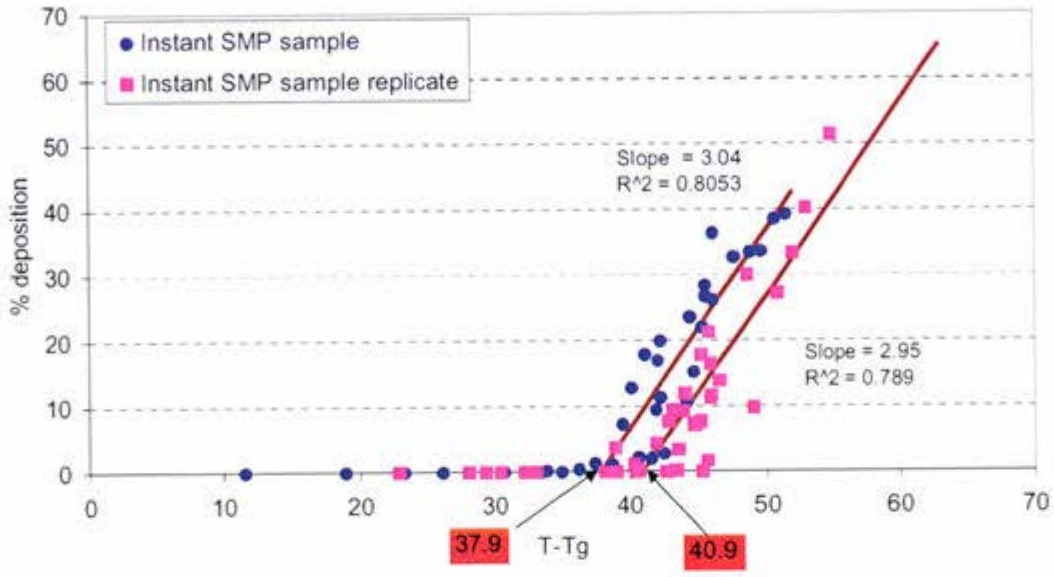

Figure 4.6 **% deposition plotted against T-T_g for four different temperature data sets of replicates.**

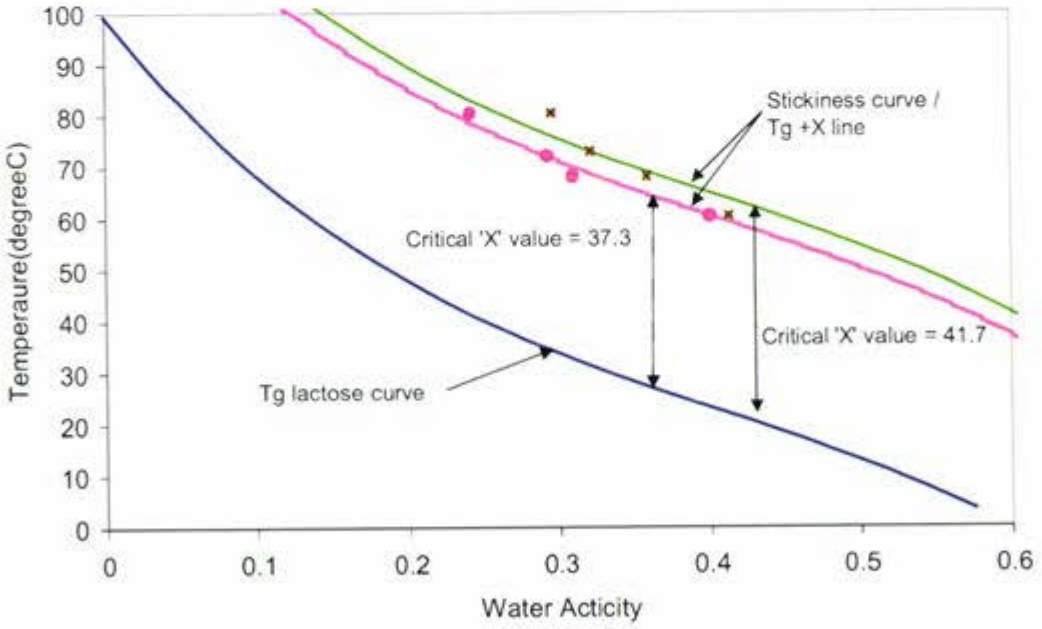

Figure 4.7 **The stickiness curve of the instant SMP in comparison with the replicate.**

The percentage error for the two sets of data were calculated as below:

(1) The critical 'X' value from T-T_g plot: 39.4±3.0 °C (7.6%)

Sample: 37.86°C, Slope = 3

Replicate: 40.93°C, Slope = 3

(2) The critical 'X' value from fitted stickiness curve: 39.5±4.4 °C (11.1)%

Sample: 37.3°C

Replicate: 41.7°C

The critical 'X' value obtained from the (T-T_g) plot method has a less error than the fitted stickiness curve method. This is because the effects of RH and temperature are combined by using the T_g parameter and all data points are used to estimate the "X". Whereas the fitted stickiness curve method contains the error from finding the point at a particular RH at each fixed temperature. The "X" values from the two methods are within their error bounds and hence are not significantly different.

The replicate has a practically higher critical "X" value by both methods. The replicate used the same sample three months later. The difference maybe due to some of the amorphous lactose crystallising during the three months' storage. Reports show the glass transition of amorphous lactose is depressed to 24°C at a critical water activity of 0.37 [Roos and Karel (1991b) , Jouppila and Roos (1994a), Bandyopadhyay *et al.* (1987)]. The water activity (Aw) of both samples was measured and the replicate had a higher Aw (0.398 @23.5°C) which is on the edge of the lactose crystallisation condition. When lactose crystalises, it tries to array itself and therefore decreases in free volume. It will release water as free water, hence increasing the water activity. Because it contains crystalised lactose, it also reduces the stickiness by having less amorphous lactose to contribute to the instantaneous sticky point. The other possible explanation of this difference is just due to experimental error.

4.3 CRITICAL 'X' VALUE OF POWDERS

4.3.1 Skim Milk Powders (SMP)

Three different specifications of SMP plus one replicate were tested and the critical "X" values determined from T-T_g plots and the fitted stickiness curves (Table 4.1). The critical "X" value varied from 37.3°C to 42°C. The slopes varied from powder to powder, with instant powder 2 having a distinctively lower slope than the other skim milk powders tested, making it a lot less sticky than other skim milk powders at equivalent conditions above their critical "X" values. The reason for this is unknown. The composition data showed relatively small differences compared to the other skim milk powders tested. It might have differed in particle size or density or other physical properties that were not identified, or it could be an outlier. The data analysis for individual SMPs in Table 4.1 can be found in Appendix A2.

Table 4.1 A summary table of critical "X" value of SMP tested.

Skim Milk Powders	Fat (%TS)	Lactose (%TS)	Protein (%TS)	Critical "X" $_{(T-Tg)}$ (°C)	Slope (T-T_g)	Critical 'X' $_{(fitted\ stickiness\ curve)}$ (°C)
Instant SMP 1	0.62	57.84	34.27	37.9	3.04	37.3
Instant SMP 1 (replicate)	0.62	57.84	34.27	40.9	2.95	41.7
Instant 2	0.79	52.98	38.19	39.7	0.34	38.1
Medium Heat SMP*	0.83	53.01	38.05	40.2	3.33	40.3
	0.80	57.56	34.63	N/A	N/A	41.2

*Chatterjee (2003) particle-gun rig experimental result (temperature below 50°C)

4.3.2 Whole Milk Powders (WMP)

Five WMP samples were tested and the critical 'X' values found are shown in Table 4.2. The critical 'X' value was in a range of 33.7°C to 40.2°C and slope varied from 0.4 to 1.2. The slope characterized individual powders. It plays a big role in

determining how fast the powder will stick in response to different conditions. The data analysis for individual WMPs in Table 4.2 can be found in Appendix A2.

Table 4.2 A summary of critical "X" value of WMP tested.

Whole Milk Powders	Fat (%TS)	Lactose (%TS)	Protein (%TS)	Critical "X"$_{(T-Tg)}$ (°C)	Slope (T-Tg)	Critical "X"$_{(fitted\ stickiness\ curve)}$ (°C)
Agglomerated	31.09	37.82	25.91	38.0	0.78	37.5
High heat	27.38	38.33	27.07	33.7	0.42	34.0
Regular 1	28.44	40.68	24.9	37.1	1.21	35.5
Instant	29.75	39.77	24.69	38.2	0.36	40.2
Regular 2	26.94	40.93	25.91	40.0	1.07	39.4
WMP*	27.96	42.48	24.65	N/A	N/A	48.6

* Chatterjee (2003) particle-gun rig experimental result (temperature below 50°C).

Comparing the critical "X" values from SMP and WMP powders shows them to be overlapping with each other, despite their different fat contents and lactose contents. The lactose content was higher in SMP and relatively lower in WMP. Looking at the average value from WMP (37.4±2.9°C) and SMP (39.4±1.7°C), the error bands overlap with each other (95% confidence interval). These average values are from the T-T_g plot. Despite the difference in types of powders, particle size, compositions, spray drier, atomizing system and process setup conditions, SMP and WMP are essentially sticky at similar points. However, they are different in degrees of response to the changes in temperature and RH conditions. In general, the slope of SMP is much higher than WMP; at any particular condition that exceeds the stickiness curve, WMP deposits are lighter than SMP. This could be due to the lower lactose content of WMP compared to SMP which means that, despite the two types of powders having similar X factors, the SMP will build deposits faster than WMP under similar conditions and hence can be regarded as a "sticker" powder.

4.3.3 Milk Protein Concentrate (MPC) and Whey Protein Powder

The lactose content in MPC was much lower than SMP and WMP. The higher the concentration of lactose, the lower the critical "X" was found to be. Table 4.3 shows that the lower the lactose concentration, the less sensitive the powder is to air conditions because of the lower slope value. The larger "X" values indicate that a powder is more tolerant for high temperature and/or relative humidity conditions. When whey protein was fired through the gun, there was only a smear of powder deposited on the plate. However, the 1% lactose effect on powder stickiness was still evident in whey protein powder, with a critical "X" value of 50.5°C. The data analysis for individual MPC and whey protein powder from Table 4.3 can be found in Appendix A2.

Table 4.3 A summary of critical "X" value of MPC and the whey protein powders tested.

MPC and Whey protein Powders	Fat (%TS)	Lactose (%TS)	Protein (%TS)	Critical "X"$_{(T-Tg)}$ (°C)	Slope ($T-T_g$)	Critical "X"$_{(fitted\ stickiness\ curve)}$ (°C)
MPC 44	0.83	47.56	43.52	42.7	2.64	44.5
MPC 56	1.35	31.29	59.36	47.5	0.34	47.7
MPC 70	1.46	18.16	72.86	50.0	0.08	49.7
MPC 85	1.67	4.17	88.54	49.1	0.04	51.1
Whey protein	0.52	1.05	96.34	50.1	0.04	50.5

4.3.4 Specialty Powders

There are some specialty powders produced by Fonterra. These include white cheese, buttermilk, and powders containing added vitamins. The critical 'X' values for the powders tested were identified as follows Table 4.4. The data analysis for individual speciality powder from Table 4.4 can be found in Appendix A2.

Table 4.4 A summary of critical "X" value of cheese, buttermilk and GUMP powders tested.

Speciality Dairy Powders	Fat (%TS)	Lactose (%TS)	Protein (%TS)	Critical "X"$_{(T-Tg)}$ (°C)	Slope $(T-T_g)$	Critical "X"$_{(fitted\ stickiness\ curve)}$ (°C)
White cheese	42.05	27.90	21.23	28.4	2.3	28.5
White cheese*	42.05	27.90	21.23	N/A	N/A	19.4
Snack Cheese*	30.89	33.88	18.92	N/A	N/A	24.7
Buttermilk	9.33	51.3	31.92	39.3	1.3	36.9
GUMP	15.46	49.48	27.84	40.7	0.3	40.7

* Chatterjee (2003) particle-gun rig experimental result (temperature below 50°C).

Included in table 4.4 is data from Chatterjee (2003), for white cheese powder and snack cheese powder. This data was collected at a low temperature (50°C), with RH (60%) conditions. There is approximately 9°C difference in these results compared to Chatterjee (2003)'s. The reason for this difference is unknown at present, and indicates more work is needed.

4.4 AMORPHOUS LACTOSE

Amorphous lactose was made on a lab scale spray drier using the method outlined by Brooks (2000). Brooks (2000) used the blow test method to determine the critical temperature of the instantaneous stickiness point above its glass transition temperature to be 25°C. Chatterjee (2003) used the particle-gun rig at low temperatures (below 48°C) and high RH (60%) and fitted a curve to find the critical stickiness point to be 26.1°C. Amorphous lactose was tested in this work using the particle-gun rig at high temperatures with a range of process conditions (80°C) and found the instantaneous stickiness point X to be 24.2°C. When the two sets of data from the particle-gun were combined (Figure 4.8), the stickiness curve data were best fitted with an "X" value of 24.7°C.

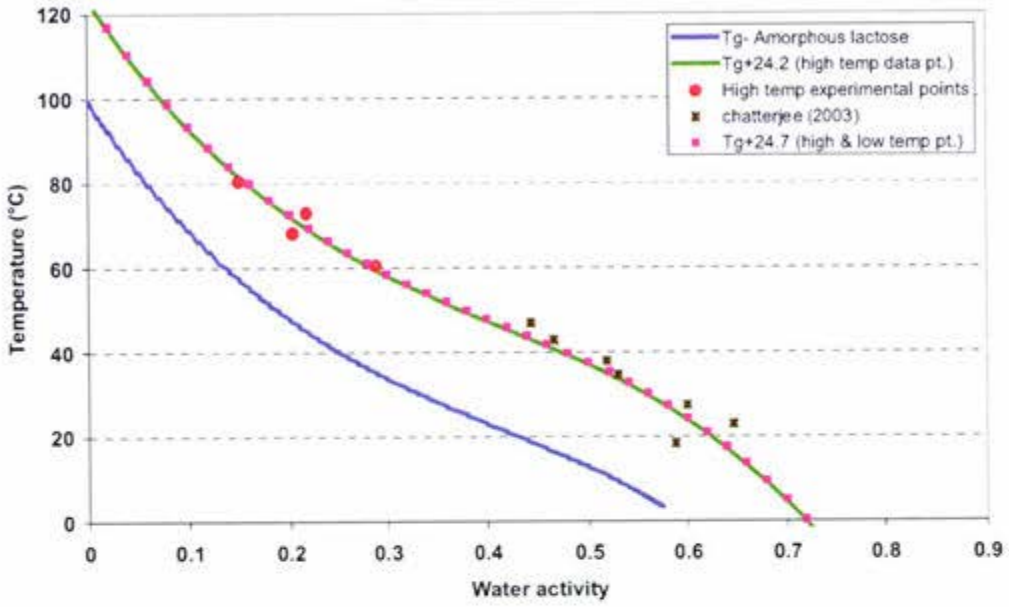

Figure 4.8 The stickiness curve of amorphous lactose with reference line T_g, including Chatterjee (2003)'s result.

The result shows that the instantaneous stickiness of amorphous lactose is around 25°C. Both the blow test and particle-gun test are in agreement. It was confirmed that the amorphous lactose instantaneous sticky point is in a range of 24 to 26°C where it will adhere to materials and where instantaneous cohesion between the particles occurs.

4.5 PREDICTION OF THE CRITICAL "X"

The original idea for generating the stickiness curves for a range of powders was to be able to predict the critical 'X' value of a powder from its known composition. The only correlation found between the critical "X" value of the powders and their composition was between the % lactose content and critical "X" and between the slope of the %deposition line/ $T-T_g$ plot and the % lactose content. This is shown in Figure 4.9 and 4.10. The correlation was found to be stronger when the lactose composition was expressed as % solid not fat (SNF). (R = 0.85 compare 0.68). The white cheese was excluded because its fat content was more than 42% and it was obviously an outlier.

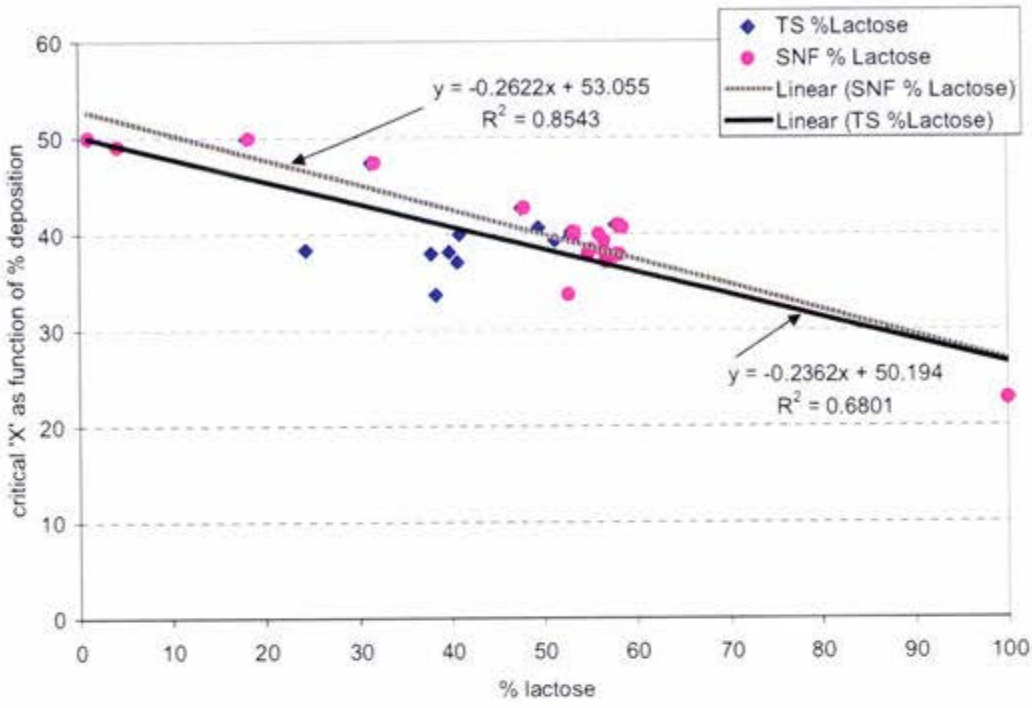

Figure 4.9 The correlation between the critical "X" value and % lactose of powder (total fat content less than 42%) tested.

A multiple regression analysis was used to fit the independent variable critical 'X' value. It was established from a set of dependent variables. %TS fat and %TS lactose was used, mainly because the two components relate to the stickiness mechanisms. Although %TS protein and %TS lactose can also be used, the resulting critical 'X' was calculated to be similar. The regression equation worked out to be as follows:

$$\text{Critical 'X'} = 53.91 + (-0.20337) * \%\text{TS Fat} + (-0.2648) * \%\text{TS lactose} \quad (\text{fat} \leq 42\%\text{TS}) \quad (4.1)$$

For any dairy powder that has fat less or equal to 42%, the critical 'X' value can be predicted from equation 4.1 with ± 10°C. Although, this 10°C error margin is large, the plot demonstrates an overall trend between the critical 'X' value and the % amorphous lactose in bulk. Since, the instantaneous stickiness of the powder has been shown to be a surface phenomenon the surface composition of a powder in relations to the critical 'X' is worth further work.

Figure 4.10 shows the slopes of the %deposition T-T_g plots versus %TS lactose in the powder. The data is scattered and for similar % lactose powders, there are a large range of slopes among the powders tested. Despite the scatter, and leaving out the 100% amorphous lactose data point, it can be seen that most powders with over 30% lactose become much more sticky quickly than powders with less than 30% amorphous lactose. A regression of the data points in the 30-60% lactose range gives 32% with a R^2 value of 0.5. It should also be noted that some powders in the range did not become as sticky as might have been expected from their %lactose content. The reasons for the non-sticky behaviours of these powders need further investigation.

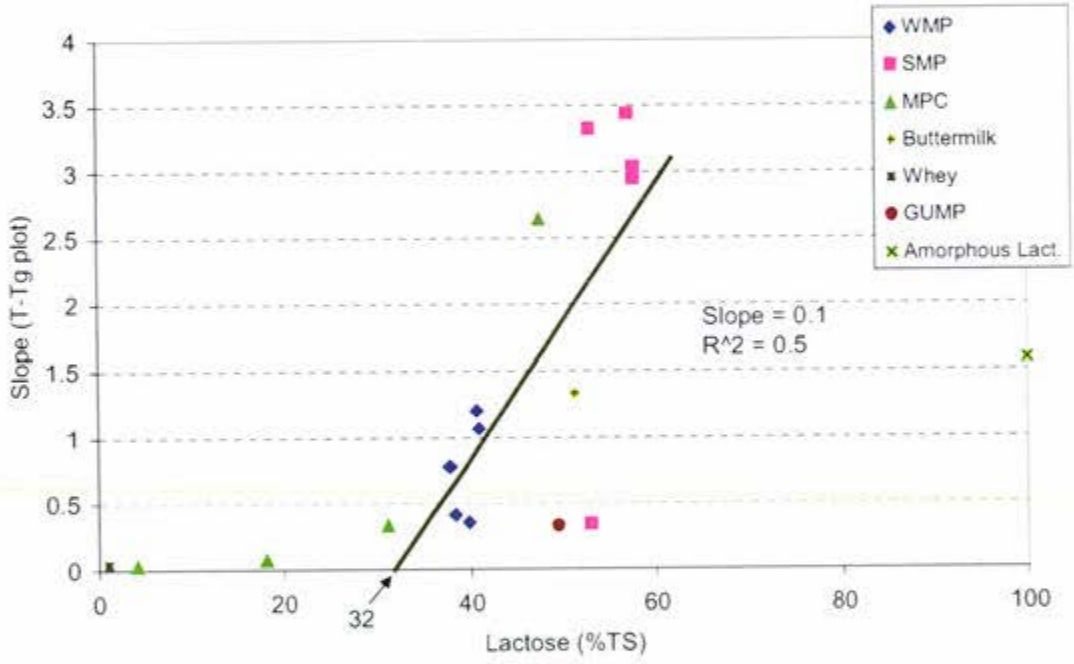

Figure 4.10 The interaction of slope as function of (T-T_g) and % lactose in bulk.

4.6 COMPARISON OF STICKINESS CURVE USING CRITICAL 'X' APPROACH

The stickiness points obtained from other researchers using different methods were fitted to a line 'X' above the T_g of amorphous lactose. The stickiness curves of similar powders, but using the different techniques, is compared.

Figure 4.11 shows sticky points of amorphous lactose measured by particle-gun rig are very close to the stickiness curve of whey powder measured by the cyclone stickiness test. The stickiness curve of SMP (57.84 lact. %TS) is also plotted. Therefore, the stickiness curve of a whey powder from the particle-gun rig can be predicted to be somewhere between the stickiness curve of amorphous lactose and the SMP, which would obtain a higher critical "X" value than the cyclone stickiness test. The difference in the critical "X" observe between the cyclone stickiness test and particle-gun rig is probably due to the different airflows and particle trajectories and the residence times between the two methods resulting in different sticky end points. Both of the stickiness curve lines are in the rubbery state of amorphous lactose. Powder particles travel in the humidified air for 1-2 minutes in the cyclone sticky test compared to a travelling time of 0.05 seconds in the particle-gun rig. A longer travelling time allows moistures to diffuse from the surface layer to the inner layer and therefore, more flow and more contact points for the particles to adhere to the walls or cohese to each other. Particle-gun rig measures the particle stickiness at the surface only and only allows enough time for the surface of the particle to equilibrate with the surrounding conditions. The powder particle in the cyclone sticky test gets stickier earlier than in the particle-gun at the same air conditions.

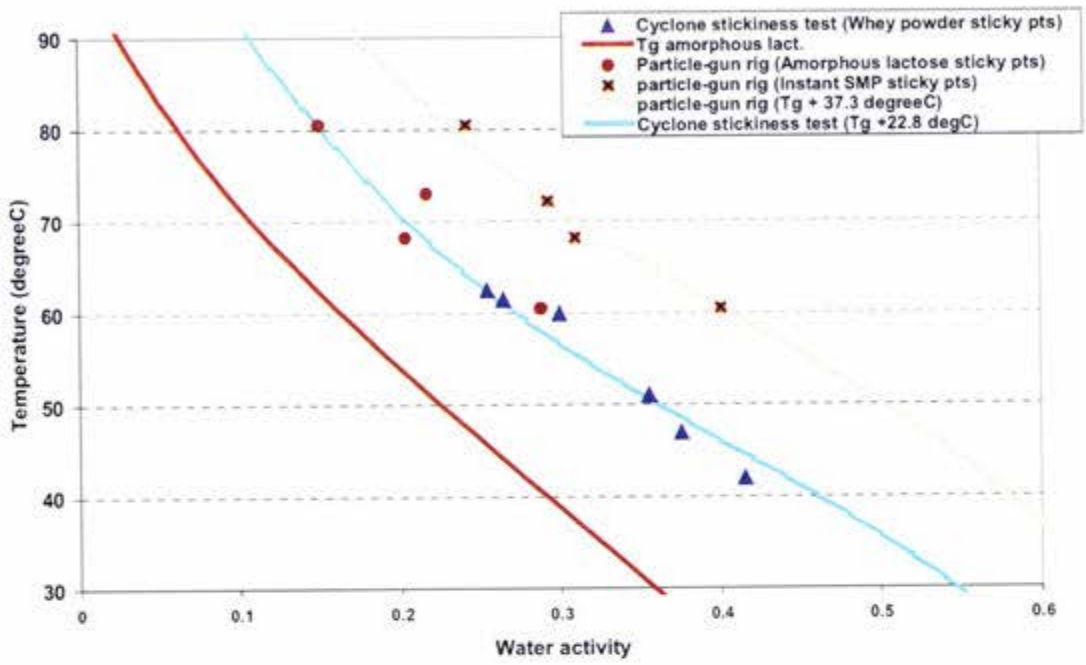

Figure 4.11 Stickiness curve of whey powder measured using cyclone stickiness test (Boonyai *et al.* (2004)) and amorphous lactose and instant SMP measured by particle-gun rig.

Figure 4.12 uses the T_g of amorphous lactose as the reference line and shows the best fit curve line critical X factor through the skim milk powder sticky end point data obtained from various different techniques. The stirrer test results in a lower critical 'X' value of 17.5°C and the fluidised-bed rig had the value of 21°C and particle-gun rig had the largest critical 'X' value of 41.3°C. The increase in the critical 'X' measured indicates that the stickiness of powder is a function of the particle velocity. In the stirrer test, the powder particles are in an almost stationary state and cohesion stickiness is measured. Although particles tested in the fluidised-bed were moving when the stickiness end-point was measured, the velocity at which the particles were moving were relatively slow compared to the particle-gun rig. These differences in sticky point critical X measurement are due entirely to the differences in the technique used, and indicate that the level of stickiness is a function of the dynamics of the particle as well as the air conditions. Real blockage data from actual plants will be needed to establish which of the techniques is most appropriate for relating this data into usable curves for industry.

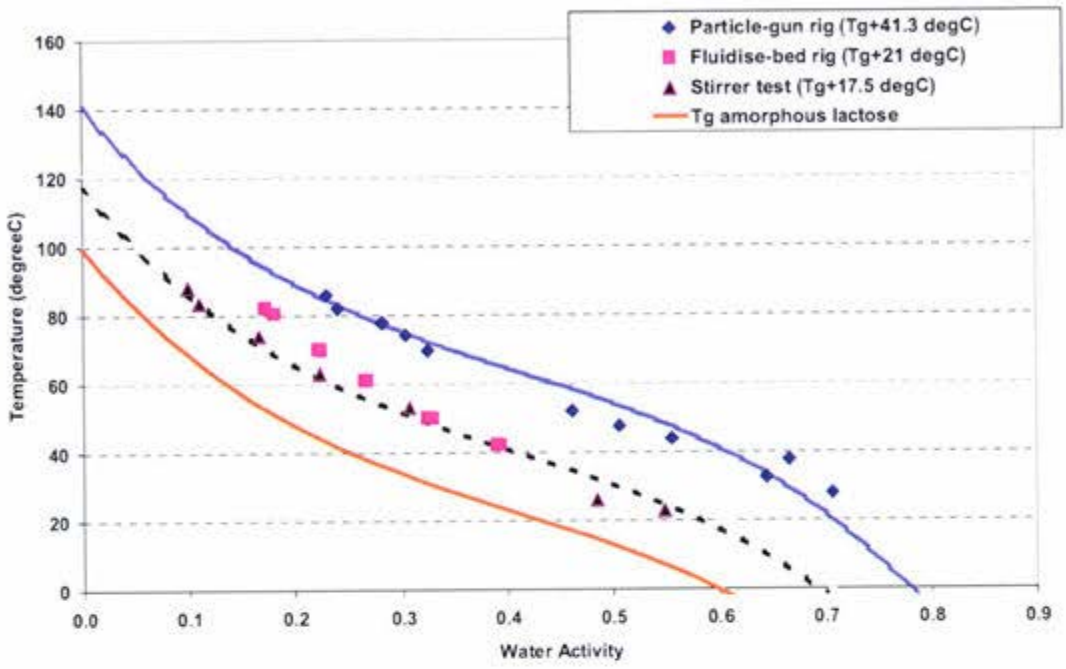

Figure 4.12 Stickiness curve of SMP measured by particle-gun rig (Chatterjee (2003)), fluidised-bed rig (Chatterjee (2003)), and stirrer test (Hennigs *et al.* (2001)).

4.7 CLOSURE

This work has established the process of obtaining the instantaneous stickiness point for various dairy powders using a particle-gun rig. The critical "X" values for WMP, SMP and MPC have been found to vary between 34°C and 51°C. A plot of %deposition versus $T\text{-}T_{g(lactose)}$ successfully combined the temperature and relative humidity factors. This indicates that it is the properties of amorphous lactose causing sticking in dairy powders. The critical 'X' value is the temperature that exceeds the T_g of amorphous lactose when instantaneous stickiness occurs. In addition, the particle-gun rig demonstrated that powders with greater than 30% amorphous lactose are more likely to cause blockages than powder with less than 30%. Both the critical 'X' value and the slope are unique to the powder. The stickiness curve or T_g+X line is useful for mapping plant operating conditions on a chart form and the slope enables a decision to be made about how close to the critical point a plant should be run for a particular powder.

For powders that have a total fat content less than 42%, the stickiness is mainly due to amorphous lactose when T_g is exceeded by the critical "X" value of the powder. A

regression equation (equation 4.1) was generated, based on the critical 'X' value obtained from the experimental data of various dairy powders, to correlate the effects of composition on X. Although an overall trend is observed, further study is required to investigate the surface composition in relationship with the critical 'X'.

Comparison of the particle-gun rig X factor with the X factor measured by other techniques shows that the factor is a function of the technique used with higher kinetic energy particles giving high X factors for similar powders. More work is required to relate this work to industrial experience.

CHAPTER 5

STICKINESS DUE TO FAT

5.1 INTRODUCTION

Foster (2002) showed that sticking and caking problems due to the fat-melting mechanism is only significant when the total fat content is higher than or equal to 42%, resulting in a high level of surface fat. There was a linear relationship between the total fat content and the surface fat content expressed in terms of the specific surface area.

White cheese powder and high/low fat cream powders were tested and are classified in the high fat content powder category. The fat effect of these powders is discussed in this chapter. During the process, these powders were exposed to high temperatures and all the surface fat was molten, causing smearing on the wall and cohesion with each other.

5.2 WHITE CHEESE POWDER (42.05 %TS fat)

A similar stickiness pattern to other dairy powders was observed at a particular temperature with changing humidity (Figure 5.1). The stickiness point at an increased temperature occurred at a decreased relative humidity. There was a small amount of 1% initial deposition. Because the % deposition scale on Figure 5.1 is large, the trend is not so obvious. A constant deposition at temperatures above 60°C shows at high temperatures all the surface fat was molten, causing a constant adhesion rate. However, there was still a temperature and humidity effect on the % deposition.

Chatterjee (2003) used the particle-gun rig for white cheese powder at the low temperature range, below 50°C. He found that at increased temperature conditions, the initial deposition increased with the same pattern. Fat-melting was affected by the temperature changing. A linear relationship between % deposition and temperature was found for white cheese powder at temperatures below 50°C.

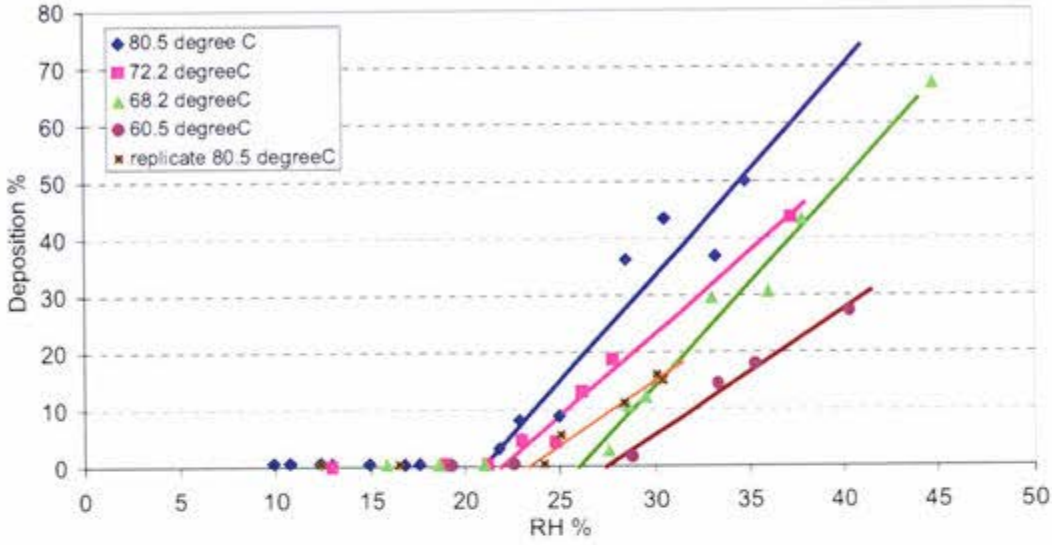

Figure 5.1 Deposition of the spray dried white cheese powder (42.05 %TS fat) tested on the particle-gun rig.

Since the stickiness is effected by both temperature and humidity of the air condition, the T-T_g parameter was used to combine those two factors as shown in Figure 5.2. The data for different air temperatures, although more scattered than the low fat dairy powders, still congregate around a single line with a common initial stickiness point. The initial stickiness point for the white cheese powder was observed at an "X" of 28.35°C. This shows the increasing stickiness is due to an amorphous lactose mechanism starting at this point. A constant deposition (ranging 0.5–0.8 %deposition) before the critical T-T_g point indicates the surface fat was molten at high temperature and was the cause of initial adhesion.

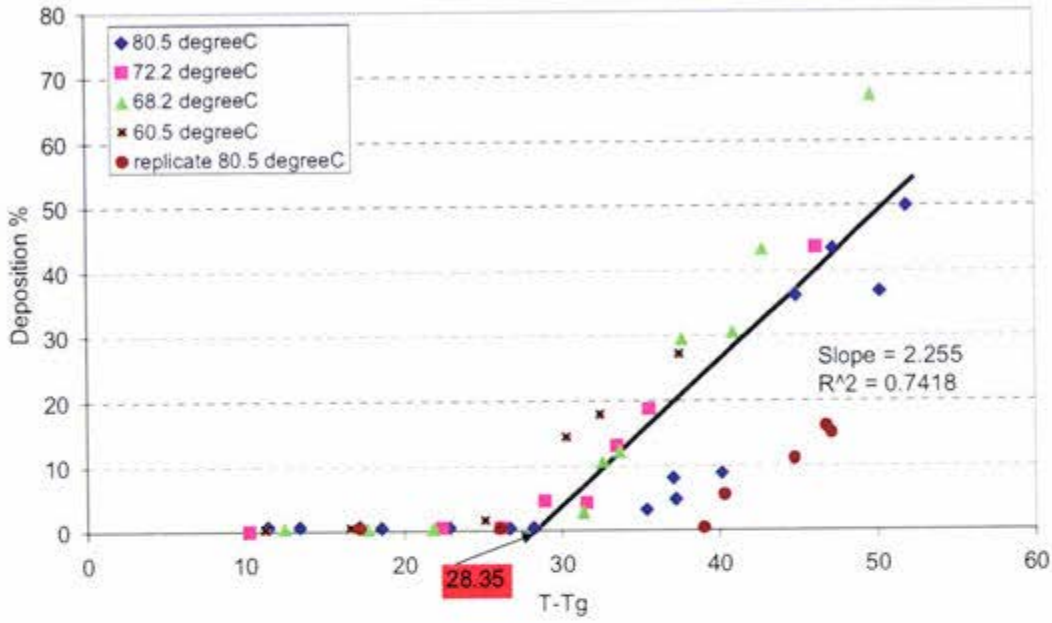

Figure 5.2 The cheese powder (42.05 %TS fat) stickiness points at temperatures above T_g of amorphous lactose.

The RH of the air at the individual stickiness points at a particular temperature were identified from Figure 5.1 and then they were used to fit a curve above the T_g of lactose calculated from both the Gordon-and-Taylor equation and the cubic equation. 'X' was found to be 22.6°C and 28.5°C respectively (Figure 5.3). The data points from Chatterjee (2003) are also plotted. The curve from the Gordon-and-Taylor equation fits both the high and low temperature data sets. In most cases the cubic equation gave a better fit. The reason it did not in this case is unknown. Despite the difference between the two T_g +X curves, for typical process conditions the likely region lies within the marked "box" on Figure 5.3. The two curves almost superimpose on top of each other in this region; therefore, either curve can be used as the stickiness curve.

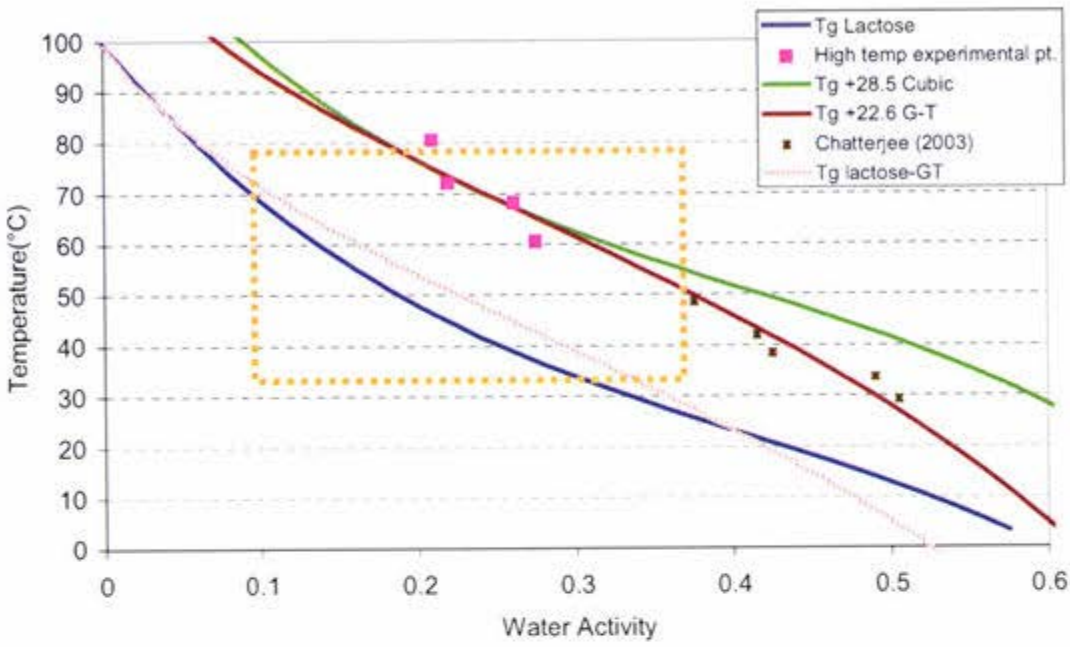

Figure 5.3 The stickiness curve for cheese powder (42.05 %TS fat) including the fitted T_g +X line from the Gordon-and-Taylor equation and fitted T_g+X line from cubic equation.

5.3 LOW FAT CREAM POWDER (55.84 %TS fat)

Again, the % deposition of dry powder versus RH% (Figure 5.4) shows adhesion phenomena are dependent on temperature and relative humidity of the air. At constant temperature and by increasing the humidity, a point is reached where there is a dramatic increase in % deposition, indicating instantaneous stickiness. For each temperature, a similar trend line is observed and the intercept of the trend line was identified to be the start of instantaneous stickiness at that particular temperature and RH condition. Increasing the temperature reduced the RH at which this point occurs. Since the powder is classified as one of the high fat powders, it is expected that an initial deposition will be seen. This is shown in Figure 5.5 when the % deposition scale has been expanded.

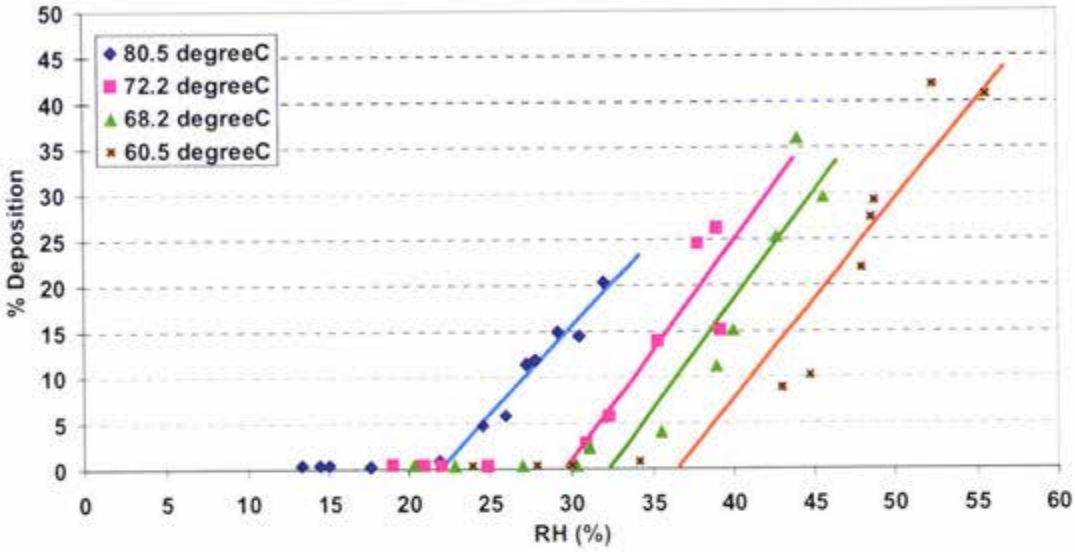

Figure 5.4 Deposition of the spray dried low fat cream powder (55.84 %TS fat) tested on the particle-gun rig.

Figure 5.5 illustrates the fat effect on initial deposition. Clearly an initial 0.5% deposition within the temperature range between 60-80°C has occurred. In the temperature range, all the fat on the surface will be molten, and therefore, a constant deposition was observed. In contrast with low fat powders, such as WMP or SMP, the initial deposition was virtually zero. In those cases, amorphous lactose was the only mechanism responsible for the powder stickiness.

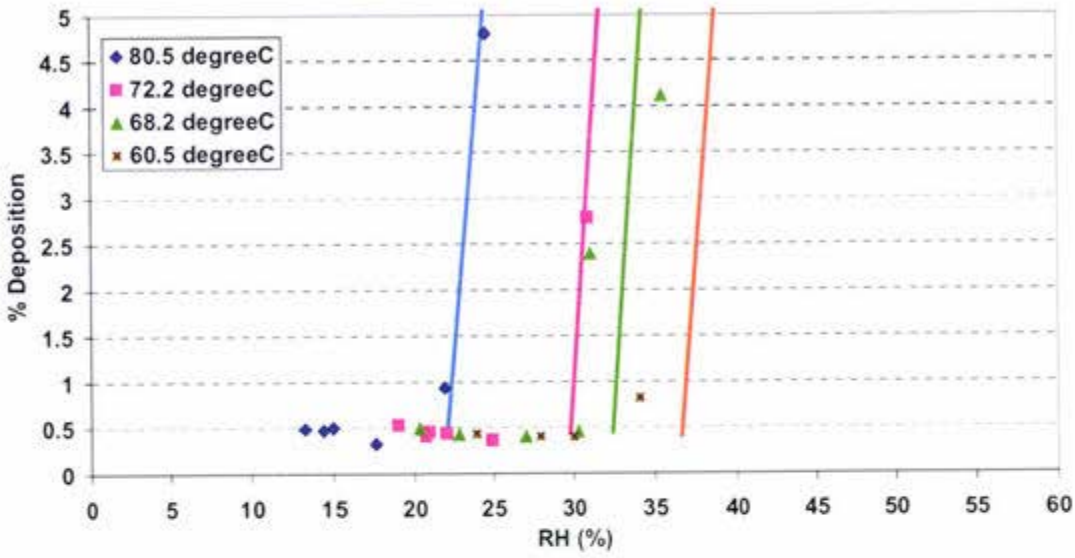

Figure 5.5 Close-up of the deposition of the low fat cream powder (55.84 %TS fat) tested on the particle-gun rig.

With low fat cream powder, both fat-melting and amorphous lactose mechanisms contribute to the powder stickiness. The lactose mechanisms can be distinctively seen in Figure 5.6, with the different temperature data being reduced to one line when plotted against $T-T_g$. The critical $T-T_g$ was identified to be 36.9°C, where powder particles start to stick on the plate over and above the initial deposition. This critical "X" value of 36.9°C was achieved by various combinations of temperature and relative humidity conditions. Comparing this critical 'X' value, the white cheese powder (28.35°C) is much lower than the low fat cream powder. This is due to the higher lactose composition in white cheese powder than cream powder (27.9 %TS versus 24.37%TS). On the other hand, more initial deposition was expected in the cream powder because of its higher fat content. There was no significant increase within experimental error in deposition caused by the increased fat content. This might be due to the fact that at these higher temperatures all the fat is molten, and for both powders there is already sufficient fat to have an effect.

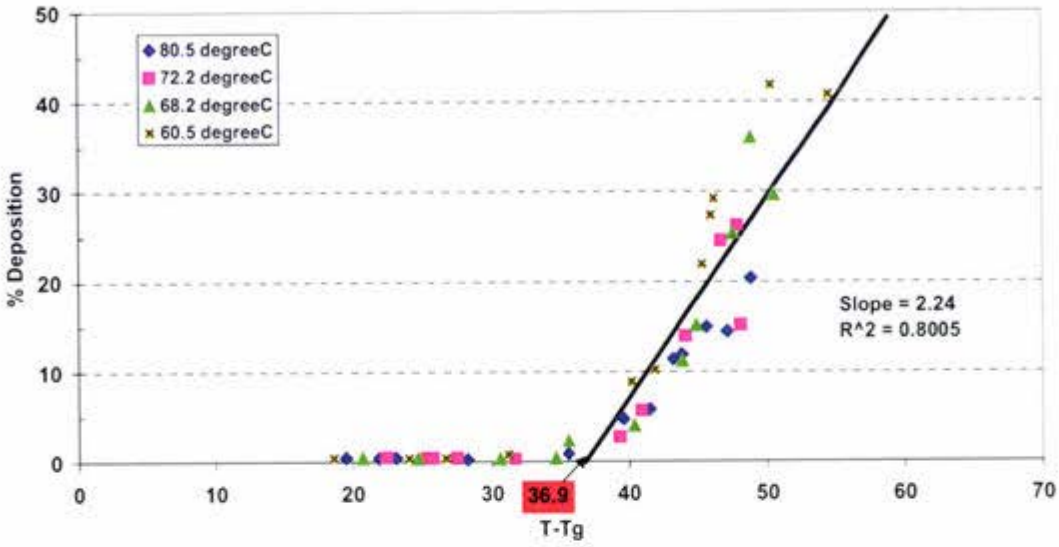

Figure 5.6 The low fat cream powder (55.84 %TS fat) stickiness points at temperatures above T_g of amorphous lactose.

Figure 5.7 shows the stickiness curve of T_g + 35.9°C was the best fit from the cubic equation of T_g for amorphous lactose. This value corresponds to the point where there is additional % deposition over the fat-melting mechanism when the powder was exposed to high process temperatures. The fat mechanism is only dependent on the temperature, not the relative humidity. The critical "X" values obtained from Figure 5.6 and 5.7 are statistically the same.

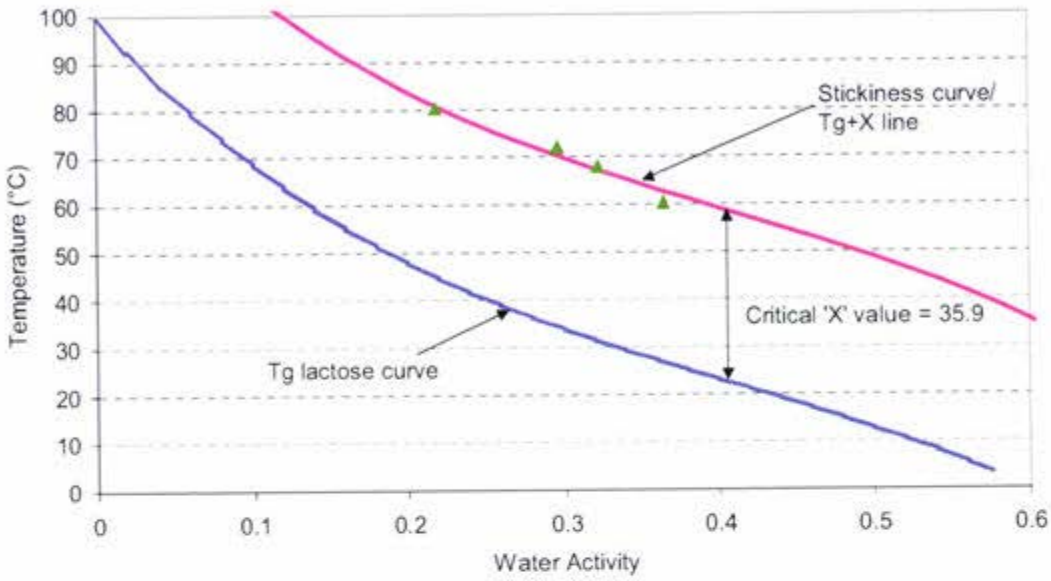

Figure 5.7 The stickiness curve for low fat cheese powder (55.84 %TS fat) including the T_g+X line.

5.4 HIGH FAT CREAM POWDER (71.79 %TS fat)

The high fat cream powder contained 71.79% TS fat and is used for manufacturing ice cream, bakery products and powdered drinks, soups, and dip. A constant initial adhesion due to fat-melting was expected in the high temperature range. This was because fat is completely molten at 40°C. However, the trend is slightly different from that seen for low fat cream powder (CP55). Figure 5.8 shows 10% deposition of powder at 60°C and 5% particle deposition above 68°C. The difference is clearly due to different fat content in the powder and exposure temperatures. The fat effect on the % deposition is further studied in the following section.

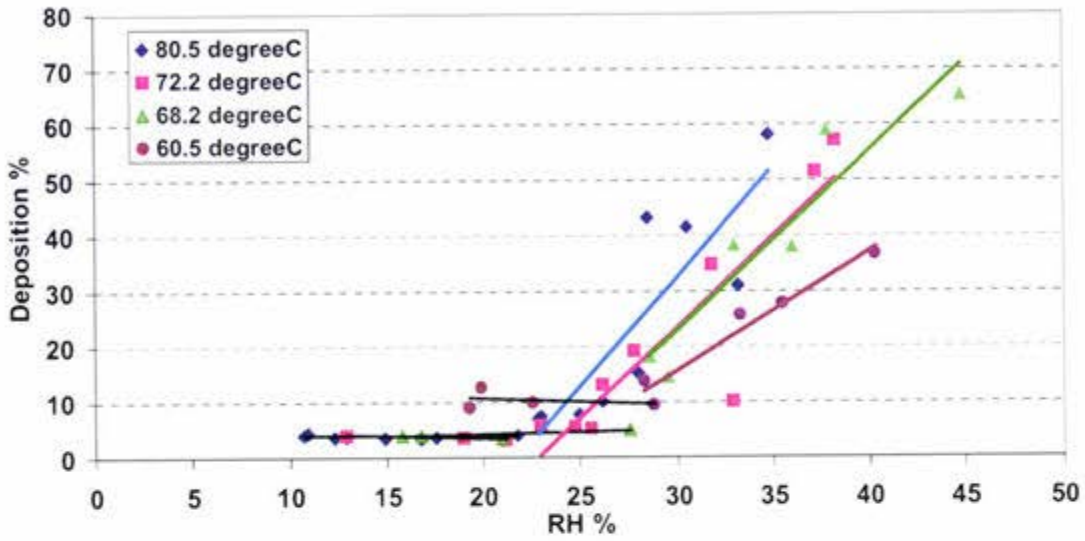

Figure 5.8 Deposition of the spray dried high fat cream powder (71.79 %TS fat) tested on the particle-gun rig.

The amorphous lactose effect is also obvious in Figure 5.8. A T-T_g plot (Figure 5.9) was used to combine the temperature and RH effects on powder deposits. The data points are quite spread and a range of critical T-T_g values (25-35°C) can be determined. Although the amorphous lactose effect is observed, there was major deposition due to the molten fat mechanism.

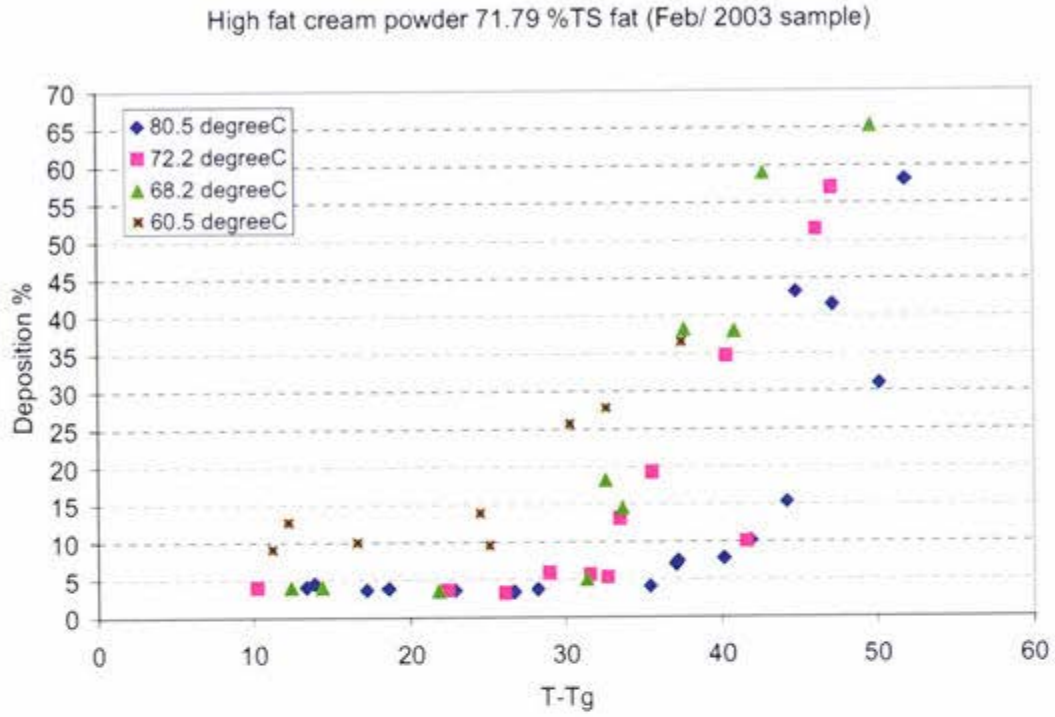

Figure 5.9 The stickiness of high fat cream powder (71.79 %TS fat) caused by molten fat and amorphous lactose.

5.5 STICKINESS DUE TO FAT-MELTING MECHANISM

The molten fat effect of high fat powder as an initial % deposition is observed in Figures 5.5 and 5.8. It is dependent on temperature only. Therefore, the following experiment was carried out to observe the % deposition as a function of temperature, while keeping the RH low to ensure there was no lactose effect. Low/ high fat cream powders were used to demonstrate the molten fat effect.

For low fat cream powder (CP 55), increasing the temperature from 30°C to 78°C caused more powder particles to stick to the plate. The relationship is linear as shown in Figure 5.10. Possible explanations are: As temperature is increased, the fat on the surface becomes less viscous and more flow can occur. The increased temperature also decreases the surface tension of the fat, which enables more fat to flow out of the capillaries in the powder particles, increasing the amount of surface fat. These effects combine to increase the % deposition that occurs as temperature is increased.

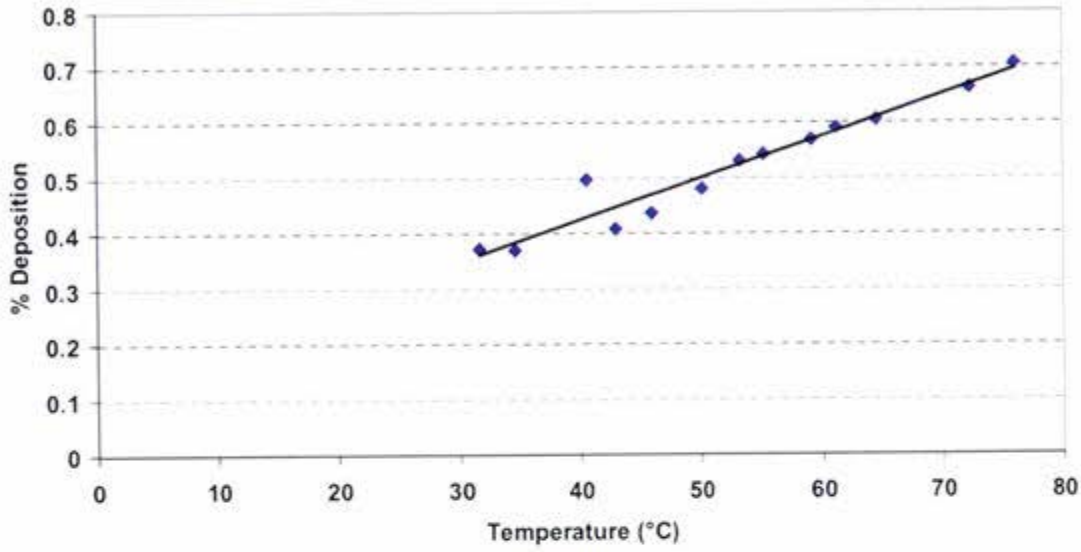

Figure 5.10 Deposition due to fat in low fat cream powder tested on the particle-gun rig with increasing air temperature and keeping RH low to avoid the amorphous lactose mechanism.

The % deposition due to fat for high fat cream powder (HFCP) is different from low fat cream powder (LFCP). Overall, at the same temperature, HFCP has a higher % deposition than LFCP. For example, at 30°C, approximately 0.35% of LFCP stuck to the plate, compared with 5% of HFCP deposited on the plate. This is because high % fat in bulk leads to a higher surface fat content [Buma (1971a),Foster (2002), Fäldt *et al.* (1993)].

The other difference is that the shape of the HFCP stickiness due to the fat curve as a function of temperature (Figure 5.11) is very different from LFCP (Figure 5.10). The high temperature range (above 60°C) data points, collected for the 2003 sample, are the intercepts of the horizontal lines from Figure 5.8. Data points at temperatures below 50°C are from Chatterjee (2003) using the same method for identifying the initial % deposition.

Due to the shortage of the 2003 sample, the stickiness caused by molten fat for the whole temperature range could not be carried out. However, a 2001 sample was found in the lab and used to do the experiment. The 2001 sample gave much higher % deposition

than the 2003 sample at the same temperature, but they have a similar shaped curve. The curve from the 2001 sample was shifted upwards. A linear relationship between % deposition and temperature over the range 28°C-45°C was observed. This increase in % deposition may be explained by an increase in temperature, causing more surface fat to melt. When the temperature exceeded 45°C, a decrease in % deposition was observed. A possible explanation is that since the majority of the particles were made of fat, as temperature increases with all the molten fat, the structure of the particle collapsed and became liquid and less viscous. When it hit the plate, it splashed and some of the particle splashed outside the stainless steel plate, causing less deposition to be recorded. The higher the temperature, the less viscous the particle became and when it contacted with the plate, it broke into smaller droplets of liquid particles.

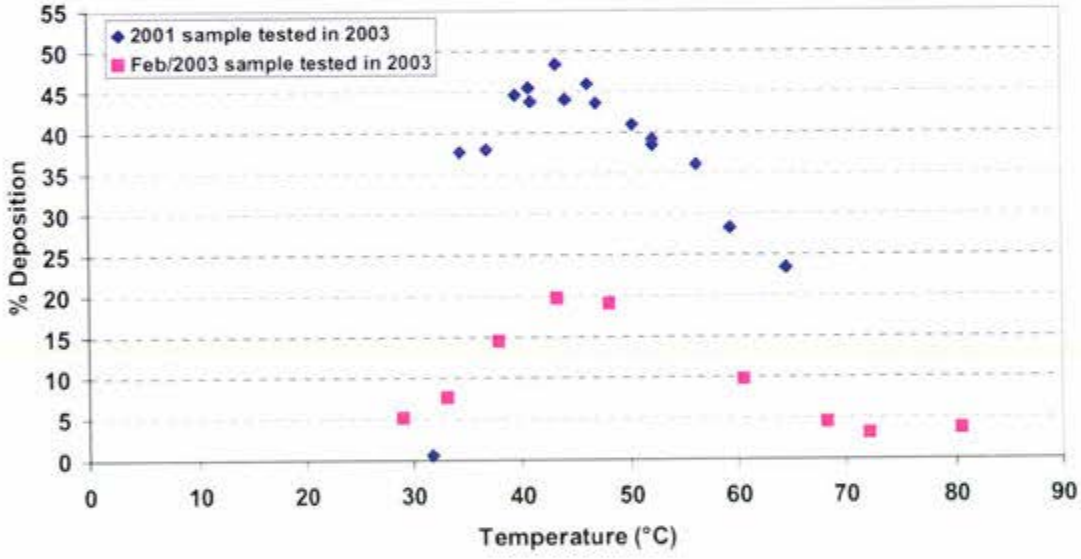

Figure 5.11 Deposition due to fat in high fat cream powder (2001 sample and 2003 sample) tested on the particle-gun rig.

The distinctive upward shift of the curve in the 2001 sample is shown in Figure 5.11. The best explanation of the 2001 sample having higher deposition than the 2003 sample lies in its age. The water activity and temperature of the 2001 and 2003 samples were measured before experiments took place (0.42 at 24.0°C and 0.39 at 22.5°C respectively). The water activity meter is Decagon, model CX1 and has been upgraded to CX2. The report shows the glass transition of amorphous lactose is depressed to 24°C at

a critical water activity of 0.37 [Roos and Karel (1991b), Jouppila and Roos (1994a), Bandyopadhyay *et al.* (1987)]. The result shows that amorphous lactose in the particle, crystalised during storage, which causes more fat to be present on the surface as the lactose crystals push the fat outwards [Fäldt and Bergenstahl (1996a), Fäldt and Bergenstahl (1996b)]. A quick test was used to check the powder for lactose crystals by observing the powder under a microscope through polarizing filters. Crystalline lactose re-rotates the plane of polarized light, allowing it to be observed under two opposing polarizing lenses. Amorphous lactose does not re-rotate the light and thus darkness is observed. Figure 5.12 shows there were lactose crystals in the 2001 CP 70 samples. They were not observed for the 2003 sample.

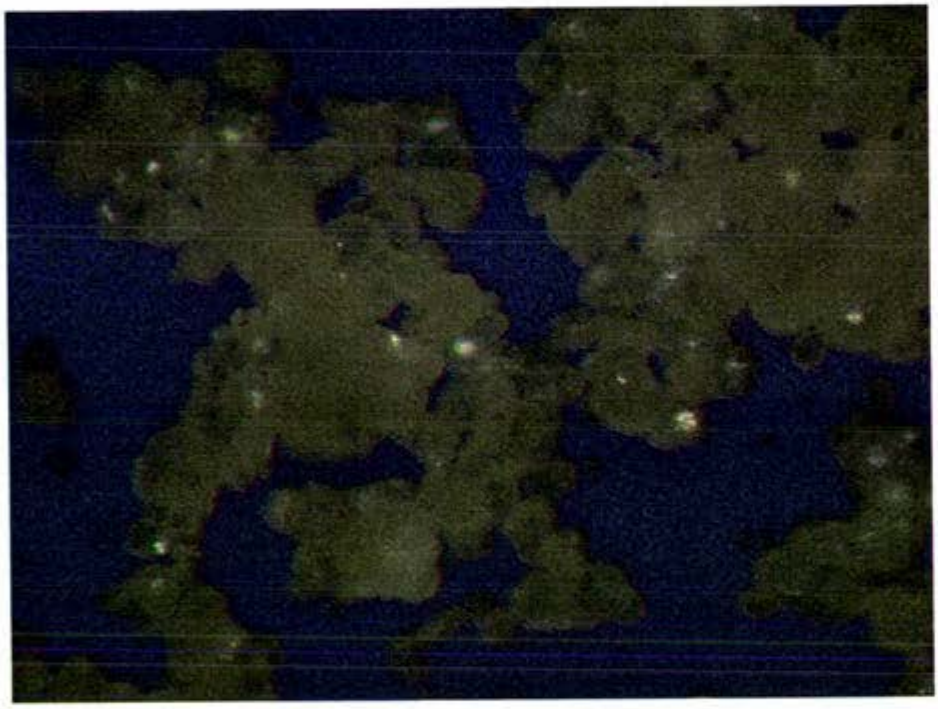

Figure 5.12 2001 high fat cream powder sample was checked for crystalline lactose under a polarising microscope at 50X magnification.

5.6 CLOSURE

This work has mainly focused on the stickiness of high fat dairy powders. Molten fat has a significant effect, causing smear and stickiness problems during processing. However, the amorphous lactose effect is still present, especially for white cheese and low fat cream powders in T-T_g plots. A linear relationship between the % deposition and temperature indicates all surface fat was molten and more fat pooled from adjacent capillary fat as temperature increases. Extreme high fat in CP70 showed a slightly different trend in % deposition as a function of temperature. This was possibly due to the decreased fat viscosity, causing the powder to become much less viscous and flow to a point that when it hit the plate, it splashed and the breakup droplets did not land on the plate. Over long storage time, amorphous lactose crystalised and pushed encapsulated fat to the surface, giving higher deposition for the 2001 sample compared to the 2003 sample.

CHAPTER 6

IMPLEMENTATION OF STICKINESS CURVE IN A PLANT - PRELIMINARY WORK

6.1 INTRODUCTION

The ultimate use of a stickiness curve is to be used in the plant environment. The stickiness curve profile has temperature versus water activity / relative humidity and is used as a reference line to map process temperature and relative humidity outlet conditions. It is generated by fitting a best line through the experimental stickiness points (particular temperature and relative humidity) at a temperature "X" above T_g for the amorphous sugar present (usually lactose in dairy powder). This critical "X" value can be estimated using the composition of the powder from the regression equation obtained in Chapter 4.

Up to this point, instantaneous stickiness has proven to be a surface phenomenon with the surrounding air condition in equilibrium with the powder surface. Hence, the spray drier outlet temperature and relative humidity are vital information as they represent the powder surface temperature and water activity. Therefore, they are essential to control stickiness on particle surfaces and adhesion of particles to clusters.

Using the skim milk powder (lactose 57.19%TS, fat 0.52%TS) as a case study, the estimated critical "X" value was compared with actual experimental data. It was produced from Fonterra, Specialty Powder Unit (SPU), Longburn. By talking to the operators with respect to the operation procedure for controlling the process. There are two common operator parameters used. These are air inlet temperature and liquid production rate that affect the outlet temperature and relative humidity.

Once the plant condition has been mapped on the stickiness curve, it enables the determination of whether the powders are sticky or not and what action can be taken to prevent blockages in the drier and/or cyclone, due to a sticky layer deposition on the walls, and what action can be taken to maximize the drier capacity if it's under processed. An Excel spreadsheet was compiled to solve the mass and energy balance around the

spray drier and was used to observe the effect on $T-T_g$ of changes to inlet air temperature and product flow rate. These can then be mapped on the stickiness curve. Recommendations on what parameters to change allow optimization of the process, for either increased throughput or lower energy costs.

6.2 CASE STUDY

This exercise was undertaken to demonstrate the process of implementing this research into practical use. The procedures were divided into three sections:

6.2.1 Determination of critical "X"

Instantaneous stickiness is a surface phenomena, therefore, the surface of the particle leaves the drier in equilibrium with the drier outlet air temperature and relative humidity, and these conditions determine whether a particle becomes sticky or not.

Temperature and relative humidity parameters are therefore used to construct the stickiness curve profile. Sticking is caused by the amorphous lactose being exposed to conditions that exceed the T_g of lactose, hence reducing the viscosity to a point that forms liquid bridging with the wall or other particles. The critical "X" temperature above T_g lactose is the point at which powder becomes instantaneously sticky and is determined either from experiment or by the regression equation given in Chapter 4 (for any powder that has total fat less than 42%). This can be useful when developing a new product with the critical "X" being estimated from its composition. In this case, SMP contains 0.52 %TS fat, 57.19 %TS lactose and the critical "X" and was calculated to be 38.7°C for the particle-gun conditions.

The other possible way to estimate this critical "X" value is to measure it experimentally on the particle-gun rig. The same procedures were employed in which the % deposition of powder on the plate was measured at a constant temperature and increasing RH of the air condition. The percentage deposition of dry powder was plotted against the $T-T_g$ parameter, which was used to combine the temperature and RH effects. The $T-T_g$ axis intercept of the trend line (38.0°C) is identified to be the critical "X" value for instantaneous stickiness to occur, shown in Figure 6.1.

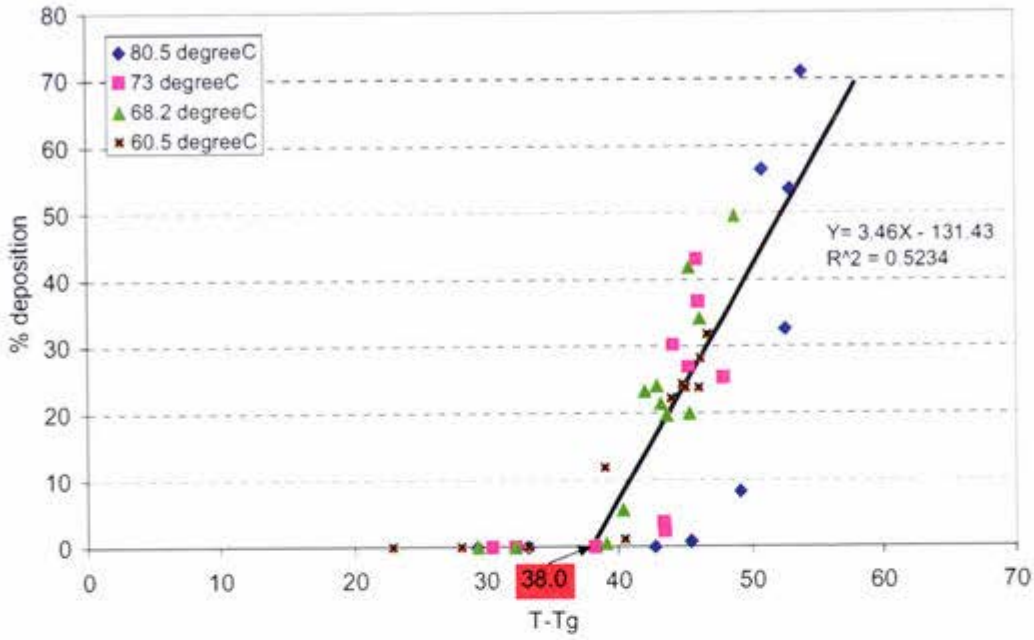

Figure 6.1 The T-T_g plot of the SMP and the critical 'X', determined to be 38°C.

Four stickiness points at particular temperatures were collected from the % deposition versus relative humidity plots. A best-fit stickiness curve of those four stickiness points resulted in "X" temperature difference above the T_g lactose line. The critical "X" found in this way was 40.7 °C as shown in Figure 6.2.

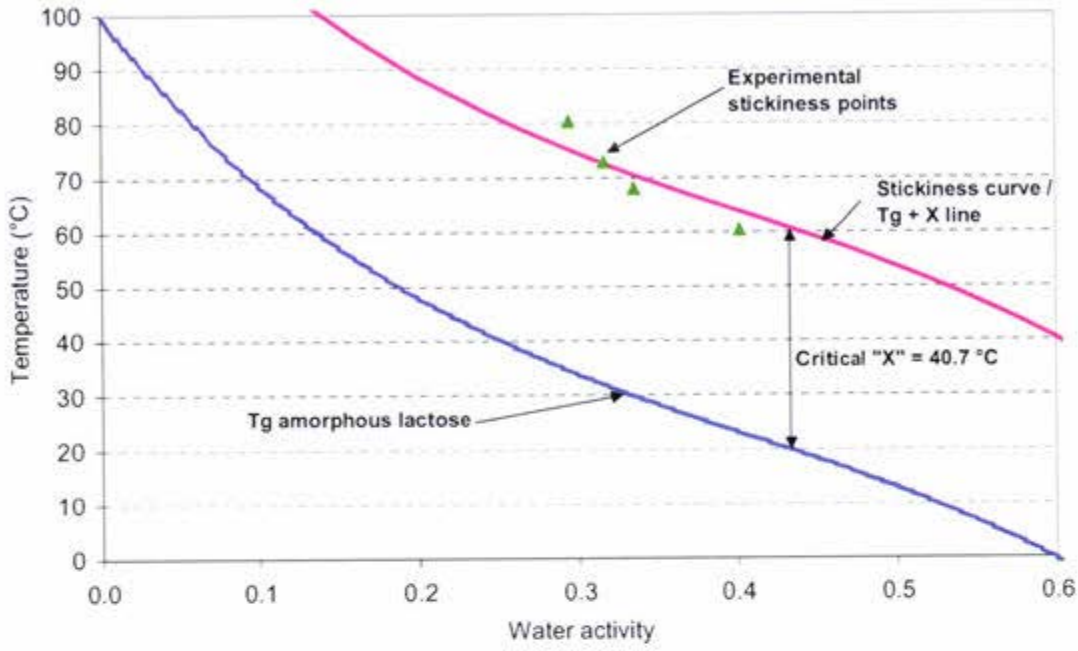

Figure 6.2 The stickiness curve of the SMP is fitted line through experimental points.

The samples were grouped in the skim milk powder category. The critical "X" value obtained from the T-T_g plot of five different specification SMP powders used was found to be 40.3±2.2 °C (95% confident interval). The critical "X" value for whole milk powder was calculated to be 37.4 ±3.0 °C with 95% confidence interval. These "X" values apply to the powder at the condition the particle-gun was run at 20 ms^{-1}, and using a flat stainless steel plate at 90° to the flow.

6.2.2 Constructing stickiness curve and mapping plant conditions

Whichever way was used to determine the critical "X" value for a powder, the result was within the 95% confidence error band.

For the case examples being considered here, the average value of SMP and its error bar are included to construct the stickiness curve as shown in Figure 6.3. The sticky and non-sticky regions were identified; any temperature and/or water activity/ relative humidity combination which exceeds the T_g+40.3°C line possible to cause the powder to become instantaneously sticky. In order to control the stickiness problem in the drier,

cyclone and ducts, the outlet air temperature and humidity that would be in equilibrium with the particle surface, have to be kept below the stickiness line.

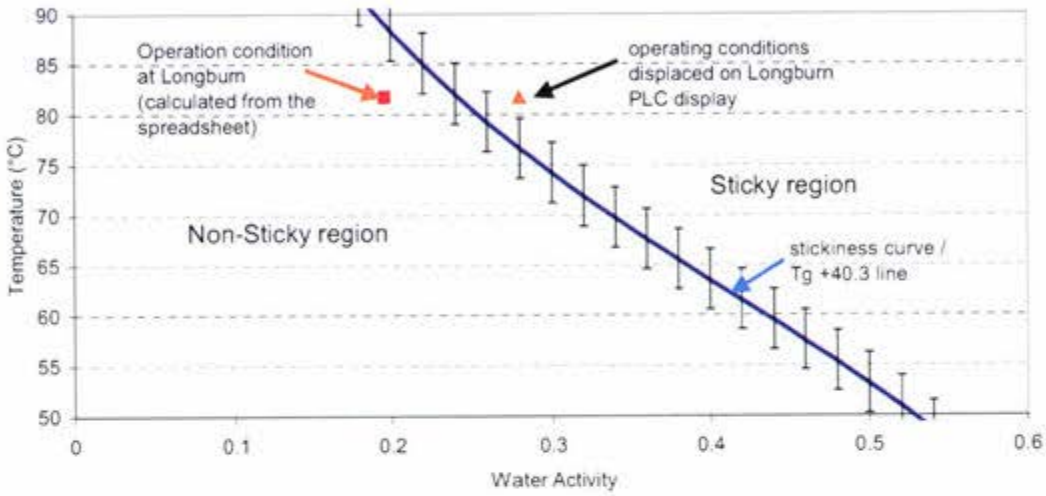

Figure 6.3 The stickiness curve constructed from the average critical "X" of SMP with ±3 error bar.

Fonterra's Speciality Powder Unit (SPU), Longbum site, produces a wide range of powders, including SMP and cream powders. The drier outlet air temperature is measured and humidity is calculated from the running parameters of the spray drier. Chatterjee (2003) outlined the step-by-step humidity calculation. The PLC displayed the outlet temperature and relative humidity of the outlet air when the SMP was made to be 81.8°C and 27.95%(or A_w= 0.2795) respectively. The values are plotted on Figure 6.3 and show it to be in the sticky region.

The outlet relative humidity was also calculated from the spreadsheet based on the total heat and mass balance around the spray drier. The input information includes the liquid production rate, the solids concentration of the feed, the inlet air flow rate, humidity and inlet/outlet air temperature. The percentage heat loss from the drier was assumed to be 5%, however, it can be adjusted for any particular driers' performance to be matched when running on water during startup. The air flow rate was not normally measured, and it can be adjusted by the valve. The spreadsheet enables the determination

of the air flow rate. In the case of the SMP, the air flow rate and outlet relative humidity were determined to be 6.7 $kg.s^{-1}$ and 19.6% (or A_w= 0.196) respectively. The calculation does not include the fluidized bed. The calculated condition is also plotted in Figure 6.2.

There is about 8% RH difference between the outlet relative humidity found between the Longburn displayed value and the calculated value from the spreadsheet. This discrepancy makes a big difference in interpreting whether the powder is sticky or not. Therefore, the reason for the discrepancy needed to be determined. A simple mass balance calculation was carried out to check the calculation base on the process inlet, the outlet air temperature, the concentrate flow rate and total solids concentrate in feed. The equations programmed into the drier PLC were traced back to the basic equations and checked. One of the assumptions was the RH is independent from air flow rate and constant values were used. Although different assumptions were made to calculate the outlet RH, including the fluidised-bed, a similar result of 15% RH was obtained both from the spreadsheet and programmed equations. It was found that the equation for calculating the saturated pressure ($P_{sat.}$) in the PLC had a constant value and the source of this figure could not be traced. The saturated pressure is a function of outlet temperature. If the programme can be corrected to calculate $P_{sat.}$ correctly, the correct RH will be displayed. There is a correction being made in the Longburn PLC programme while the plant is not processing because of its being the off-season period. It is recommended to recheck RH display with calculated RH once the plant has start to process.

6.3 SPRAY DRYING PROCESS OPTIMISATION

In order to gain some knowledge about spray drier operating control, discussions were held with the operators involved with the powder production at Longburn.

The percentage moisture of the final dried powder was kept below its maximum specification. Product with a high moisture content lowers the T_g of lactose and has an effect on $T-T_g$. It causes particles to stick to the wall or with each other, blocking the cyclone or causing problems in later stages. In that case, the operator can either increase the outlet temperature or increase the SFB inlet temperature to lower the moisture content

of the final product. Samples are collected from the bottom of the drier and are checked frequently for their moisture level.

Providing everything else is kept constant, including other powder components, particle size, density, drier fittings (nozzle size, angle of spray) and percent of total solids, the outlet temperature can be increased by reducing the production throughput. (i.e. concentrate feeding rate). Increasing the inlet temperature and keeping the same product flow rate would result in the same effect of increasing the outlet temperature. On the drier, the inlet temperature and outlet temperature have independent set points.

The exhaust fan which is taking all the air out of the drier is set at –3mm WG vacuum point and operates with the exhaust valve 90% fully open. Above –3mm WG, a vacuum effect could not be provided. Therefore, always set the exhaust to that value. Any dramatic reduction in vacuum means hardly any air is going through, and no change of fan reading indicates that there is a cyclone blockage in the process line. The pressure readings in the drier are a measure of the level of powder product in the drier. However, if the pressure reading drops fast, it means more powder is accumulating in the chamber and therefore a blockage is occurring in the chamber.

The Excel spreadsheet enables us to visualise the effect of inlet temperature, outlet temperature and production rate on the stickiness parameter ($T-T_g$) in a dynamic way. Figures 6.4 and 6.5 demonstrate these effects using the SMP as an example.

6.3.1 Effect on X via different inlet temperature and production rate

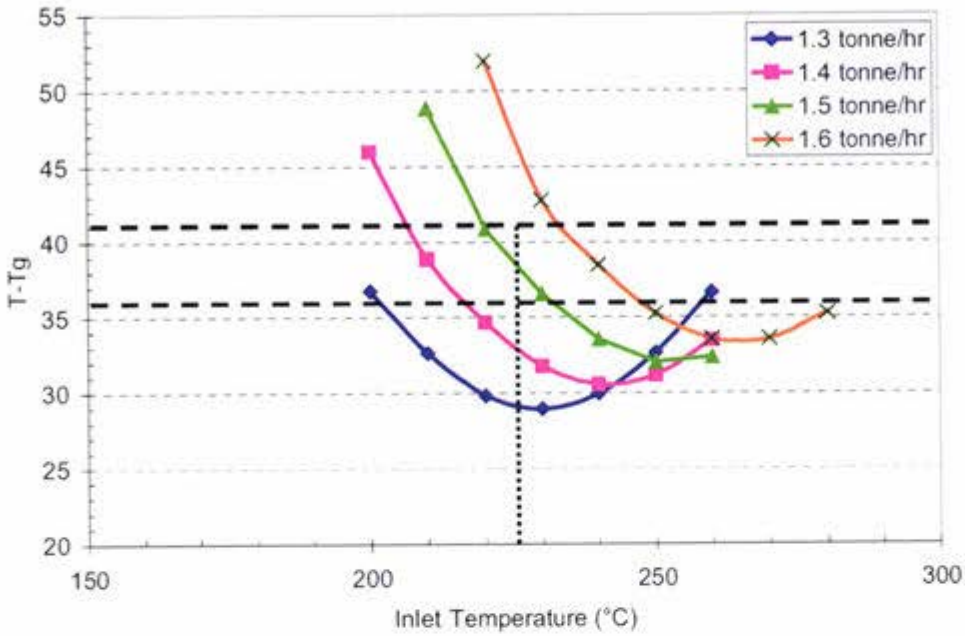

Figure 6.4 Effect of dry product throughput and inlet temperature on T-T_g

Figure 6.4 shows the effects of dry product throughput on T-T_g, as a function of inlet temperature (the dotted line at 225°C is for the SMP), while Figure 6.5 shows the effect of dry product throughput on the outlet temperature. The critical T-T_g for instantaneous stickiness of the skim milk powder falls between 36°C-41°C with a 95% confidence interval (Chapter 4). The ideal condition for the plant is to run the drier with a T-T_g below this range. This is because with any temperature and/or humidity combined condition that results in T-T_g above 41°C, the powders are definitely sticky, and above 36°C they are probably sticking and will cause a problem. The drier was running at 1.4 tonne per hour of dry product, and the T-T_g was below the lowest bound; hence there is an opportunity to push the drier harder. There are two ways to move the process conditions closer to the band. It can be done either by increasing the production rate from 1.4 tonne per hour to 1.5 tonne per hour and keeping the outlet temperature at 81°C by increasing the inlet air temperature to 235°C, or reduce the inlet temperature from 225°C to 220°C. In this way the plant can save energy and therefore money.

6.3.2 Effect on X and outlet temperature via different production rate

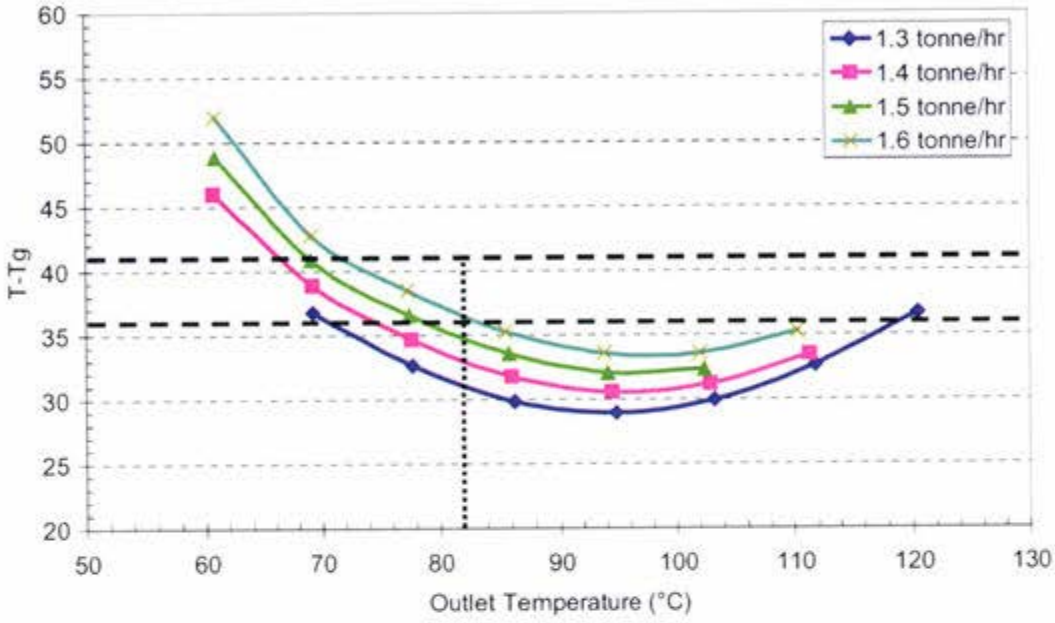

Figure 6.5 Effect on dry production rate and outlet temperature on $T-T_g$

Increasing the production rate is the more practical thing to do in the plant, because the outlet temperature is adjusted by the liquid production rate, as mentioned earlier. At a constant outlet temperature, increasing the production rate would result in increasing $T-T_g$.

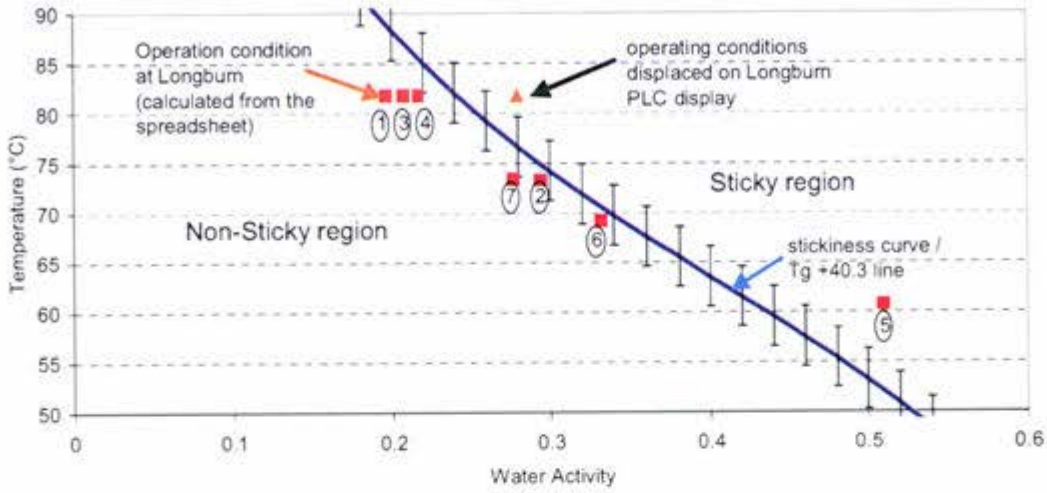

Figure 6.6 Demonstration of the possible changes that could effect the drier outlet conditions.

Table 6.1 The possible experimental matrix for variation in the solids production rate, inlet temperature and corresponding $T-T_g$.

DATA PT.	SOLIDS PROD. RATE	INLET TEMP.	OUTLET TEMP.	$T-T_G$	RH%	A_W
1	1.4 tonne/hr	225	81.8	33.1	19.6	0.196
2	1.5 tonne/hr	225	73.3	38.6	29.4	0.294
3	1.5 tonne/hr	235.2	81.8	34.9	20.7	0.207
4	1.6 tonne/hr	246	81.8	36.6	21.7	0.217
5	1.5 tonne/hr	210	60.8	48.9	51	0.51
6	1.4 tonne/hr	210	69.2	38.9	33.2	0.332
7	1.4 tonne/hr	215	73.4	36.7	27.7	0.277

The temperature and water activity data plotted on the stickiness curve in Figure 6.6 are from Table 6.1. It shows the changes recommended above based on the spreadsheet calculation and recommends the best way to optimize the process. The first data point is the current processing condition at Longburn for the SMP. The second data point has increased production rate to 1.5 tonnes per hour and kept the same inlet temperature, which resulted in both an increase in outlet temperature and humidity. The critical $T-T_g$ is not exceeded but it does lie within the error bars for the stickiness lines, and problems may be experienced. The plant is operating near or at its limit. The third data point has increased inlet temperature while keeping the production rate at 1.5 tonne

per hour and outlet temperature, the outcome condition is very similar to the current production but is closer to the sticky point lines. The fourth data point has increased the production rate to 1.6 and uses an increased inlet temperature to produce the same outlet temperature as the current production. The RH % is increased but the critical $T-T_g$ is not exceeded. The fifth data point has 1.5 tonne/hr and a reduced inlet temperature of 210°C. It has reduced the outlet temperature to 60.8°C and increased the RH to 51%, indicating the product is very moist and will be sticky. The sixth data point has the current product rate and a reduced inlet temperature of 210°C, which resulted in a reduced outlet temperature of 70°C and 38.9% RH and the critical $T-T_g$ is not exceeded, but is within the error bands and is very close to the stickiness curve. The last data point has the current production rate and a reduced inlet temperature of 215°C (5°C higher than the sixth data point), giving the same production as the current conditions but at lower energy costs. The best recommended process conditions are data points 7 and 4. It depends on whether the company wants to save energy or increase production.

In a general trend, changing the production rate and keeping the same outlet temperature shifts the point sideways. Either changing the inlet temperature and keeping the production rate the same or changing the production rate and keeping the inlet temperature the same shift the point vertically.

If data point 7 was chosen, reducing the inlet temperature would mean saving money on the energy cost. A simple heat based calculation found approximately $ 11.34 can be saved per hour based on an assumed energy cost of $0.17 kwh. If the plant continually processes for 20-30 hours before a nozzle wash, it would save $ 340.2 of powder. The whole production normally runs for 30 days.

If data point 4 was chosen, the production rate can be increased by 0.2 tonnes in dry production rate, a 14% increase in production throughput.

6.4 CLOSURE

Dairy powder stickiness during processing is a surface phenomenon, and therefore the outlet air temperature and relative humidity is assumed to be in equilibrium with the surface of the powder particle. For a dairy powder, there is a critical "X" value for instantaneous stickiness. The very first step is to be able to identify this critical "X" value. There are several different ways to do it from the data obtained with the particle-gun rig. All the values obtained were not significantly different for the SMP tested. It is in a range of 36°C - 41°C with a 95% confidence interval. The next step was to map the plant condition on to the stickiness curve (T_g + 'X' line), and any adjustment can be made to approach or move away from the stickiness curve. The main two parameters responsible for such adjustments are the inlet air temperature and the production rate. An Excel spreadsheet enabled the solution of the problem in a dynamic way, especially to relate the inlet/outlet temperature and production rate with the $T-T_g$ parameter. For this particular skim milk powder, processing at the Longburn site, the best recommendation for reducing energy is to reduce the inlet air by 10°C, hence reduce outlet temperature to 73.4°C and keep the same production rate. The other option is to increase the solid production rate from 1.4 tonnes/hr to 1.6 tonnes/hr.

CHAPTER 7

CONCLUSIONS AND RECOMMENDATIONS

The particle-gun rig has been used to measure the onset of instantaneous stickiness of dairy powders. Its dynamic setup has shown the stickiness phenomena is a function of temperature, relative humidity, and composition of the powder. It has shown that the stickiness behaviour is a function of the surface conditions since there was insufficient time (<0.05 s) for the particles in the particle-gun to have anything but the surface to be affected by the air conditions the particle was subjected to. This technique does not need to pre-condition the powder, as the surface was assumed to be in equilibrium with the surrounding condition. The particle-gun rig has enabled stickiness data to be collected under air temperature and RH conditions similar to those found in the exit of spray driers. It also enables the rate at which stickiness develops in a powder to be investigated as a function of RH and temperature. Further study is required to observe the velocity and angles of contact on effects of instantaneous stickiness in more detail.

There were two ways of identifying the critical "X" value from raw data of % deposition versus RH at constant temperatures. The first was to identify the instantaneous stickiness point at a particular relative humidity for each temperature tested. Then a stickiness curve was fitted to the experimental stickiness point at those temperatures above the T_g of amorphous lactose. The best fit using a least squares error fit of "X" was identified to be the critical value for instantaneous stickiness. The other way was to plot % deposition against the $T-T_g$ parameter for combining temperature and relative humidity effects. This was done successfully, indicating that the stickiness was due to the T_g of amorphous lactose being exceeded and was a function of temperature and RH. The critical "X" value was identified as the x-intercept in the $T-T_g$ plot and the slope of the trend line detects the sensitivity of the stickiness in response to condition changes. Various dairy powders were tested for the critical "X" value. These powders included WMP, SMP, MPC and cheese powders. The critical "X" value of SMP varied from 37°C to 42°C; WMP varied from 33°C to 40°C; and MPC varied from 42.7°C to 51°C. The variation between the powders depends on their composition. There was a positive linear

relationship formed between the critical "X" value of a powder and the powders' lactose content.

Cream powders and white cheese powder are catalogued under the high fat powders (i.e. total fat content equal to or more than 42 %). The liquid bridges formed by molten fat were a function of temperature. However, amorphous lactose also contributed to the stickiness when the T_g amorphous lactose was exceeded. Both effects are observed in $T-T_g$ plots for high fat powders.

It has been shown that the stickiness of dairy powders was caused mainly by the amorphous lactose content, as the stickiness is a function of both temperature and RH. The glass transition temperature of amorphous lactose correctly predicts the effects of temperature and RH; all the stickiness powders as shown by the $T-T_g$ plots collapsed these data to a single line. This line starts at a critical $T-T_g$ value for a powder, known as the critical "X" value, which shows that the glass transition temperature needs to be exceeded by a constant amount in order for the powder to become instantaneously sticky. The slope of the trend line in the $T-T_g$ plot shows the sensitivity of the powder to stickiness in response to the temperature and/or relative humidity changes. Both the critical 'X' value and the slope are unique to the powder. They also show that powders with greater than 30% amorphous lactose become more sticky quicker once the critical X factor above T_g is exceeded.

In this work, "X" has been measured using a particle-gun rig at a velocity of $20ms^{-1}$ which is typical of the velocities of the powders in the ducting of spray driers.

For powders that have a total fat content less than 42%, the stickiness is mainly due to amorphous lactose when T_g is exceeded by the critical "X" value of the powder. A regression equation (equation 4.1) was generated, based on the critical 'X' value obtained from the experimental data of various dairy powders, to correlate the effects of composition on X. Although an overall trend is observed, futher study is required to investigate the surface composition in relationship with the critical 'X'.

Once the critical "X" for a particular powder was identified, the stickiness curve was generated on a temperature versus relative humidity/water activity plot. It enables operators to map the plant operating conditions on the stickiness curve for a particular powder being produced, and adjustment can then be made to optimize the process by moving the operating condition toward or away from the stickiness curve. The surface of the particle is assumed to be in equilibrium with the drier outlet air temperature and relative humidity, and it is these conditions which are used to map the plant operating point on the graph. The case study on the SMP has demonstrated the procedure to implement this work in an industrial environment. The drier outlet temperature and production rate are the two parameters that control the outlet conditions. An Excel spreadsheet was constructed, based on the energy and mass balance around a spray drier. It related the two adjustable parameters with the $T\text{-}T_g$ parameter and was used to solve the problem in a dynamic way. In the case of the SMP, the objective was to push the drier to its limit and move the point towards the stickiness curve. The best recommendations are either to reduce the inlet air by 10°C in order to save on energy or to increase the concentrate feeding rate to 3.2 tonnes/hr (or solid production rate of 1.6 tonnes/hr), a 14% increase in production throughput.

Fonterra Te Repa site implemented the stickiness curve and uses it to monitor the process conditions so that the chamber, cyclone and ducting blockages due to stickiness can be avoided. These are continuously under review and updating with the latest knowledge being used to control the process in an efficient and a dynamic way.

Several factors were kept constant throughout this experimental work. These included the air velocity of the particle-gun rig, stainless steel plates and powder particle fired to the plate at 90°. Further work is recommended to investigate the factors of varied air velocity, different coating of the plate, and other angles of contact that have an effect on the critical "X" value for a powder.

REFERENCES

Adhikari, B., Howes, T., Bhandari, B.R., & Truong, V. (2001). Stickiness in Foods: A Review of Mechanisms and Test Methods. International Journal of Food Properties, 4(1), 1-33.

Aguilera, J.M., del Valle, J.M., & Karel, M. (1995). Caking Phenomena in Amorphous Food Powders. Trends in Food Science and Technology, 6, 149-155.

Bandyopadhyay, P., Das, H., & Sharma, G.P. (1987). Moisture Adsorption Characteristics of Casein, Lactose, Skim Milk and Chhana Powder. Journal of Food Science and Technology, Vol. 24, Jan/Feb.

Bhandari, B. (2001). Glass Transition in Relation to Stickiness during Spray Drying. Food Technology International, 64-68.

Bhandari, B.R., Datta, N., & Howes, T. (1997). Problems Associated with Spray Drying of Sugar-rich Foods. Drying Technology, 15(2), 671-684.

Bhandari, B.R., & Howes, T. (2000). Glass Transition in Processing and Stability of Food. Food Technology in Australia, 52(12), 579-585.

Bhandari, E.R., & Howes, T. (1999). Implication of Glass Transition for the Drying and Stability of Dried Foods. Journal of Food Engineering, 40, 71-79.

Bloore, C. (2000). Developments in Food Drying Technology overview. International Food Dehydration Conference – 2000 and Beyond, Carlton Crest Hotel, Melbourne, Australia.

Boonyai, P., Bhandari, B., & Howes, T. (2004). Stickiness Measurement Techniques for Food Powders: A Review. Powder Technology, 145, 34-46.

Bronlund, J. E. (1997). The Modelling of Caking in Bulk Lactose. PhD thesis, Massey University, Palmerston North, New Zealand.

Brooks, G.F. (2000). The Sticking and Crystallisation of Amorphous Lactose. Masterate Thesis. Massey University, Palmerston North, New Zealand.

Buma, T.J. (1971a). Free Fat in Spray-dried Whole Milk. 2. An evaluation of methods for the determination of free-fat content. 3. Particle size. its estimation, influence of processing parameters and its relation to free-fat content. Netherlands Milk Dairy Journal, 25(42-80)

Buma, T.J. (1971b). Free Fat in Spray-dried Whole Milk. 4. Significance of free fat for other properties of practical importance. Netherland Milk Dairy Journal, 25, 88-106.

Burr. R. (1999). An Investigation Into Cheese Powder Caking. Diploma in Dairy Science and Technology Dissertation, Massey University. Palmerston North, New Zealand.

Chatterjee, R. (2003). Characterising Stickiness of Dairy Powders. Masterate Thesis. Massey University, Palmerston North, New Zealand.

Chen, X.D. (1994). Towards a Comprehensive Model based Control of Milk Drying Process. Drying Technology , 12(5), 1105-1130.

Chuy, L.E., & Labuza, T.P. (1994). Caking and Stickiness of Dairy-based Food Powders as Related to Glass-Transition. Journal of Food Science, 59(1), 43-46.

Crofskey, G.M. (2000). Investigation into the Caking Problems Associated with Spray Dried Cream Powders 55 and 70. 4th year Food Technology Report, Massey University. Palmerston North, New Zealand.

Dixon, A. (1999). Correlating Food Powder Stickiness with Composition, Temperature and Relative Humidity. Monash Universtity, Melbourne, Australia.

Downton, G.E., Flores-Luna, J.L., & King, C.J. (1982). Mechanism of Stickiness in Hygroscopic, Amorphous Powders. Ind. Eng. Chem. Fundam., 21, 447-451.

Foster, K.D. (2002). The Prediction of Sticking in Dairy Powders. PhD Thesis. Massey University, Palmerston North, New Zealand.

Fäldt, P., & Bergenstahl, B. (1996a). Changes in Surface Composition of Spray-dried Food Powders due to Lactose Crystallisation. Lebensm-Wiss. u- Technology, 29, 438-446.

Fäldt, P., & Bergenstahl, B. (1996b). Spray-dried Whey Protein/Lactose/Soybean Oil Emulsions. 1. Surface Composition and Particle Structure. Food Hydrocolloids, 10(4), 421-429.

Fäldt, P., Bergenstahl, B., & Carlsson, G. (1993). The Surface Coverage of Fat on Food Powders Analyzed by ESCA (Electron Spectroscopy for Chemical Analysis). Food Structure, 12, 225-234.

Fäldt, P., & Bergenstlhl, B. (1995). Fat Encapsulation in Spray-dried Food Powders. JAOCS, 72(2), 171-176.

Fäldt, P., & SjÖholm, I. (1996). Characteriszation of Spray-dried Whole Milk. Milchwissenschaft - Milk Science International, 51(21), 88-92.

Jenicke, A.W. (1964). Storage and flow of solids. Bulletin 123, Utah Engineering Experimental Station, University of Utah.

Jouppila, K., Kansikas, J., & Roos, Y.H. (1997). Glass Transition, Water Plasticization, and Lactose Crystallisation in Skim Milk Powder. Journal of Dairy Science, 80(12), 3152-3160.

Jouppila, K., & Roos, Y.H. (1994a). Glass Transitions and Crystallisation in Milk Powders. Journal of Dairy Science, 77(10), 2907-2915.

Jouppila, K., & Roos, Y.H. (1994b). Water Sorption Properties and Time-Dependent Phenomena of Milk Powders. Journal of Dairy Science, 77(7), 1798-1808.

Hennigs, C., Kockel, T.K., & Langrish, T.A.G. (2001). New Measurements of the Sticky Behaviour of Skim Milk Powder. Drying Technology, 19(3&4), 471-484.

Keir, T. (2001). Milk Powder Stickiness: A Preliminary Study. Masterate Thesis. Massey University, Palmerston North, New Zealand.

Kim, E.H.J., Chen, X.D., & Pearce, D. (2002). On the Mechanisms of Surface Formation and the Surface Compositions of Industrial Milk Powders. Drying Technology,

King, N. (1965). The Physical Structure of Dried Milk. Dairy Science Abstracts, 27(3), 91-104.

Lazar, M.E., Brown, A.H., Smith, G.S., Wong, F.F., & Lindquist, F.E. (1956). Experimental Production of Tomato Powder by Spray Drying. Food Technology, 129-133.

Le Meste, M., Champion, D., Roudaut, G., Blond, G., & Simatos, D. (2002). Glass Transition and Food Technology: A Critical Appraisal. Journal of Food Science, 67(7), 2444-2458.

Lillford, P.J., & Fryer, P.J. (1998). Food Particles and the Problems of Hydration. Trans IChem E, 76(part A), 797-802.

Lloyd, R.J., Chen, X.D., & Hargreaves, J.B. (1996). Glass Transition and Caking of Spray-dried Lactose. International Journal of Food Science and Technology, 31, 305-311.

Masters, K. (1991). Spray Drying Handbook. Great Britain: Longman Scientific & Technical .

Moreyra, R., & Peleg, M. (1981) Effect of equilibrium water activity on the bulk properties of selected food powders. Journal of Food Science, 46.

Noel, T.R., Ring, S.G., & Whittam, M.A. (1990). Glass Transitions in Low-Moisture Foods. Trends in Food Science and Technology, 62-67.

Norris, G.E., Gray, I.K., & Dolby, R.M. (1973). Seasonal Variations in the Composition and Thermal Properties of New Zealand Milk Fat - Thermal Properties of Milk Fat and their Relation to Composition. Journal of Dairy Research, 40, 311-321.

O'Donnell, A.M., Bronlund, J.E., Brooks, G.F., & Paterson, A.H.J. (2002). A constant humidity air supply system for pilot scale applications. International Journal of Food Science and Technology, 37, 369-374.

Ozmen, L., & Langrish, T.A.G. (2002). Comparision of Glass Transition Temperature and Sticky Point Temperature for Skim Milk Powder. Drying Technology, 20(6), 1177-1192.

Paterson, A.H.J., Brooks, G.F., & Bronlund, J.E. (2001) The Blow Test for Measuring the Stickiness of Powders. Conference of Food Engineering 2001, AICHE conference Noverber 4-9, 2001, Reno, Nevada.

Paterson, A.H.J., Brooks, G.F.,Foster, K.D., & Bronlund, J.E. (2004/5). The development of stickiness in amorphous lactose at constant T-T_g levels. International Dairy Journal, In Press.

Peleg, M. (1993). Glass Transitions and the Physical Stability of Food Powders. In J. Blanshard and P. Lilliford. (Editor) (Ed.), The Glassy State in Foods. 435-451. Leicestershire: Nottingham University Press.

Roos Y. (1993). Melting and Glass Transition of Low Molecular Weight Carbohydrates. Carbohydrate Research, 238-248.

Roos, Y., & Karel, M. (1991a). Phase Transitions of Mixtures of Amorphous Polysaccharides and Sugars. Biotechnol. Prog., 7, 49-53.

Roos, Y., & Karel, M. (1991b). Plasticizing Effect of Water on Thermal Behavior and Crystallisation of Amorphous Food Models. Journal of Food Science, 56(1), 38-43.

Roos , Y., & Karel, M. (1991c). Water and Molecular Weight Effects on Glass Transitions in Amorphous Carbohydrates and Carbohydrate Solutions. Journal of Food Science, 56(1), 1676-1681.

Roos, Y.H. (1995a). Phase Transitions in Foods. Academic press, INC.

Roos, Y.H. (1995b). Glass Tranistion-related Physicochemical Changes in Foods. Food Technology, 49(10), 97-102.

Roos, Y.H. (2002). Importance of Glass Transition and Water Activity to Spray Drying and Stability of Dairy Powders. Lait, 82, 475-484.

Roos, Y.H., Karel, M., & Kokini, J.L. (1996). Glass Transitions in Low-Moisture and Frozen Foods: Effects on Shelf Life and Quality. Food Technology, 50(11), 95-108.

Toy, K.I.M. (2000). Stickiness Rig: A procedure to Characterise Powder Stickiness. New Zealand Dairy Research Institute, Palmerston North, New Zealand.

Wallack, D.A., & King, C.J. (1988). Sticking and Agglomeration of Hygroscopic, Amorphous Carbohydrate and Food Powders. Biotechnology Progress, 4(1), 31-35.

Williams, M.L., Landel, R.F., & Ferry, J.D. (1955). The Temperature Dependence of Relaxation Mechaniasm in Amorphous Polymers and other Glass-forming Liquids. Journal of the American Chemical Society, 77, 3701-3707.

NOMENCLATURE

a, D	Particle radius	m
a_w	Water activity	
C_{p1}, C_{p2}	Specific heat capcity	J/k mol
k	Viscous flow constant (Eq. 2.1)	
k	Gordon and Taylor constant	
T	Temperature	°C or K
T_g	Glass transition temperature	°C or K
T_{gm}	Glass transition temperature of mixture	°C or K
T_{g1}, T_{g2}	Glass transition temperature of components	°C or K
C_1, C_2	WLF constant	
w_i, w_1, w_2	Mass fraction of components	g/g powder
x	Interparticle bridge size	m
x_i	mass fraction of component i	g/g dry basis

Greek Letters

γ	Surface tension	N/m
τ	Time/ particle contact time	s
μ, μ_c	Viscosity, Critical viscosity,	Pa.s
μ_g	Viscosity at glass transition temperature	Pa.s

APPENDIX A1

COMPOSITIONS OF POWDERS TESTED

Dry Powder Product	Fat	Lactose	Protein
	(%TS)	(%TS)	(%TS)
Agglomerated WMP	31.09	37.82	25.91
High heat WMP	27.38	38.33	27.07
Regular WMP1	28.44	40.68	24.9
Instant WMP	29.75	39.77	24.69
Regular WMP2	26.94	40.93	25.91
Instant SMP2	0.79	52.98	38.19
Instant SMP1	0.62	57.84	34.27
Medium heat SMP	0.83	53.01	38.05
SMP	0.52	57.19	34.06
Butter milk	9.33	51.3	31.92
MPC 44	0.83	47.56	43.52
MPC 56	1.35	31.29	59.36
MPC 70	1.46	18.16	72.86
MPC 85	1.67	4.17	88.54
Whey protein Isolates	0.52	1.05	96.34
GUMP	15.46	49.48	27.84
White cheese	42.05	27.9	21.23
LFCP 55	55.84	24.37	16.24
HFCP 70	71.79	13.33	12.31
Amorphous Lact.	0	100	0

Product compositions were supplied by Fonterra.

APPENDIX A2

SMP

INSTANT SMP 2

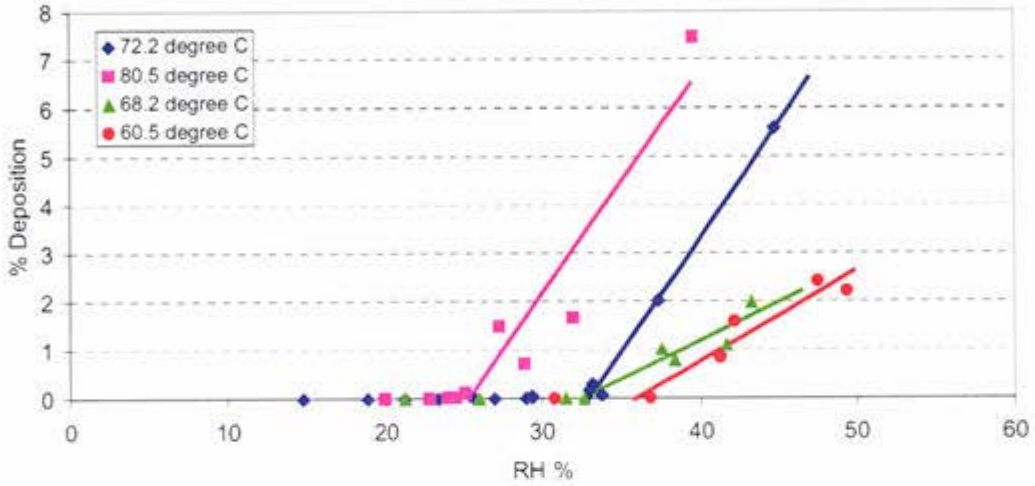

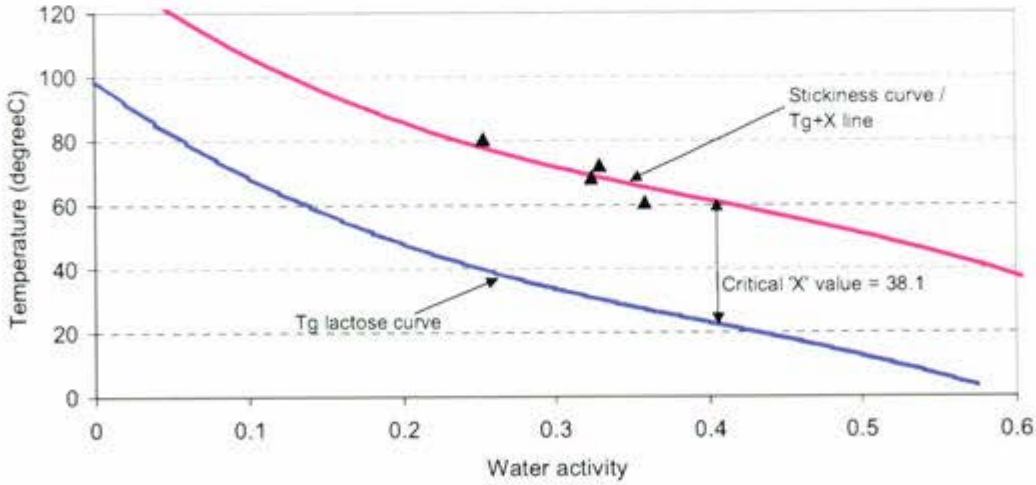

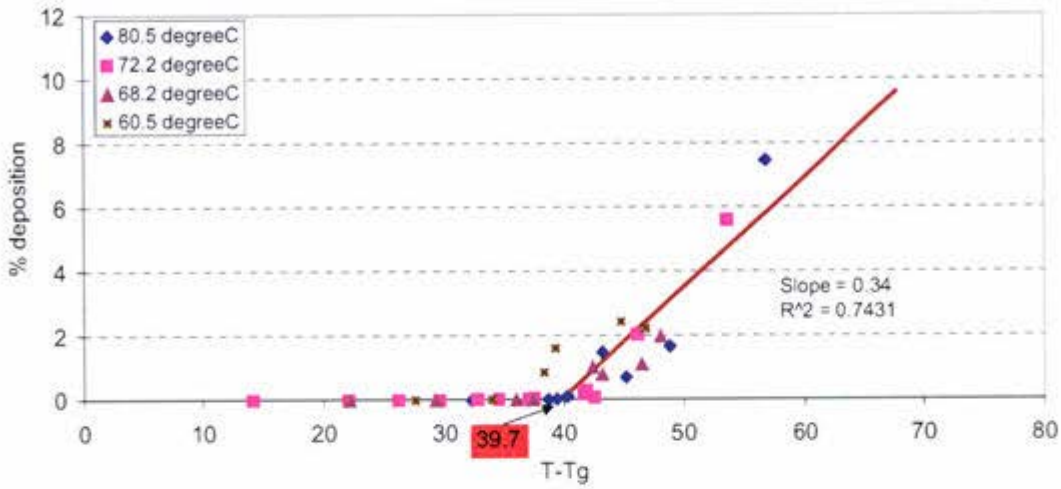
80.5 degreeC
72.2 degreeC
68.2 degreeC
60.5 degreeC
% deposition
Slope = 0.34
R^2 = 0.7431
39.7
T-Tg

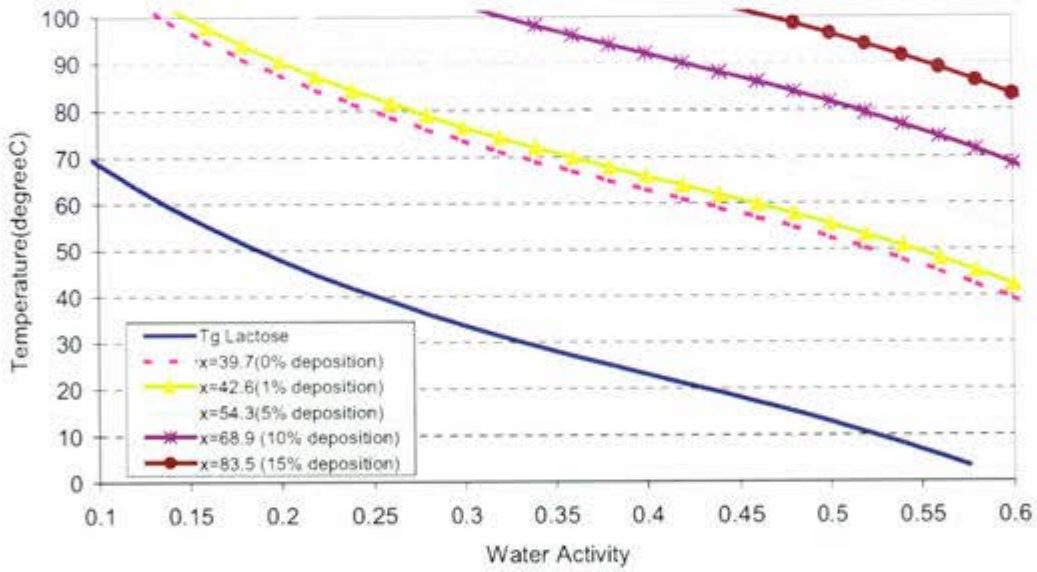
Tg Lactose
x=39.7(0% deposition)
x=42.6(1% deposition)
x=54.3(5% deposition)
x=68.9 (10% deposition)
x=83.5 (15% deposition)
Temperature(degreeC)
Water Activity

MEDIUM HEAT SMP

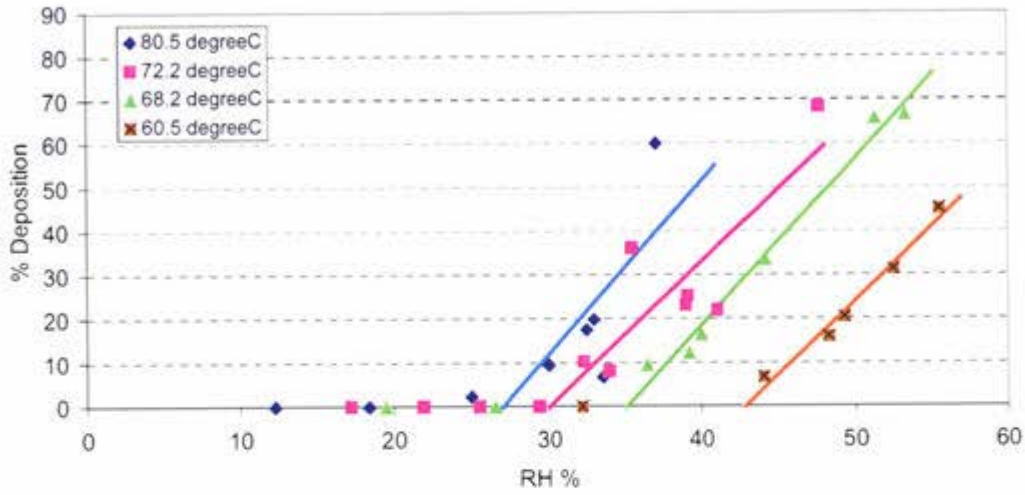

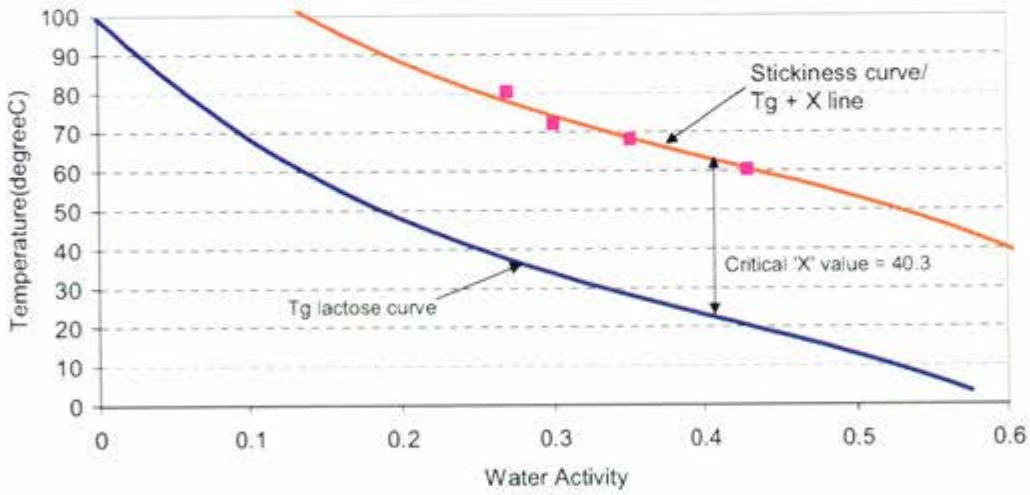

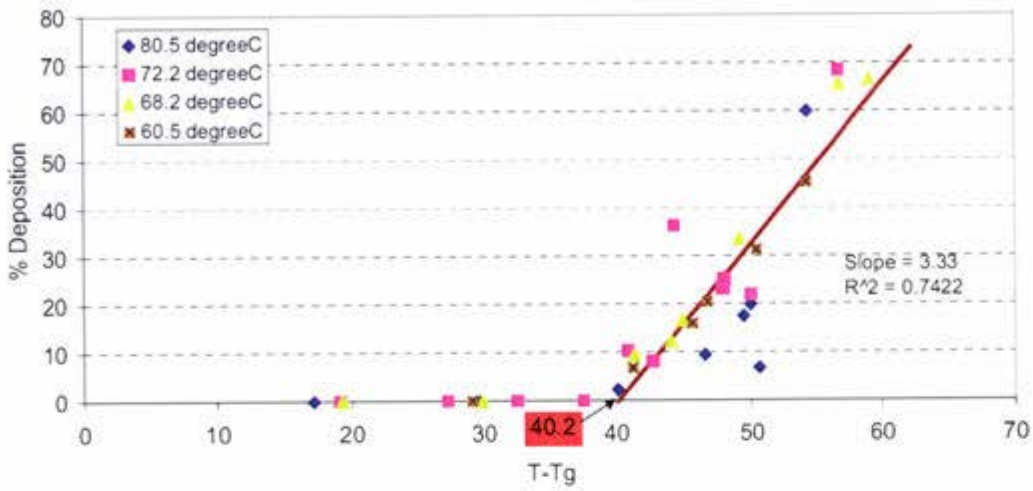
80.5 degreeC
72.2 degreeC
68.2 degreeC
60.5 degreeC
% Deposition
Slope = 3.33
R^2 = 0.7422
40.2
T-Tg

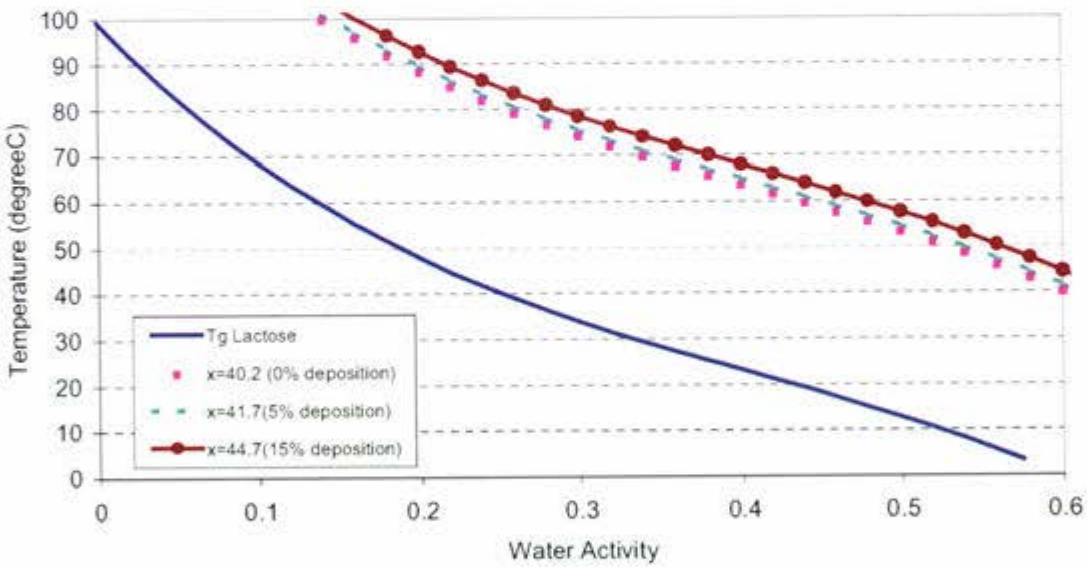
Temperature (degreeC)
Tg Lactose
x=40.2 (0% deposition)
x=41.7(5% deposition)
x=44.7(15% deposition)
Water Activity

INSTANT SMP (REPLICATE)

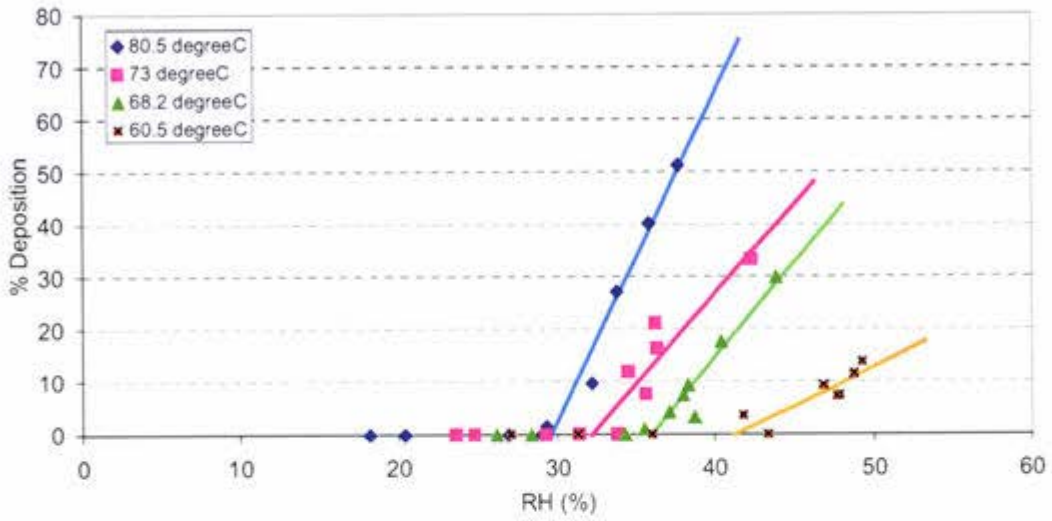

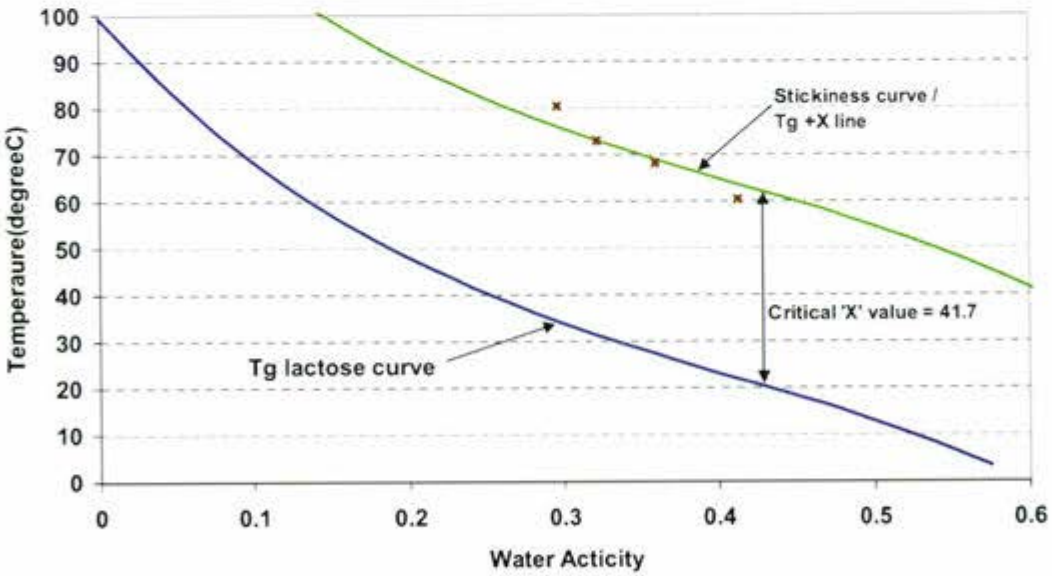

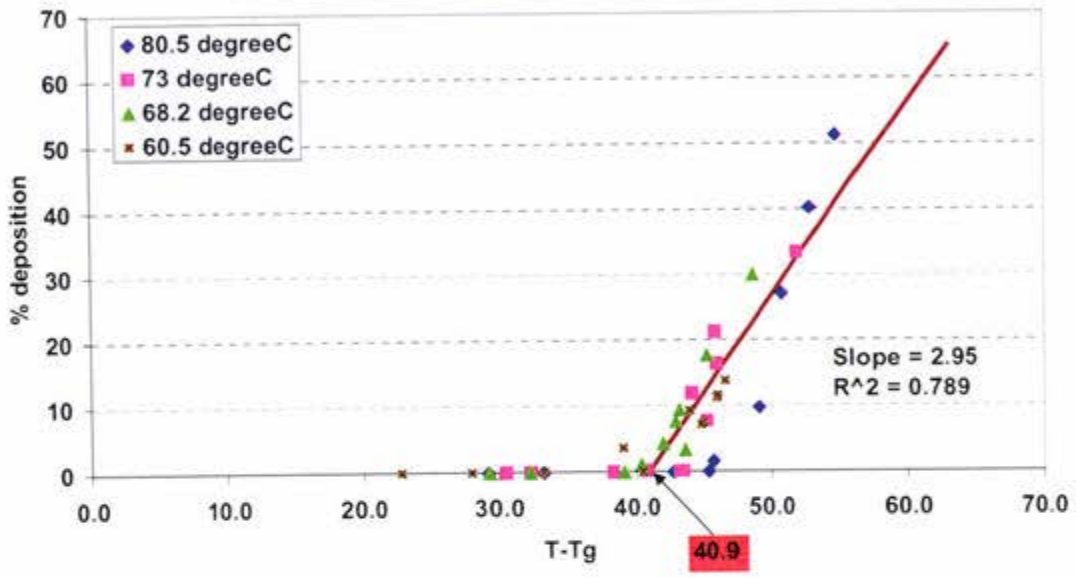
80.5 degreeC
73 degreeC
68.2 degreeC
60.5 degreeC
% deposition
70
60
50
40
30
20
10
0
0.0
10.0
20.0
30.0
40.0
50.0
60.0
70.0
T-Tg
40.9
Slope = 2.95
R^2 = 0.789

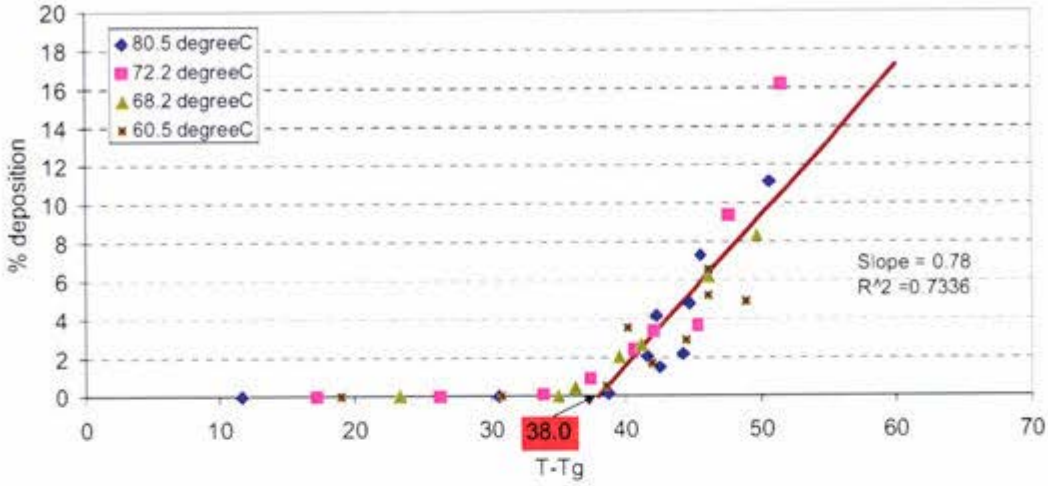
80.5 degreeC
72.2 degreeC
68.2 degreeC
60.5 degreeC
% deposition
Slope = 0.78
R^2 =0.7336
38.0
T-Tg

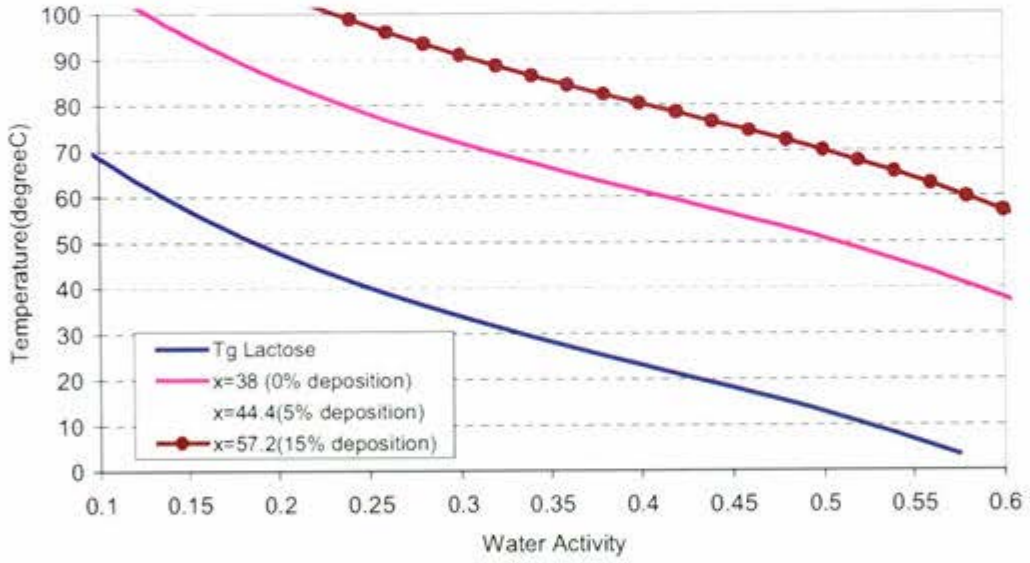
Temperature(degreeC)
Tg Lactose
x=38 (0% deposition)
x=44.4(5% deposition)
x=57.2(15% deposition)
Water Activity

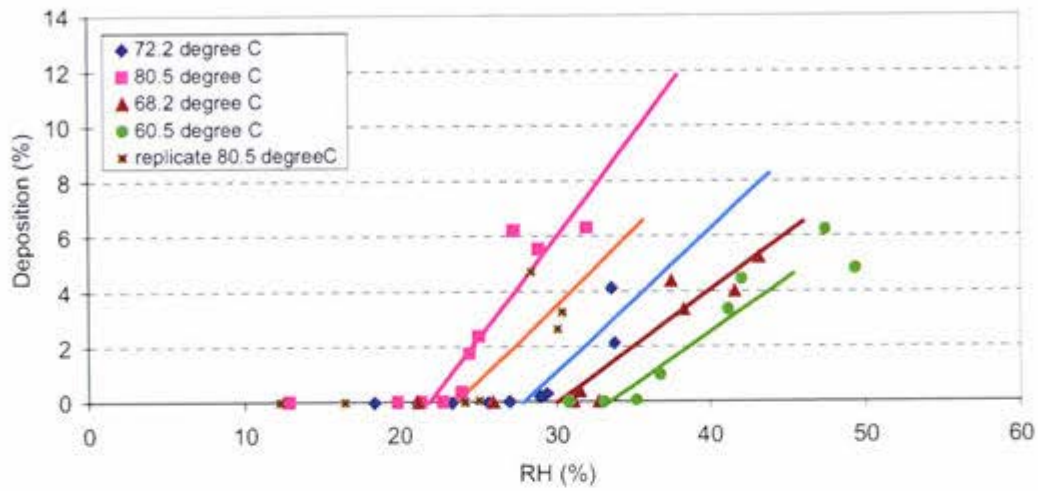
72.2 degree C
80.5 degree C
68.2 degree C
60.5 degree C
replicate 80.5 degreeC
Deposition (%)
RH (%)
0
2
4
6
8
10
12
14
0
10
20
30
40
50
60

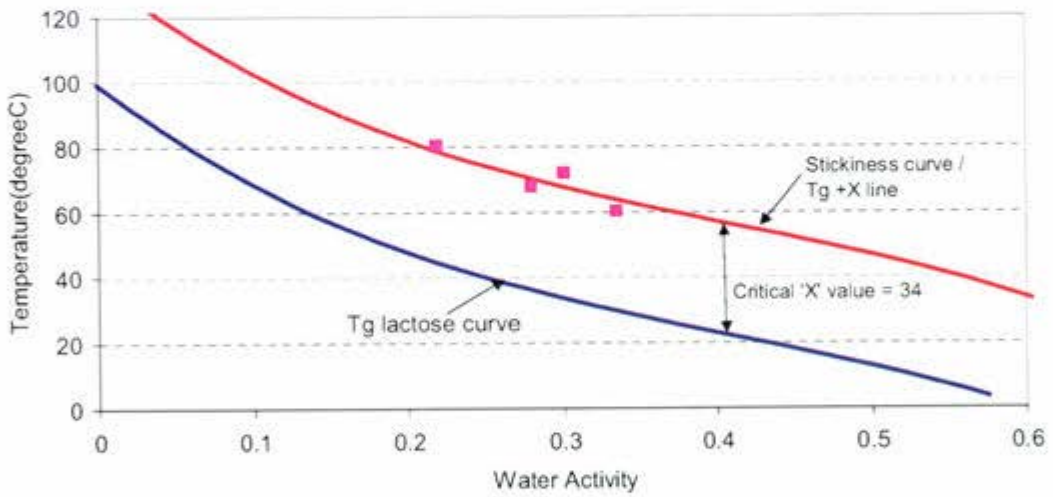
Temperature(degreeC)
Water Activity
Stickiness curve / Tg +X line
Critical 'X' value = 34
Tg lactose curve
0
20
40
60
80
100
120
0
0.1
0.2
0.3
0.4
0.5
0.6

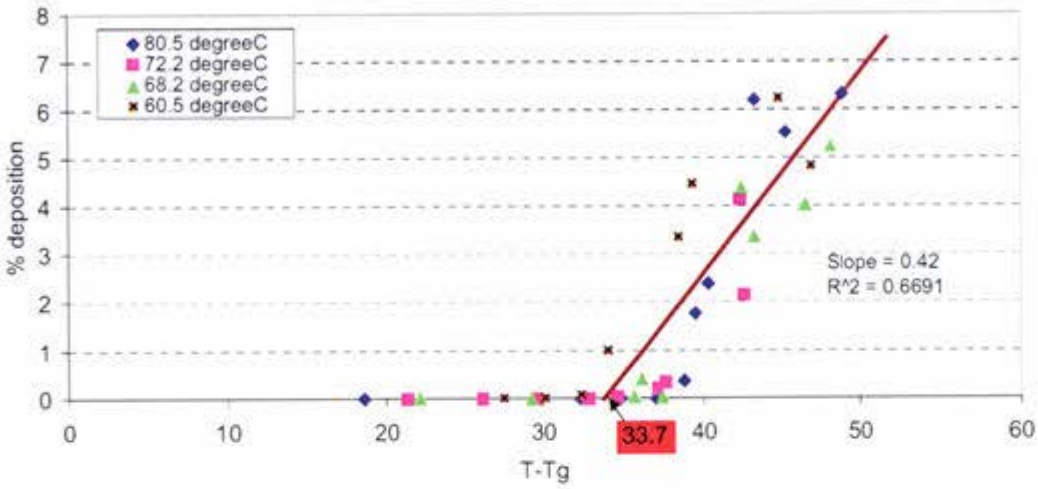
80.5 degreeC
72.2 degreeC
68.2 degreeC
60.5 degreeC
% deposition
Slope = 0.42
R^2 = 0.6691
33.7
T-Tg

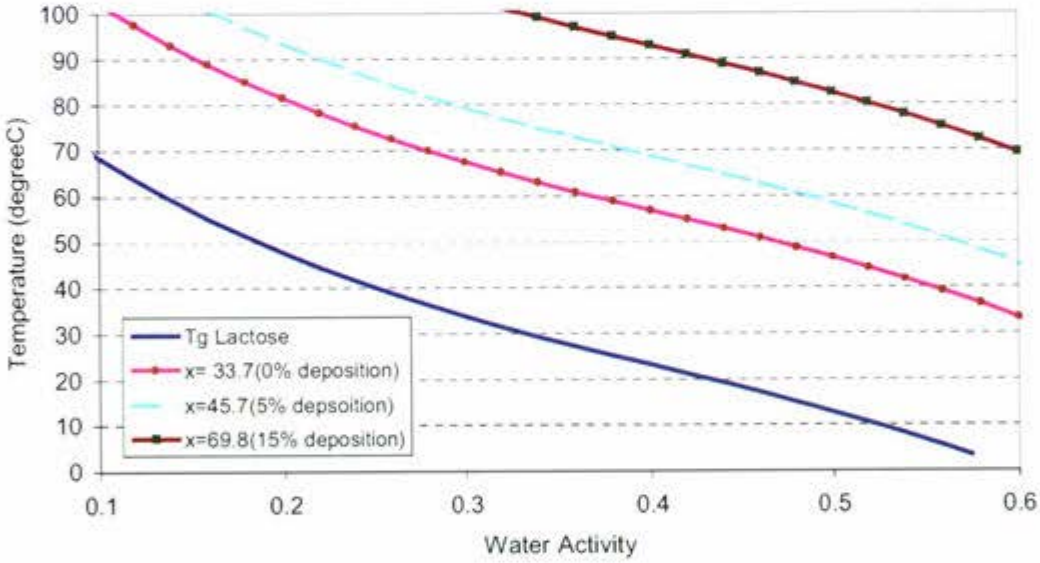
Temperature (degreeC)
Tg Lactose
x= 33.7(0% deposition)
x=45.7(5% depsoition)
x=69.8(15% deposition)
Water Activity

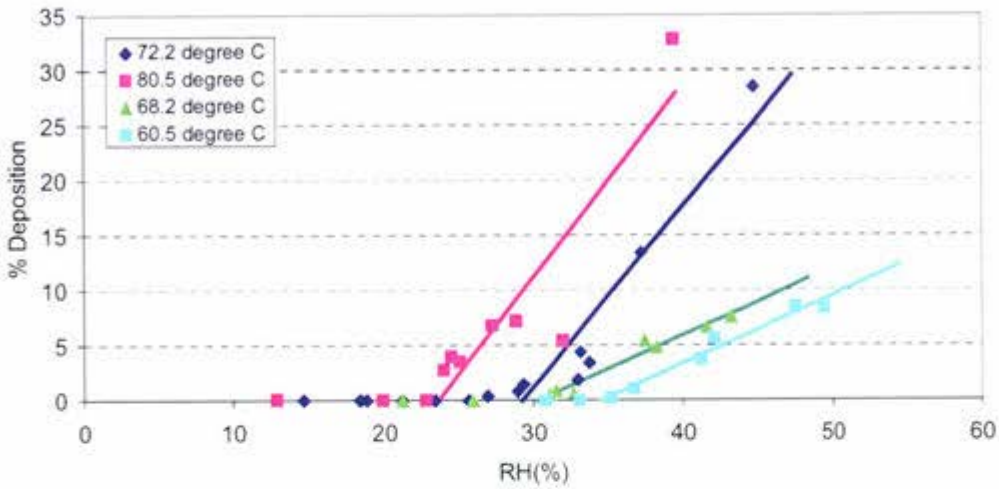
72.2 degree C
80.5 degree C
68.2 degree C
60.5 degree C
% Deposition
RH(%)
0
5
10
15
20
25
30
35
0
10
20
30
40
50
60

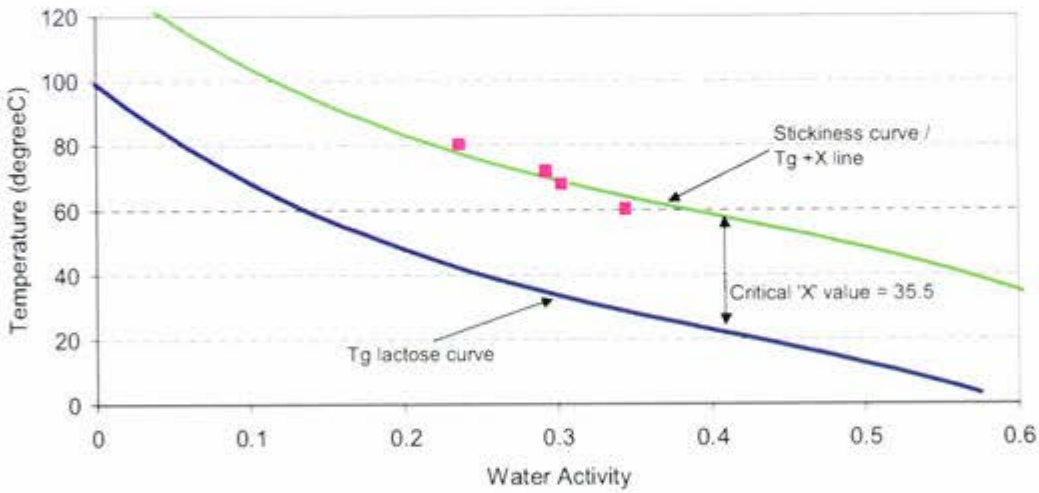
Temperature (degreeC)
Water Activity
Stickiness curve / Tg +X line
Critical 'X' value = 35.5
Tg lactose curve
0
20
40
60
80
100
120
0
0.1
0.2
0.3
0.4
0.5
0.6

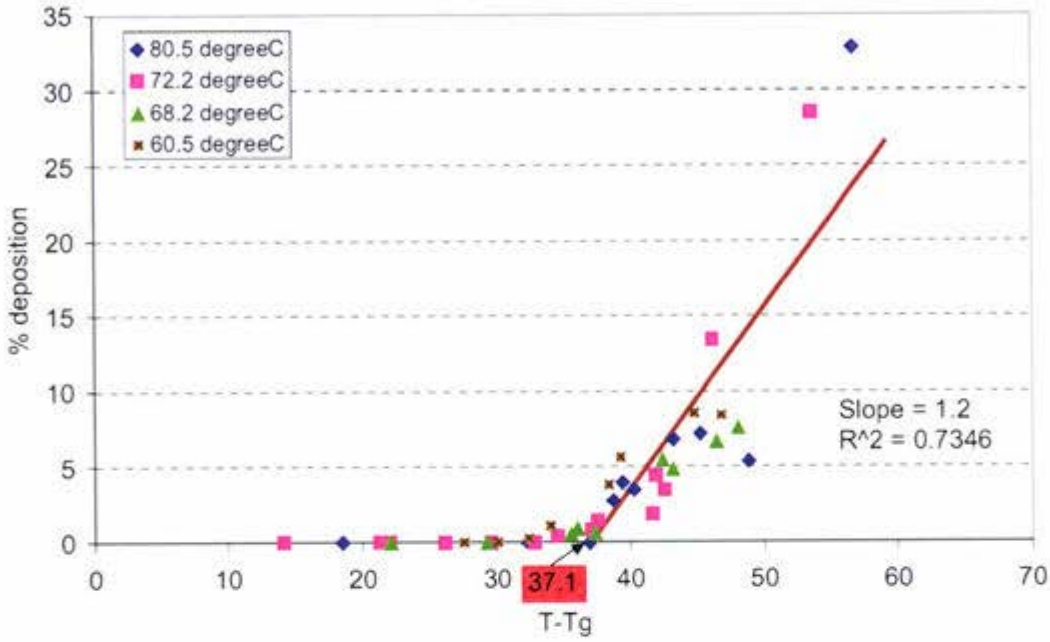
80.5 degreeC
72.2 degreeC
68.2 degreeC
60.5 degreeC
% deposition
Slope = 1.2
R^2 = 0.7346
37.1
T-Tg

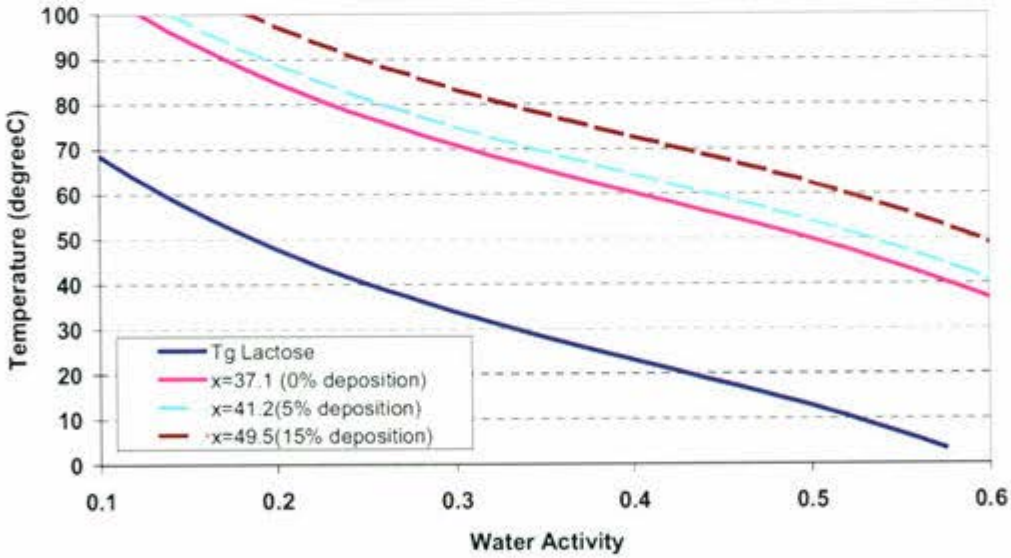
Temperature (degreeC)
Tg Lactose
x=37.1 (0% deposition)
x=41.2(5% deposition)
x=49.5(15% deposition)
Water Activity

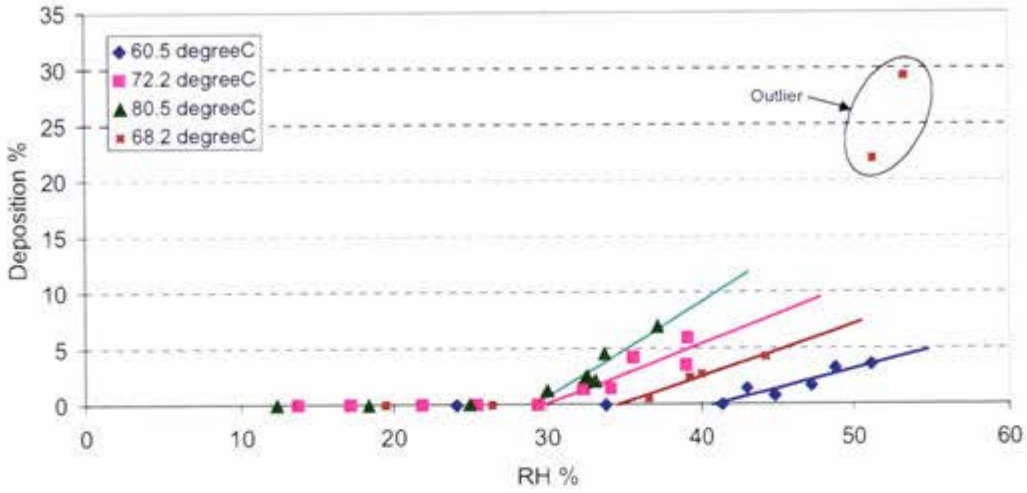
60.5 degreeC
72.2 degreeC
80.5 degreeC
68.2 degreeC
Outlier
Deposition %
RH %
0
5
10
15
20
25
30
35
0
10
20
30
40
50
60

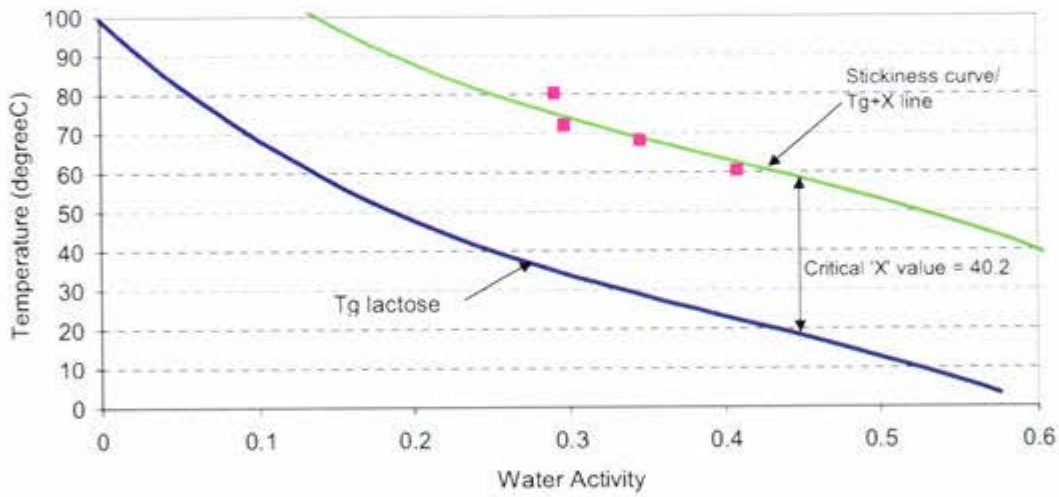
Stickiness curve/
Tg+X line
Critical 'X' value = 40.2
Tg lactose
Temperature (degreeC)
Water Activity
0
10
20
30
40
50
60
70
80
90
100
0
0.1
0.2
0.3
0.4
0.5
0.6

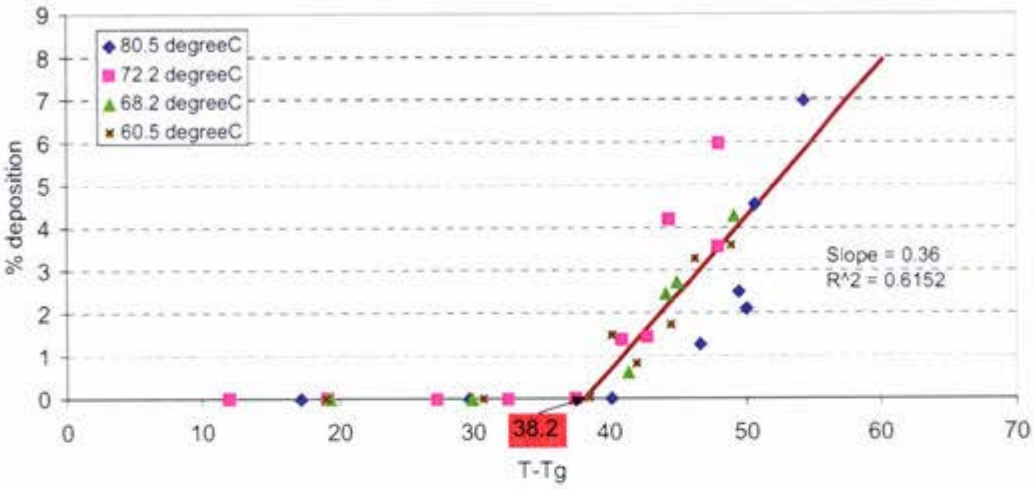
80.5 degreeC
72.2 degreeC
68.2 degreeC
60.5 degreeC
% deposition
Slope = 0.36
R^2 = 0.6152
38.2
T-Tg

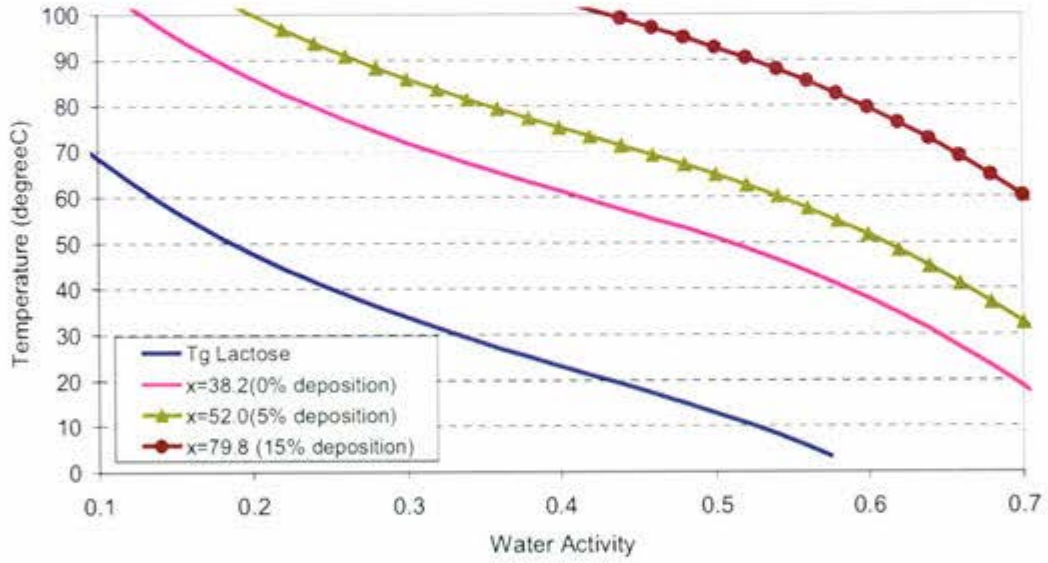
Temperature (degreeC)
Tg Lactose
x=38.2(0% deposition)
x=52.0(5% deposition)
x=79.8 (15% deposition)
Water Activity

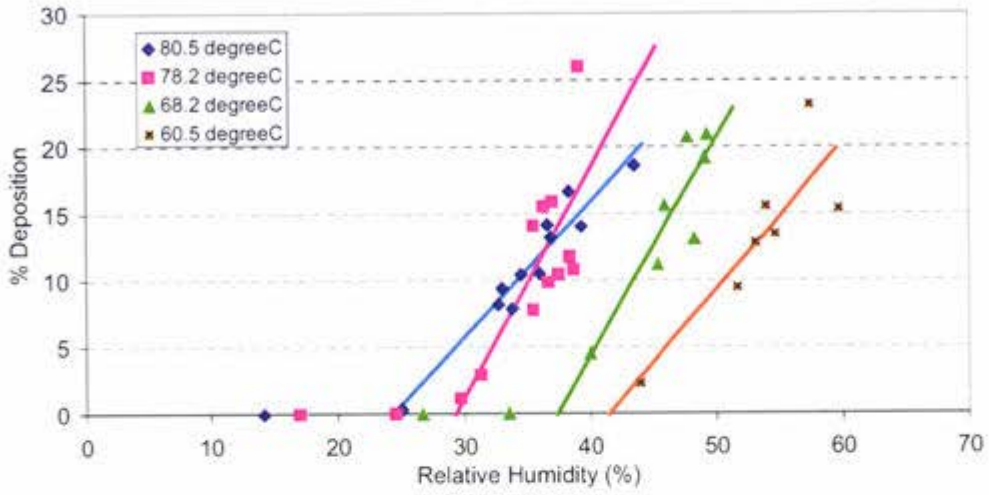
80.5 degreeC
78.2 degreeC
68.2 degreeC
60.5 degreeC
% Deposition
Relative Humidity (%)
0
5
10
15
20
25
30
0
10
20
30
40
50
60
70

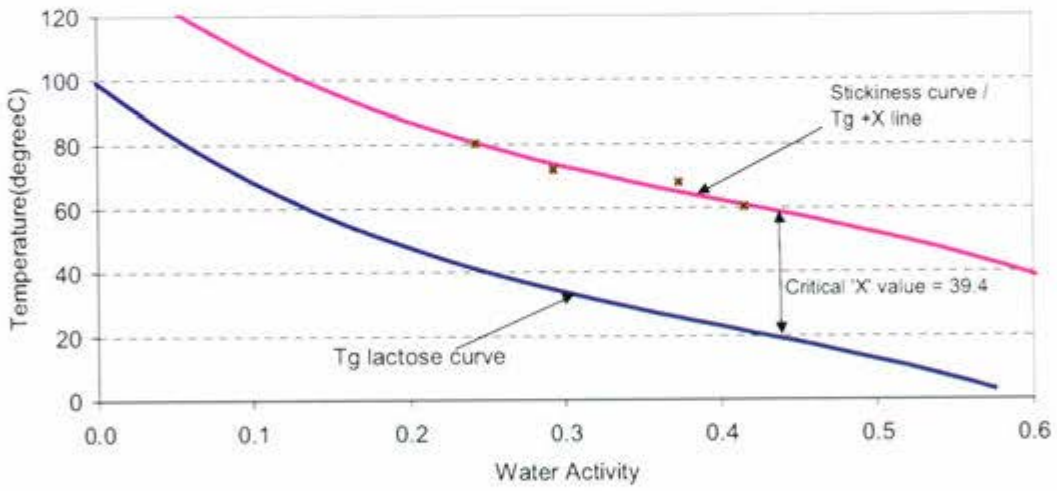
Stickiness curve / Tg +X line
Critical 'X' value = 39.4
Tg lactose curve
Temperature(degreeC)
Water Activity
0
20
40
60
80
100
120
0.0
0.1
0.2
0.3
0.4
0.5
0.6

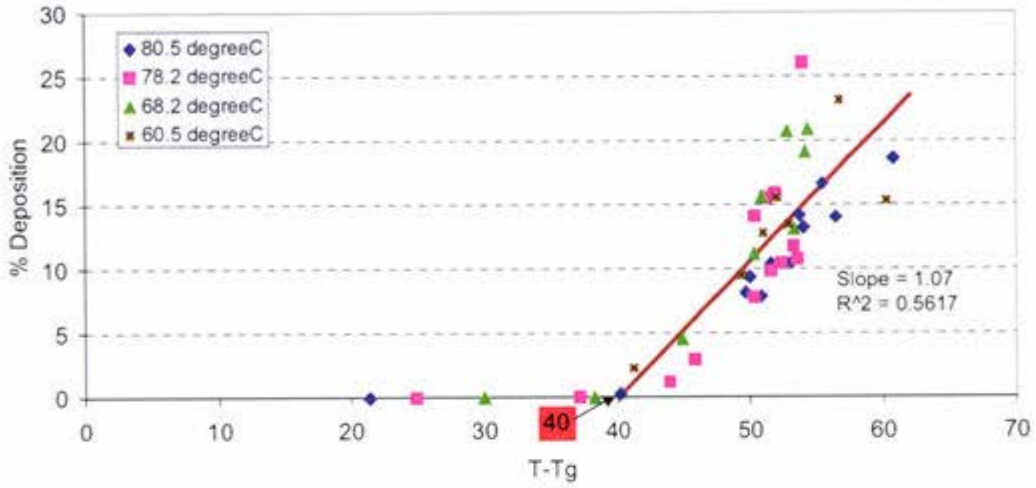
80.5 degreeC
78.2 degreeC
68.2 degreeC
60.5 degreeC
% Deposition
T-Tg
Slope = 1.07
R^2 = 0.5617
40

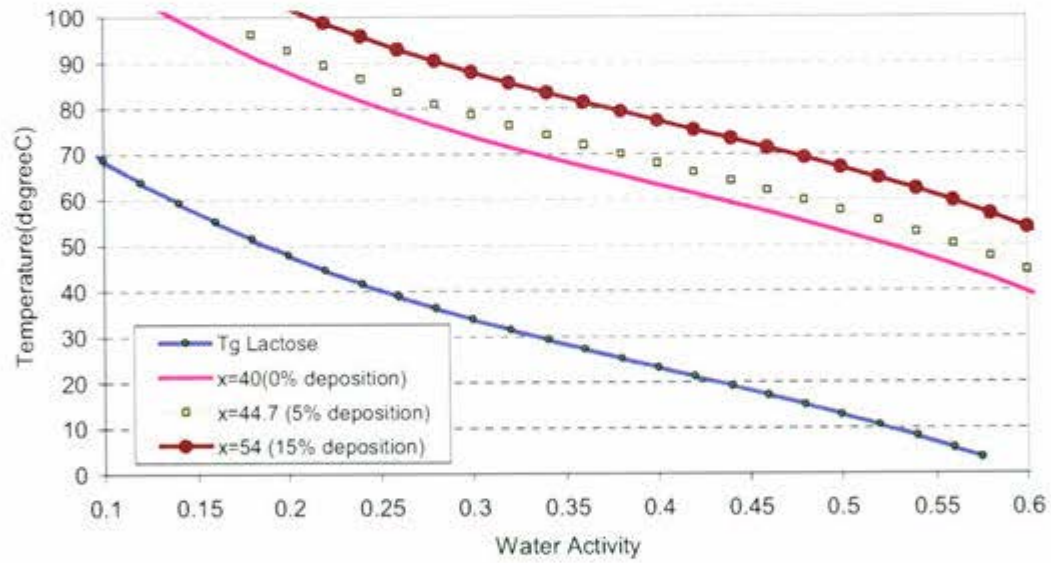
Tg Lactose
x=40(0% deposition)
x=44.7 (5% deposition)
x=54 (15% deposition)
Temperature(degreeC)
Water Activity

MPC AND WHEY PROTEIN

MPC 44

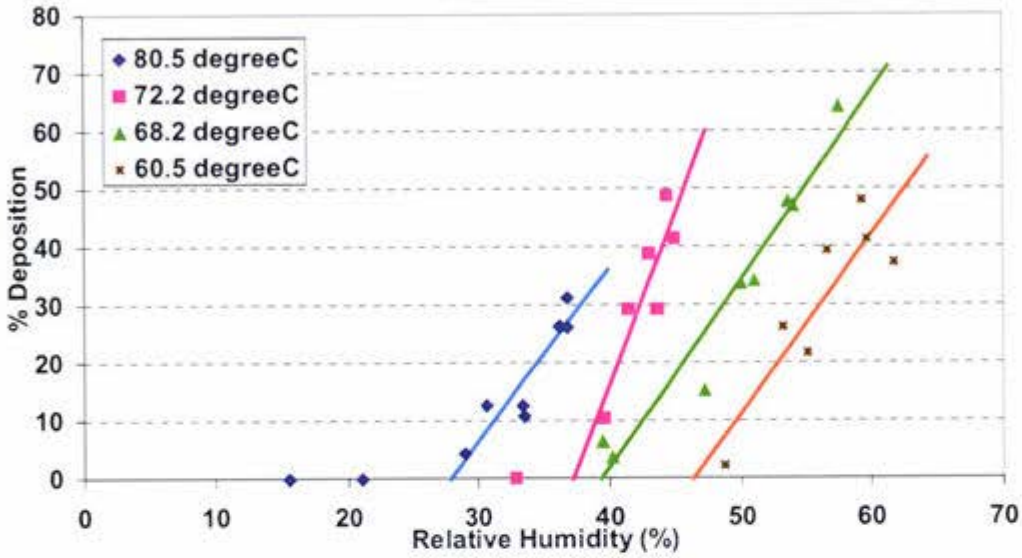

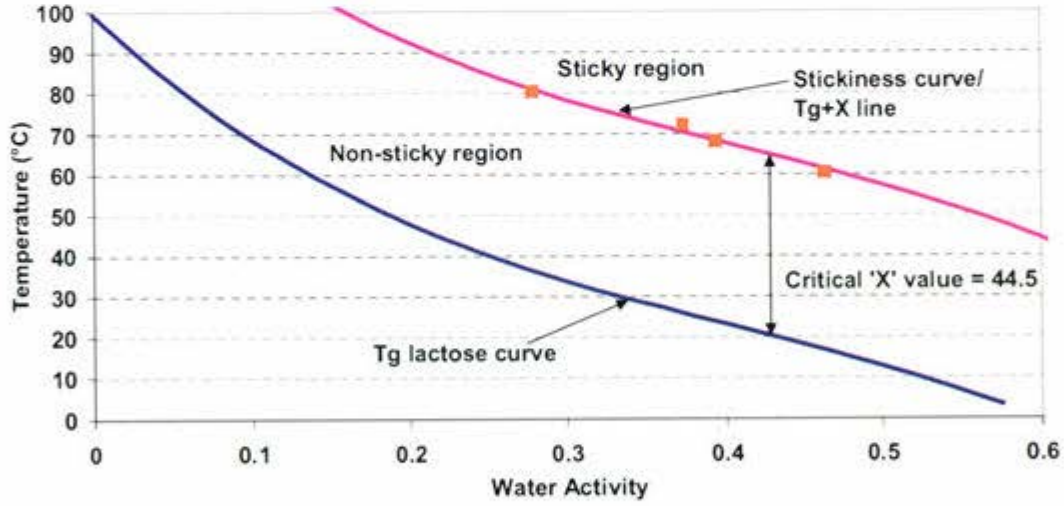

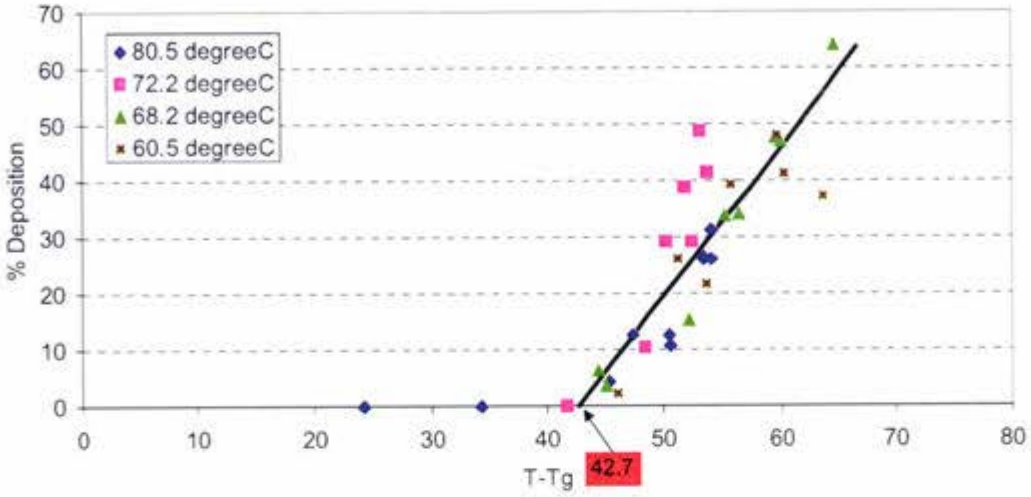
80.5 degreeC
72.2 degreeC
68.2 degreeC
60.5 degreeC
% Deposition
T-Tg
42.7

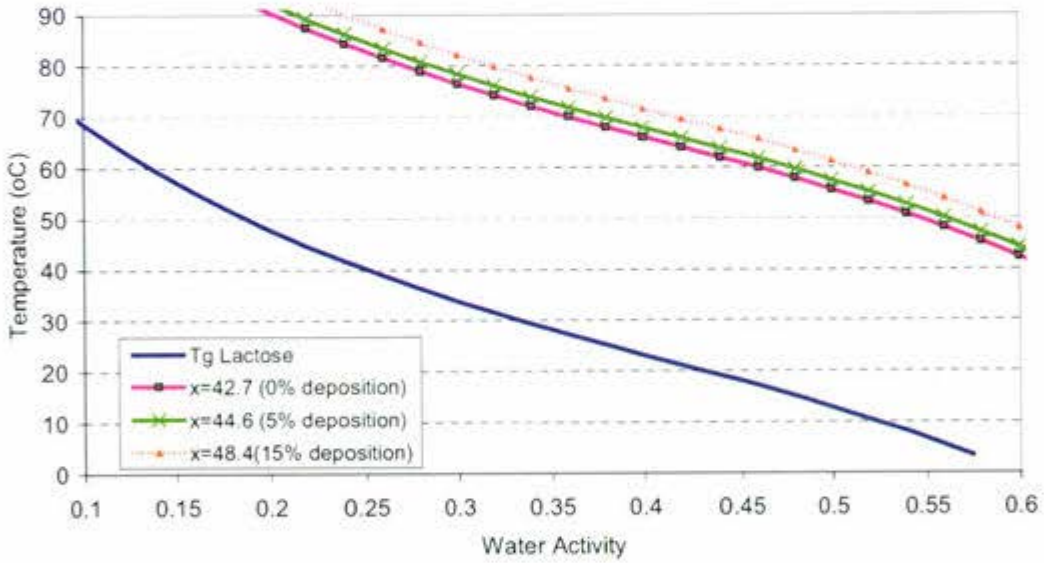
Tg Lactose
x=42.7 (0% deposition)
x=44.6 (5% deposition)
x=48.4(15% deposition)
Temperature (oC)
Water Activity

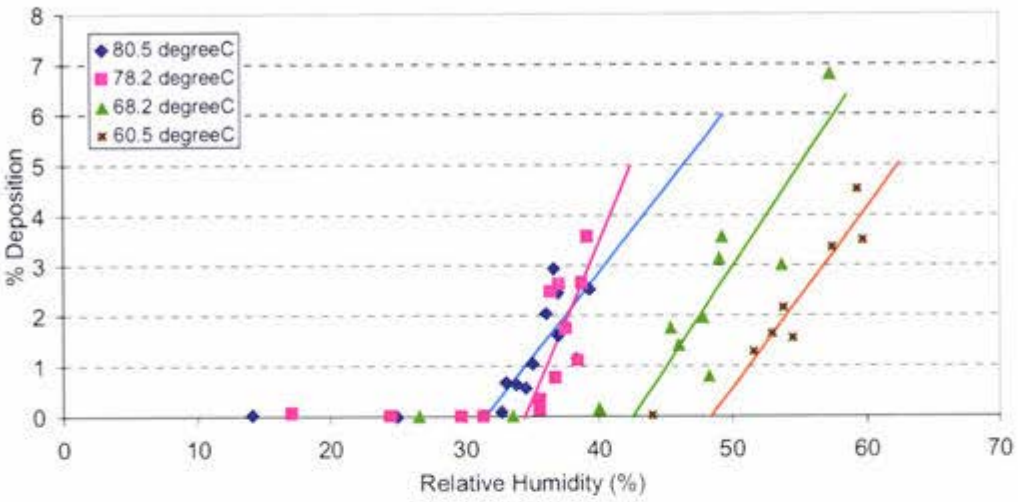
80.5 degreeC
78.2 degreeC
68.2 degreeC
60.5 degreeC
% Deposition
Relative Humidity (%)
0
1
2
3
4
5
6
7
8
0
10
20
30
40
50
60
70

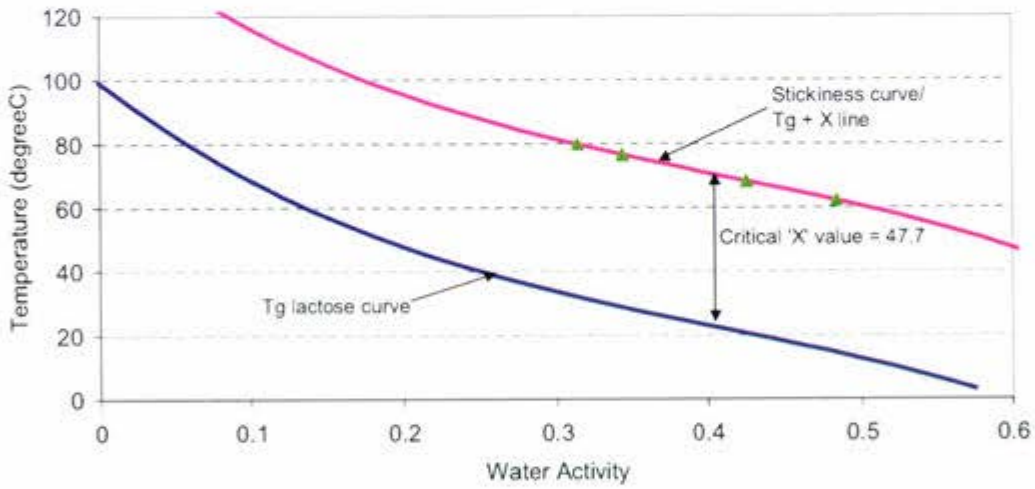
Stickiness curve/
Tg + X line
Critical 'X' value = 47.7
Tg lactose curve
Temperature (degreeC)
Water Activity
0
20
40
60
80
100
120
0
0.1
0.2
0.3
0.4
0.5
0.6

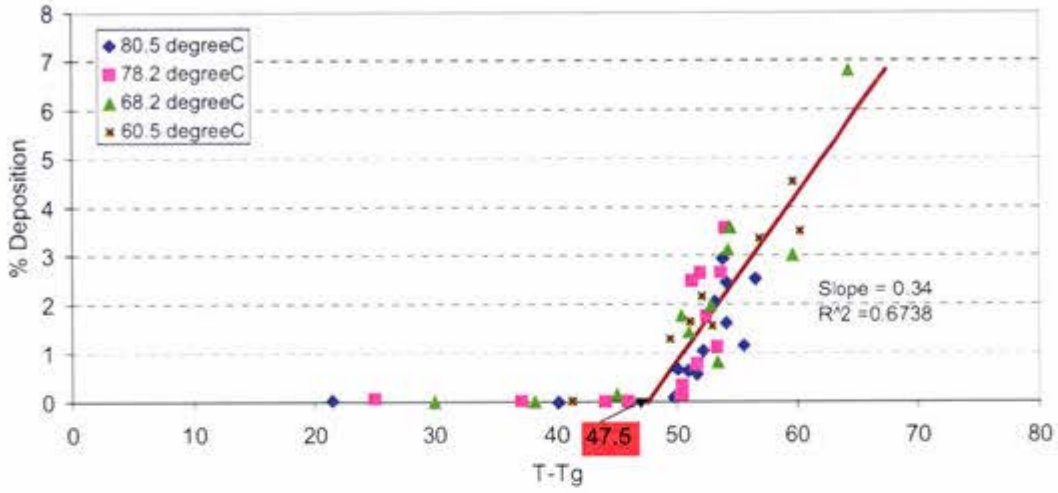
80.5 degreeC
78.2 degreeC
68.2 degreeC
60.5 degreeC
% Deposition
Slope = 0.34
R^2 =0.6738
47.5
T-Tg

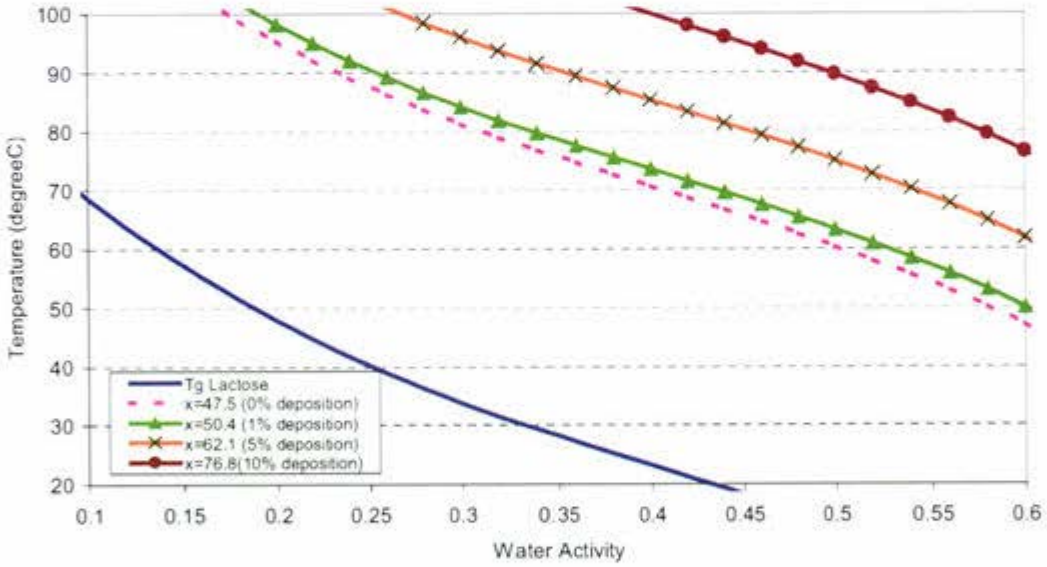
Temperature (degreeC)
Tg Lactose
x=47.5 (0% deposition)
x=50.4 (1% deposition)
x=62.1 (5% deposition)
x=76.8(10% deposition)
Water Activity

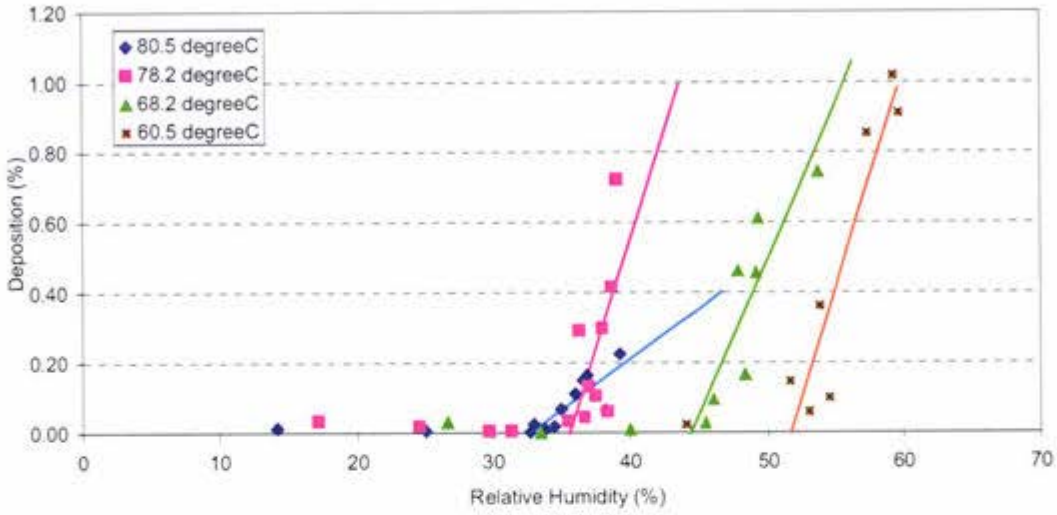
80.5 degreeC
78.2 degreeC
68.2 degreeC
60.5 degreeC
Deposition (%)
Relative Humidity (%)
1.20
1.00
0.80
0.60
0.40
0.20
0.00
0
10
20
30
40
50
60
70

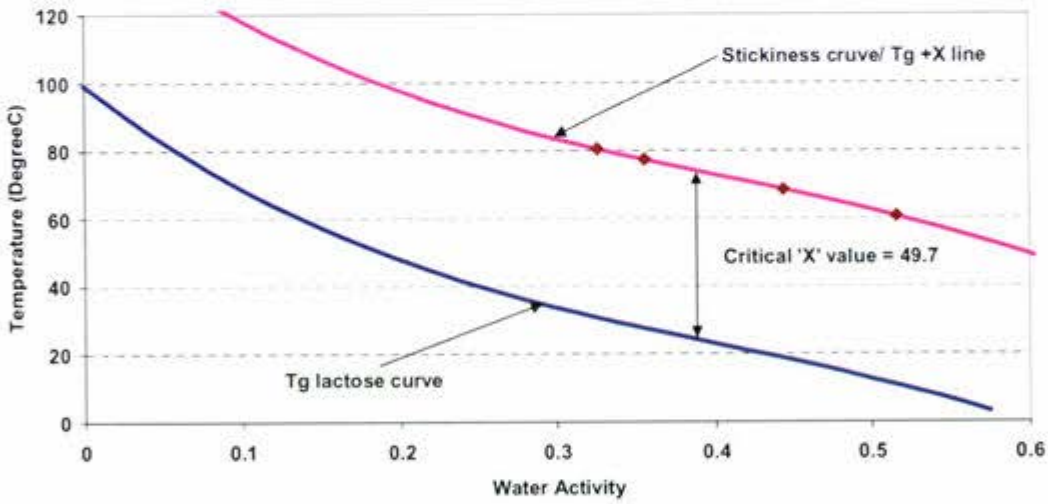
Stickiness cruve/ Tg +X line
Critical 'X' value = 49.7
Tg lactose curve
Temperature (DegreeC)
Water Activity
120
100
80
60
40
20
0
0
0.1
0.2
0.3
0.4
0.5
0.6

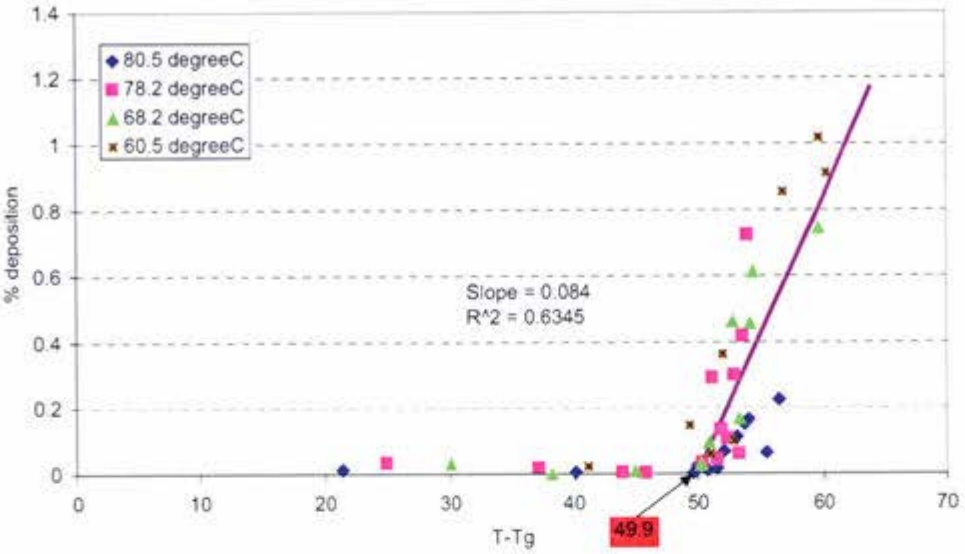
80.5 degreeC
78.2 degreeC
68.2 degreeC
60.5 degreeC
% deposition
Slope = 0.084
R^2 = 0.6345
T-Tg
49.9

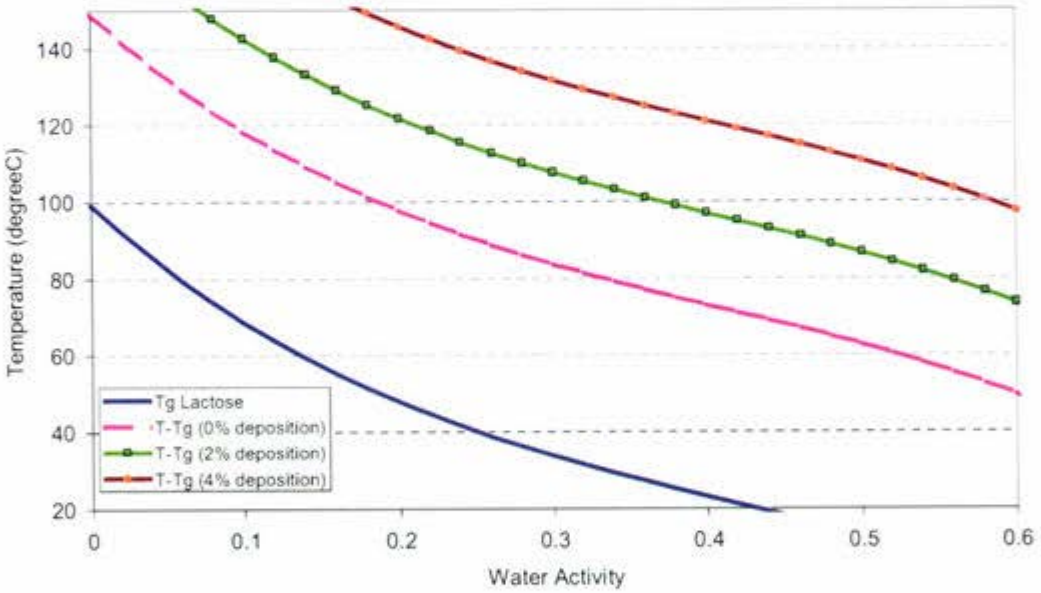
Temperature (degreeC)
Tg Lactose
T-Tg (0% deposition)
T-Tg (2% deposition)
T-Tg (4% deposition)
Water Activity

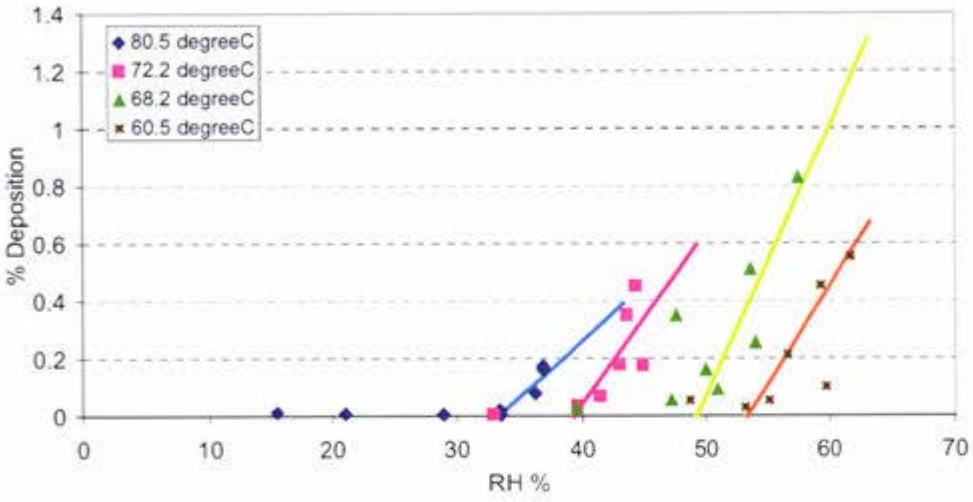
80.5 degreeC
72.2 degreeC
68.2 degreeC
60.5 degreeC
% Deposition
RH %
0
0.2
0.4
0.6
0.8
1
1.2
1.4
0
10
20
30
40
50
60
70

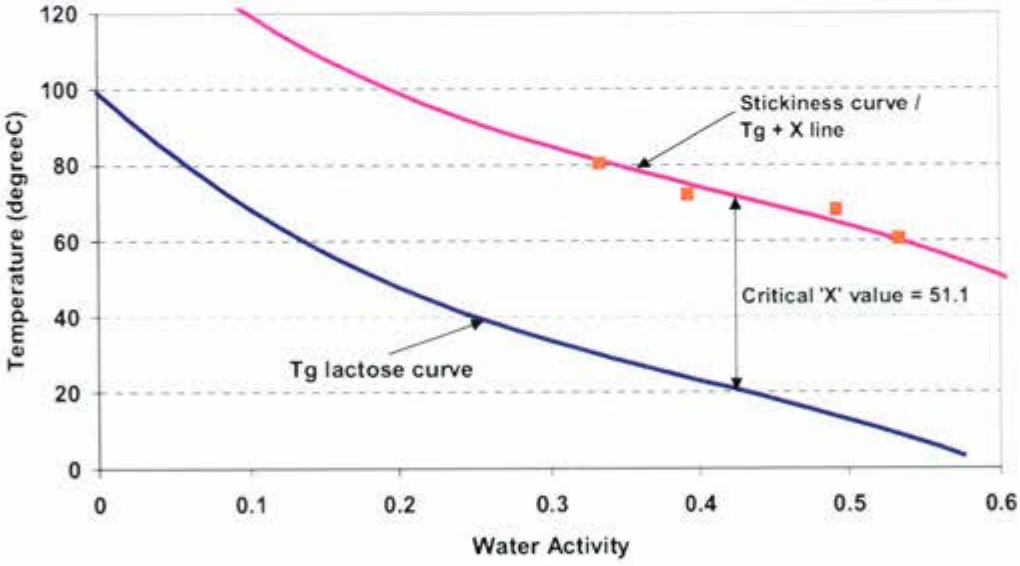
Stickiness curve / Tg + X line
Critical 'X' value = 51.1
Tg lactose curve
Temperature (degreeC)
Water Activity
0
20
40
60
80
100
120
0
0.1
0.2
0.3
0.4
0.5
0.6

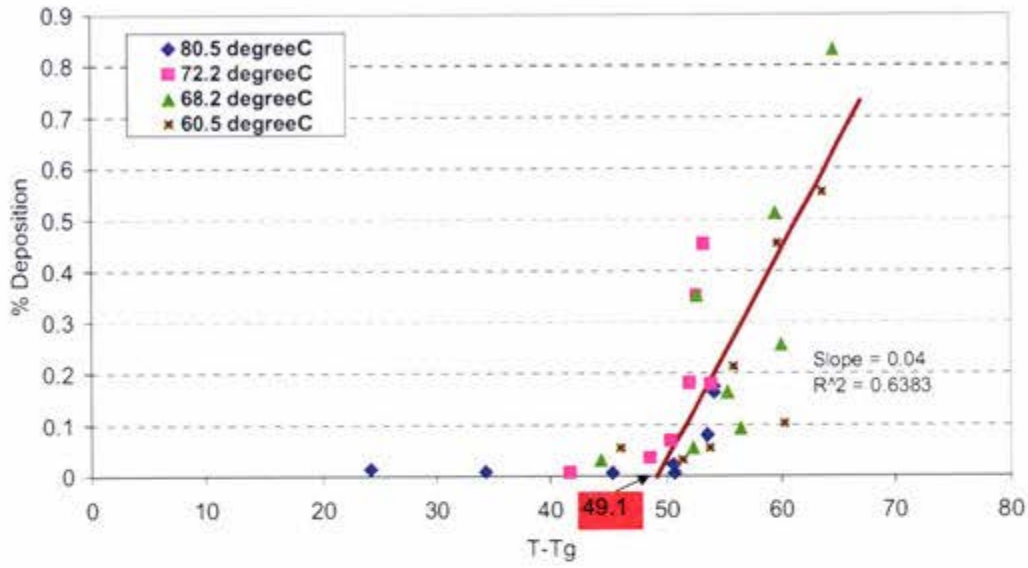
80.5 degreeC
72.2 degreeC
68.2 degreeC
60.5 degreeC
% Deposition
Slope = 0.04
R^2 = 0.6383
49.1
T-Tg

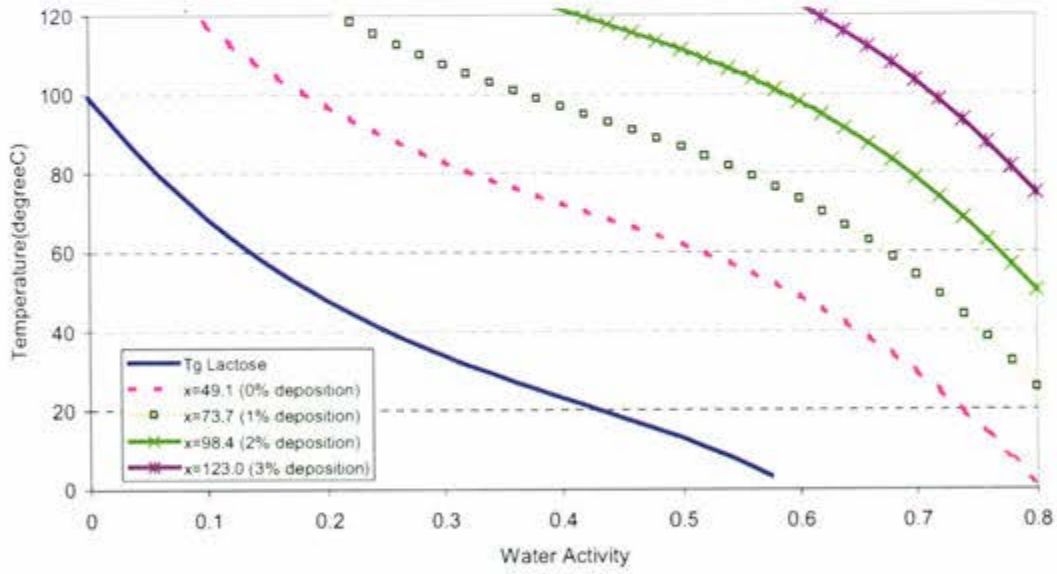
Temperature(degreeC)
Tg Lactose
x=49.1 (0% deposition)
x=73.7 (1% deposition)
x=98.4 (2% deposition)
x=123.0 (3% deposition)
Water Activity

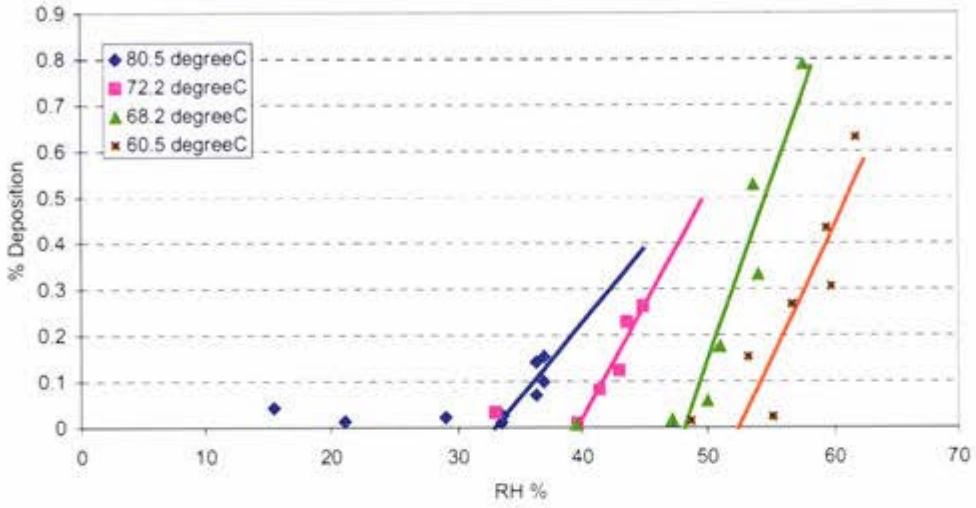
80.5 degreeC
72.2 degreeC
68.2 degreeC
60.5 degreeC
% Deposition
RH %
0
0.1
0.2
0.3
0.4
0.5
0.6
0.7
0.8
0.9
0
10
20
30
40
50
60
70

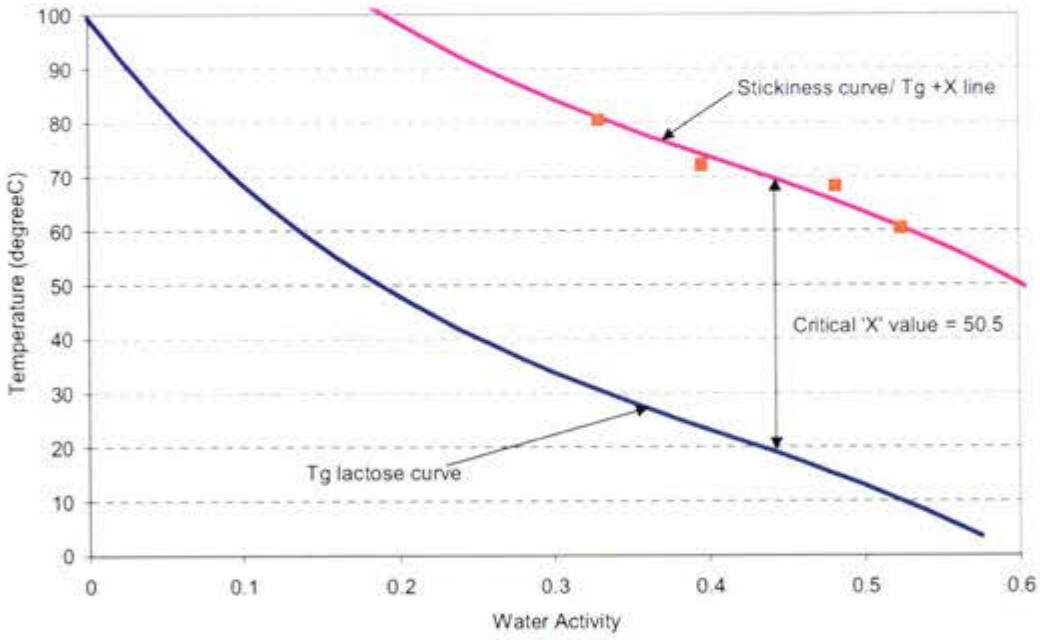
Stickiness curve/ Tg +X line
Critical 'X' value = 50.5
Tg lactose curve
Temperature (degreeC)
Water Activity
0
10
20
30
40
50
60
70
80
90
100
0
0.1
0.2
0.3
0.4
0.5
0.6

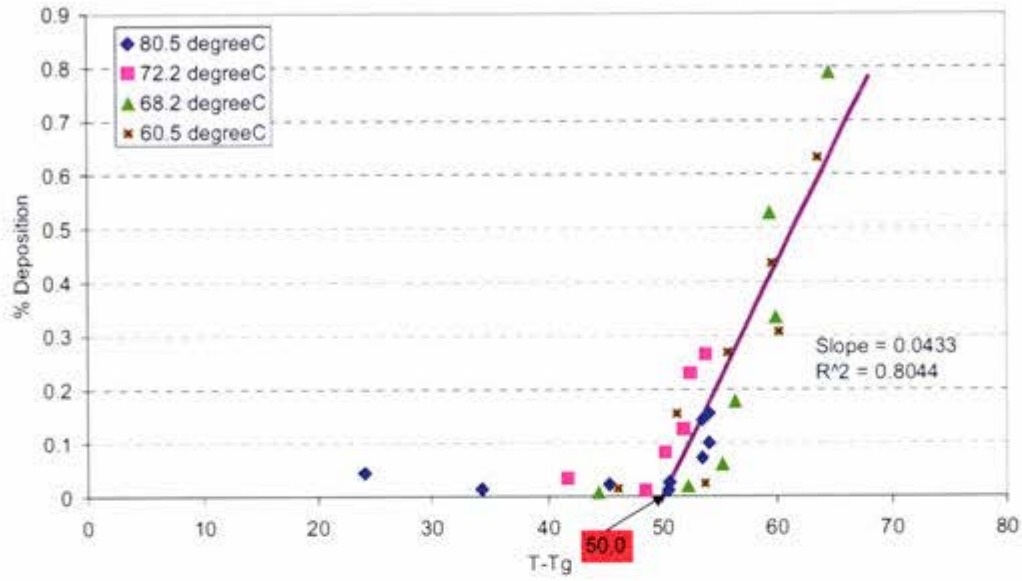
80.5 degreeC
72.2 degreeC
68.2 degreeC
60.5 degreeC
% Deposition
T-Tg
50.0
Slope = 0.0433
R^2 = 0.8044

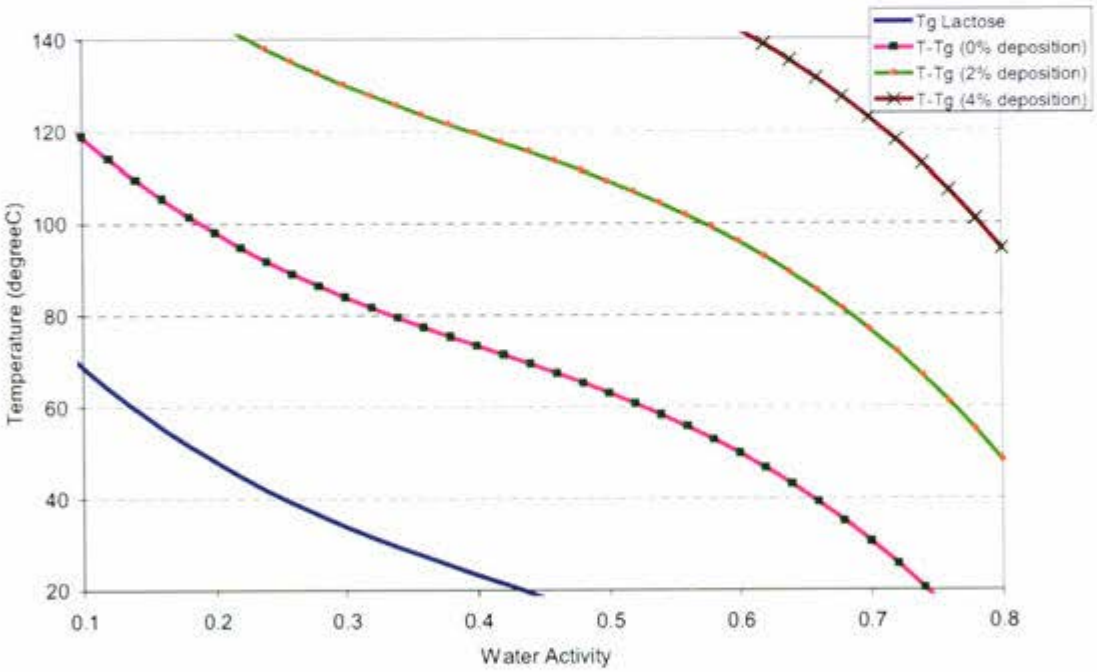
Tg Lactose
T-Tg (0% deposition)
T-Tg (2% deposition)
T-Tg (4% deposition)
Temperature (degreeC)
Water Activity

SPECIALITY

BUTTER MILK POWDER

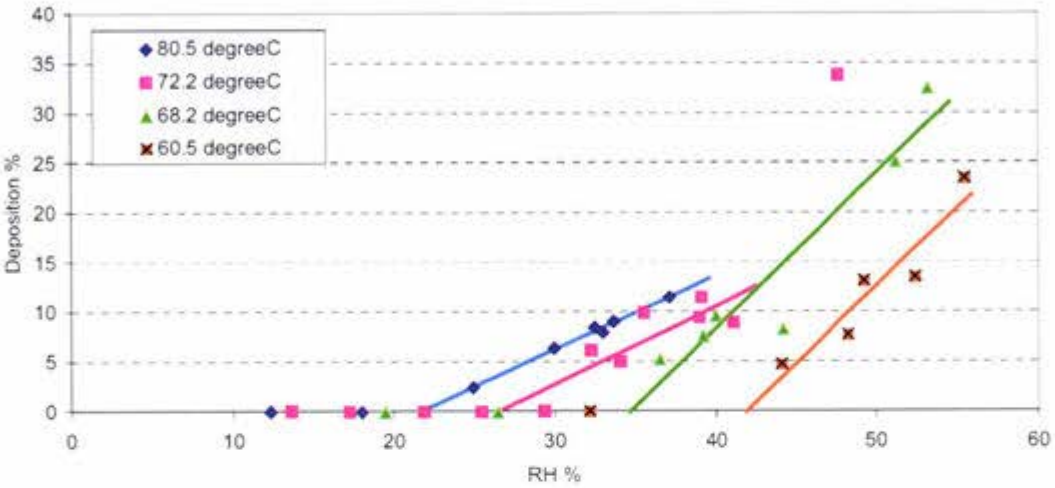

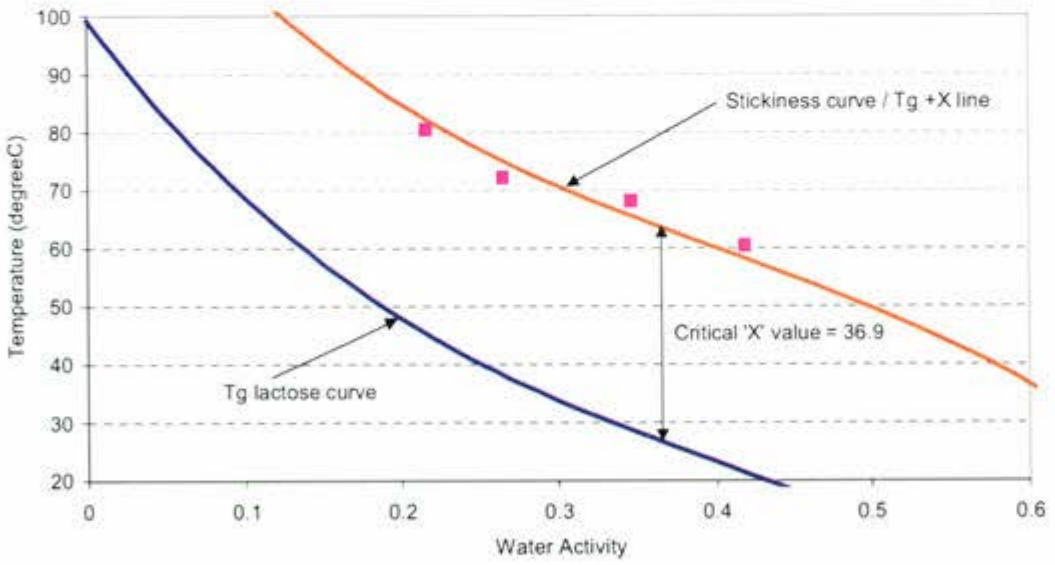

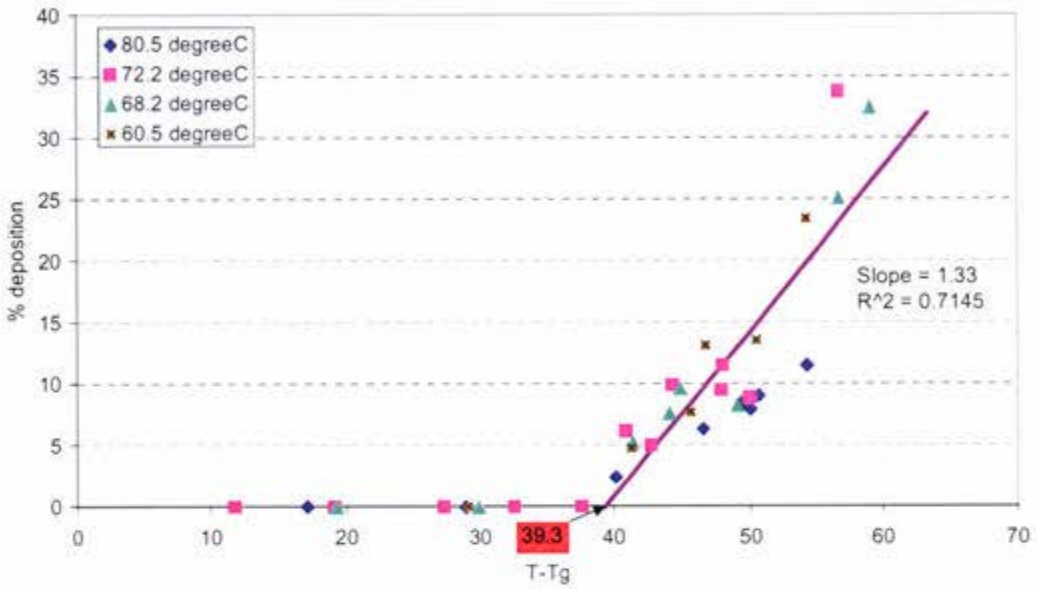
80.5 degreeC
72.2 degreeC
68.2 degreeC
60.5 degreeC
% deposition
Slope = 1.33
R^2 = 0.7145
39.3
T-Tg

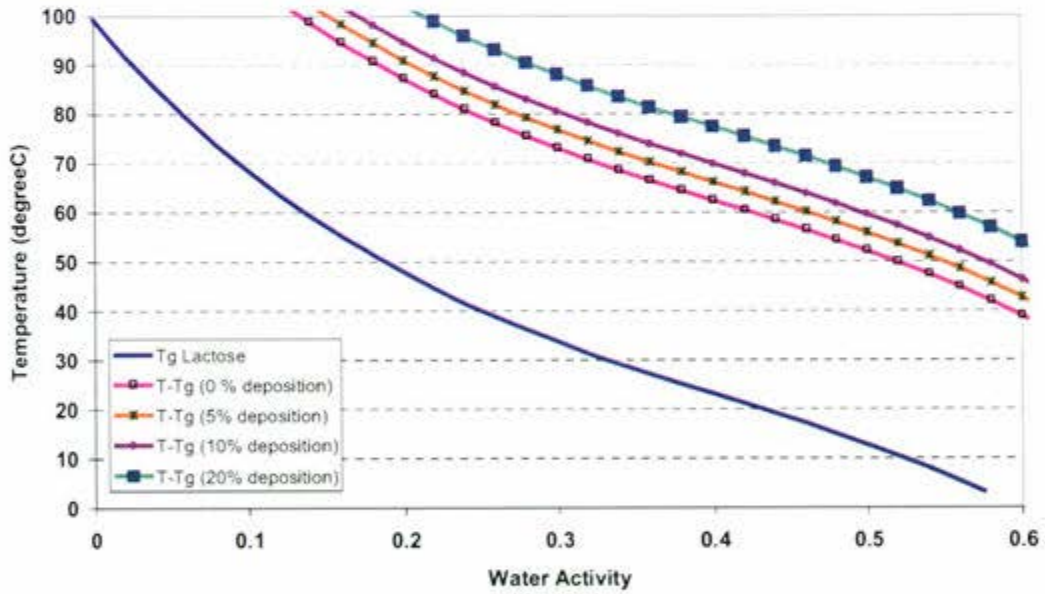
Temperature (degreeC)
Tg Lactose
T-Tg (0 % deposition)
T-Tg (5% deposition)
T-Tg (10% deposition)
T-Tg (20% deposition)
Water Activity

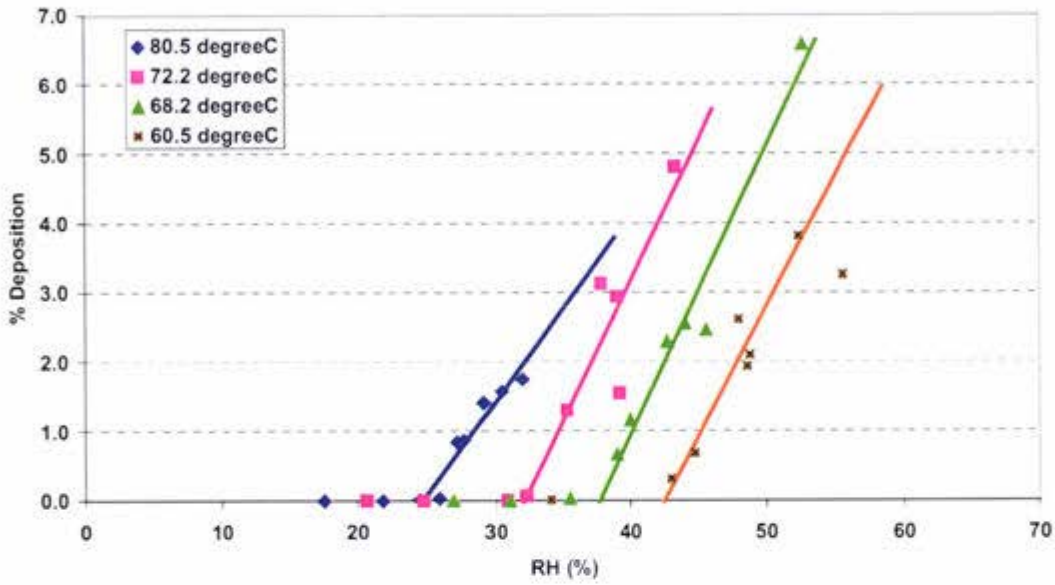
80.5 degreeC
72.2 degreeC
68.2 degreeC
60.5 degreeC
% Deposition
RH (%)
0.0
1.0
2.0
3.0
4.0
5.0
6.0
7.0
0
10
20
30
40
50
60
70

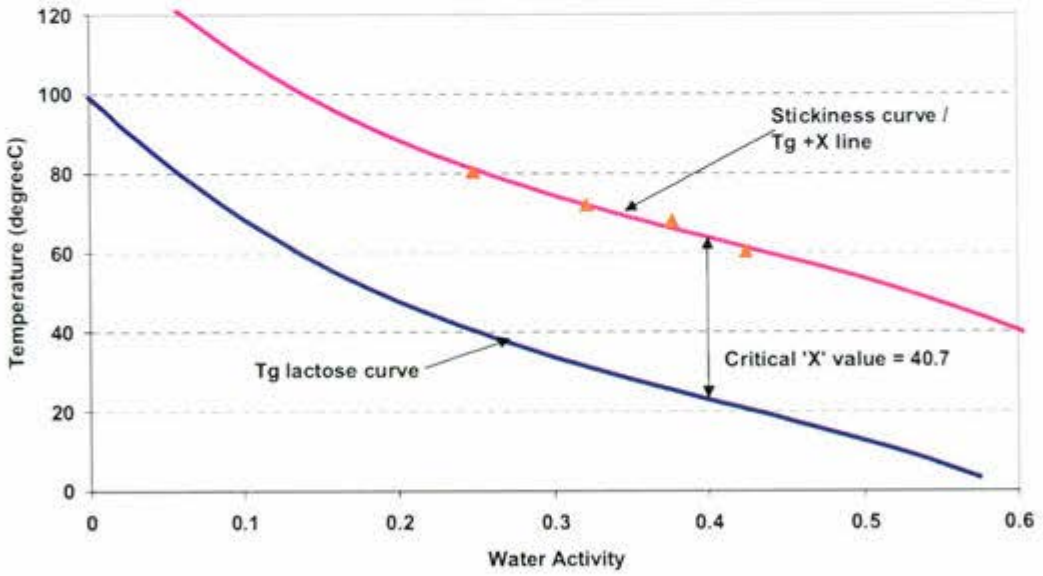
Stickiness curve / Tg +X line
Tg lactose curve
Critical 'X' value = 40.7
Temperature (degreeC)
Water Activity
0
20
40
60
80
100
120
0
0.1
0.2
0.3
0.4
0.5
0.6

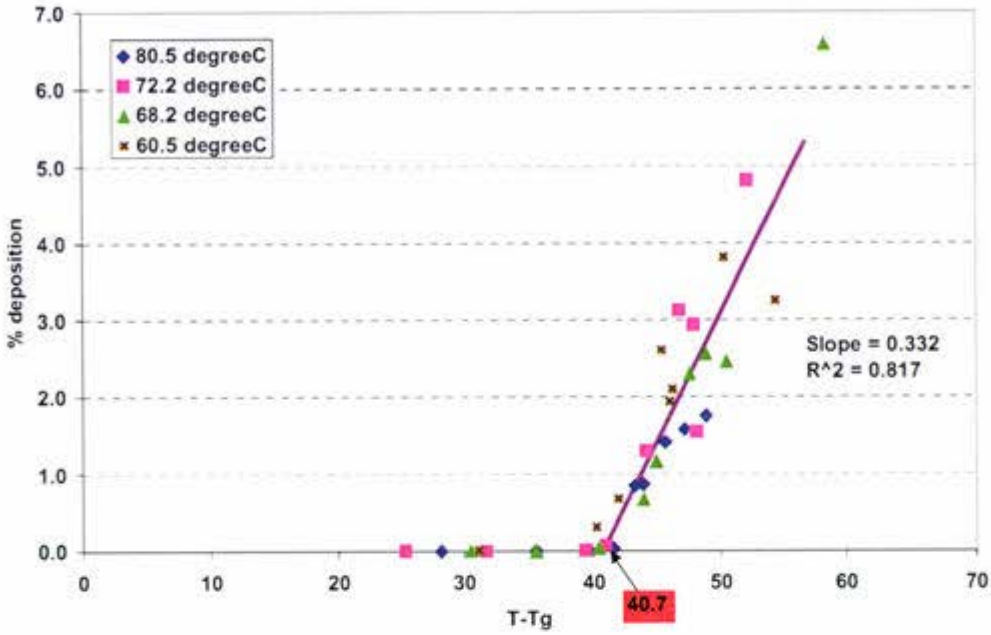
80.5 degreeC
72.2 degreeC
68.2 degreeC
60.5 degreeC
% deposition
T-Tg
Slope = 0.332
R^2 = 0.817
40.7

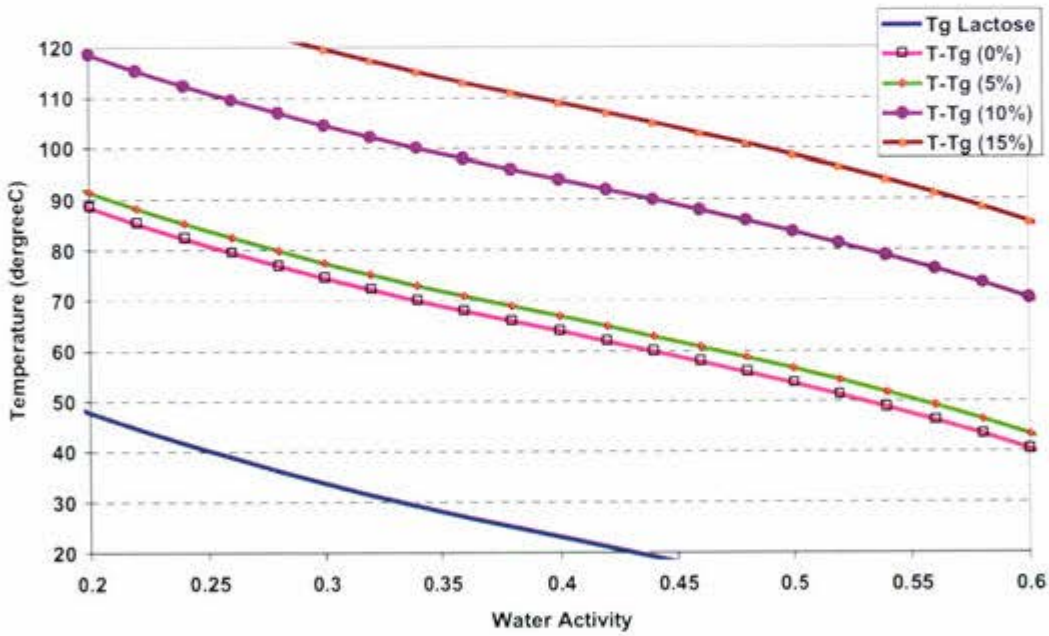
Tg Lactose
T-Tg (0%)
T-Tg (5%)
T-Tg (10%)
T-Tg (15%)
Temperature (dergreeC)
Water Activity